Charles University in Prague
Faculty of Mathematics and Physics

MASTER THESIS

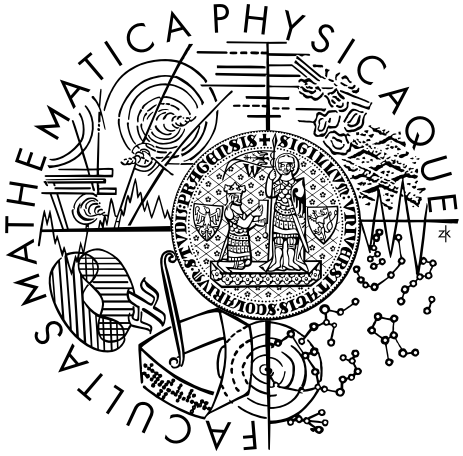

Miroslav Tomasik

Simulation of two-dimensional flow past obstacles using lattice-gas cellular automata

Institute of Theoretical Physics

Supervisor of the master thesis: Martin Scholtz
Study programme: Physics
Study branch: Mathematical modelling

Prague 2017

I declare that I carried out this master thesis independently, and only with the cited sources, literature and other professional sources.

I understand that my work relates to the rights and obligations under the Act No. 121/2000 Sb., the Copyright Act, as amended, in particular the fact that the Charles University in Prague has the right to conclude a license agreement on the use of this work as a school work pursuant to Section 60 subsection 1 of the Copyright Act.

In ..... date ..... signature of the author

Title: Simulation of two-dimensional flow past obstacles using lattice-gas cellular automata

Author: Miroslav Tomasik

Institute or Department: Institute of Theoretical Physics

Supervisor: Martin Scholtz, Institute of Theoretical Physics

Abstract: Cellular automata constitutes original computational methods, that found its application in various scientific disciplines. The special class of cellular automata, the lattice gas automata were succesfull in dealing with many challenges of hydrodynamic simulations, and they bootstraped one of the most perspective CFD methods, the Lattice Boltzmann models.

In the theoretical part, we follow the evolution of the lattice gas automata, explore the theory behind them, and from their microdynamics, we derive the hydrodynamic equations.

In the practical part, we implemented two most distinguished types of LGCA, the Pair-interaction automaton and FCHC. We applied them on the flow around obstacles of various shapes. The scientifically most relevant part concerns statistical properties of the turbulent flow simmulated by LGCA, but requires further research to conclude it.

Keywords: Cellular automata FCHC Pair-interaction Turbulence

Contents

How to use this diploma thesis

For the beginner in this field, we recommend to follow sequence of the chapters, since the theoretical part constitutes tutorial to lattice-gas cellular automata, but an experienced user can feel free to chose the topic he finds interesting.

In chapter one, we introduce the notion of cellular automata.

In chapter two, we continue with the special type cellular automata, the lattice-gas CA, that represents the original approach in CFD.

In chapter three, we present the better-known branch of LCCA, that started with FHP in two-dimensions and FCHC in three-dimensions.

In chapter four, we inspected microdynamics of FHP more theoretically and generally, so that the obtained results are valid for N-dimensional FHP-like LGCA, namely FCHC.

In chapter five, we derive macroscopic equations for FHP and FCHC.

In chapter six, we analyzed FCHC lattice and sketched FCHC collision algorithm as proposed by Henon.

In chapter seven, we introduced another successful branch of LGCA, the Pair-Interaction models. They are more comfortable to implement then FCHC in 3D, they are great model for ideal fluids, but they have some drawbacks for viscous fluids (viscosity is anisotropic).

Chapter eight concludes theoretical analysis of LGCA by showing what statistical properties does physical fluid exhibit, and that if we artificially impose its statistical properties on the LGCA, we obtain physically realistic model by every means, although this new generation of LGCA are beyond the scope of this thesis.

In chapter ten we introduce probabilistic methods that we intend to use in practical part, to inspect properties of fully-developed turbulence simulated by our models.

Practical part starts with the chapter ten, that summarizes what its content.

Chapter eleven contains general comments on the implementation.

Chapter twelve and thirteen discuss implementation of FCHC and standard algorithm of Pair-Interaction

Chapter fourteen motivates non-deterministic variant of Pair-interaction automata.

In chapter fifteen, we present results of the flow around obstacles simulated on our models.

Chapter sixteen is scientifically most challenging part, and although the obtained results are questionable from various positions, they constitute basis for the further research.

Part I

Theory

1. Cellular automata

Years before DNA and replication mechanism was discovered in living cells, John von Neumann was investigating self-replicating systems in theory, and layed basis for the "New kind of science" [4].

1.1 Game of Life

John Conway, by significant simplification of von Neumann ideas, introduced the Game of Life in 1970 that renewed general interest in cellular automata.

Depending on the initial conditions, evolution of this automaton can be chaotic, periodic or it can lead to the stable configurations.

The reason for this complexity hides in the fundamental property of Game of Life - because it is the Turing-complete, in principle any computer program can be simulated in the Game of Life, and thus any behavior can be observed.

For the purposes of this thesis, we have written a simple desktop application implementing this game, since we can easily explain the basic principles of cellular automata on it.

Let us have a rectangular grid, with black and white squares. White squares represent dead cells, black cells represent living cells. On the figure 1.1 we see such grid, that we chose for the initial state of 'Life'.

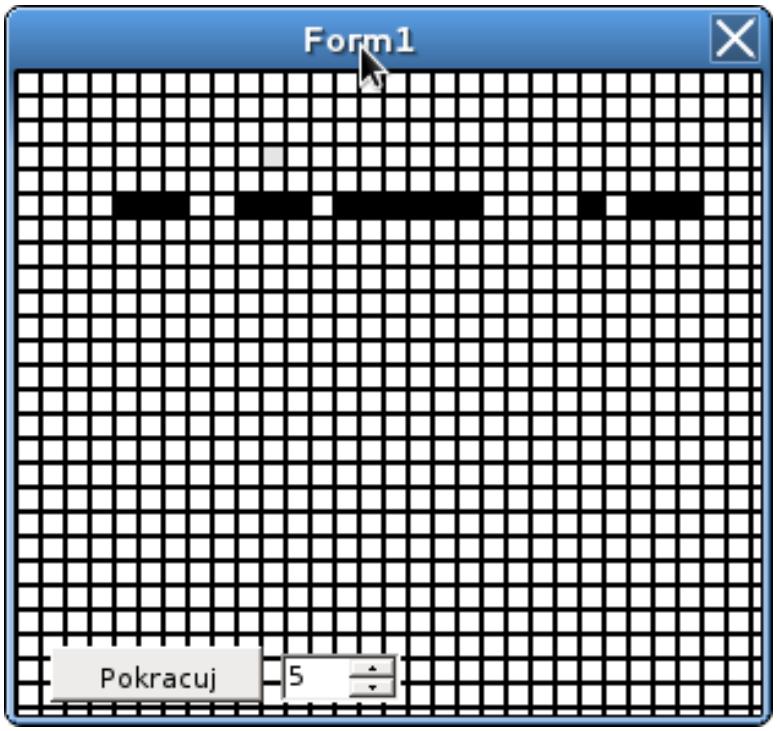

Figure 1.1: The initial state of 'Life' (at t=0)

Now we press 'Pokracuj' button and let the the Life evolve. In the discrete time steps, the grid is changing. We see that some cells are dying, but some cells are getting alive. What is the rule that kills the cell or leave it be?

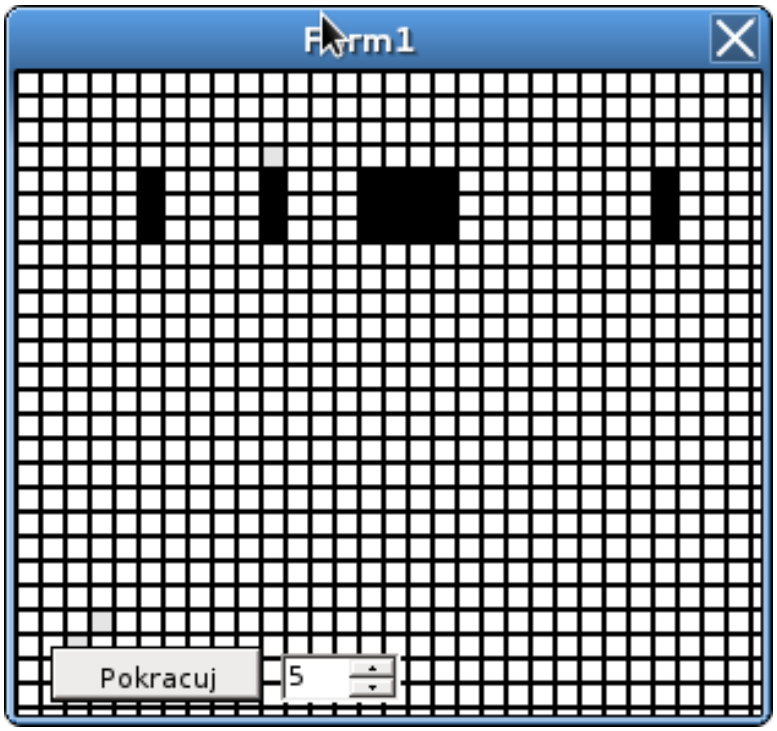

Figure 1.2: t=1

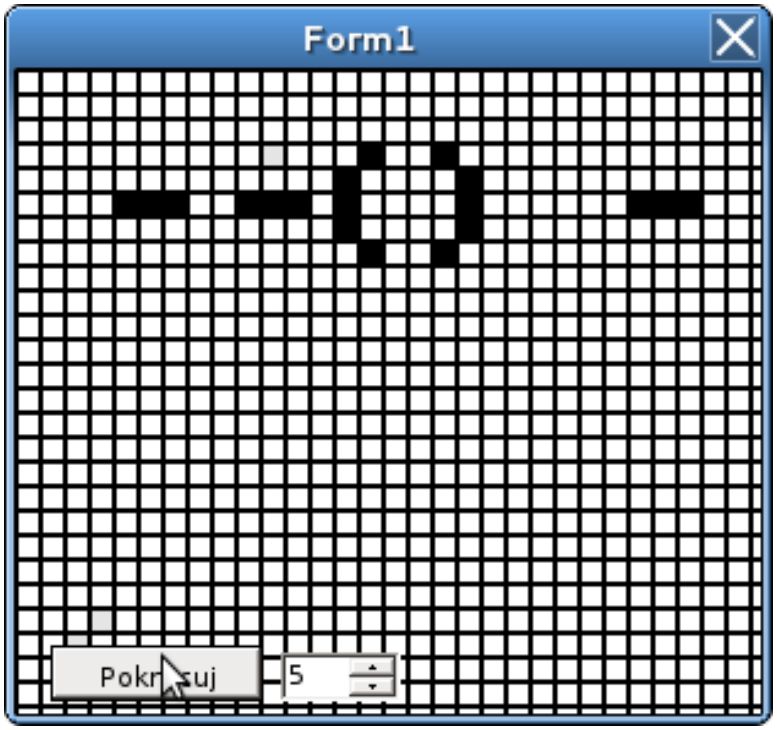

Figure 1.3: t=2

1. If the cell is alive, and 2 or 3 neighbouring cells are alive, the cell will stay alive in the next step. Otherwise it will die.

2. If the cell is dead, and **exactly** 3 neighboring cells are alive, the cell will get alive in the next step. Otherwise, it stays dead.

We see that the rule involves only the state of **the cell** and the states of **its eight neighboring cells**.

Let us proceed from this simple example to a more general setting. In the next section, we will generalize main features of 'Life' and formally define the cellular automaton.

1.2 Cellular automaton in general

1. **Position of the cells:**

   Instead of two dimensional, rectangular grid of 'Life', cells might be arranged on the regular grid of arbitrary dimensional. (Regularity follows from definition of Kubrid. In general, cells might be positioned really wildly, e.g. on Penrose lattice, or arbritrary as proposed by Feynman).

2. **Set of cell states Q:**

   In 'Life' cells can be dead or alive, but generally, set of states Q for the cell can have an arbitrary finite size.

3. **Neighborhood:**

   In 'Life', state of the cell in the next step was determined by the nearest neighboring cells. We call these cells neighborhood of range r = 1 (in the distance of 1 cell). However, the rule might involve neighborhood with the arbitrary range, see figure 3

4. **Update rule:**

   Update rule is an arbitrary bounded mapping from the *neighborhood* to the set of states Q. Since the state of the cell is determined only by the state of its neighborhood, update rules in cellular automata are local.

1.3 The most basic cellular automaton

In middle 1980s on the prestigious Princeton institute, Stephen Wolfram and his assistants were performing unusual computer experiments. They were simulating the evolution of the one dimensional cellular automata and they were analyzing the obtained patterns [11] (to a despair of their senior colleagues, who did not understand this "new kind of science")[4].

The most basic, one dimensional cellular automaton we can imagine, is the two state automaton with range $r = 1$.

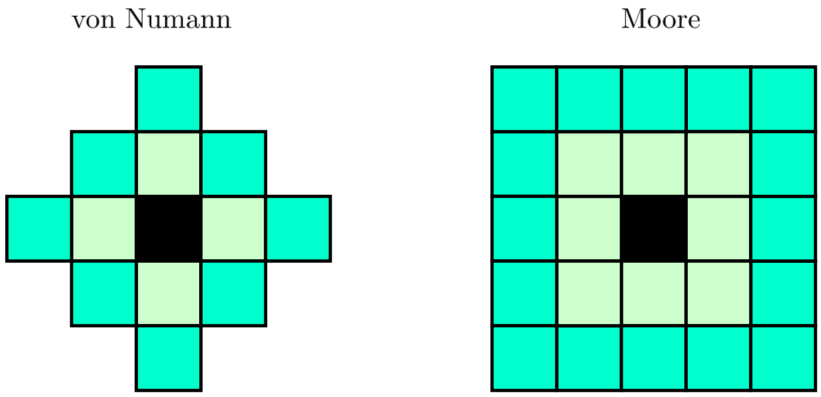

Figure 1.4: Moore's and von Neumann's neighborhood

One dimensional indicates that the cells are arranged in the row (figure 1.3), range $r = 1$ indicates that the update rule involves only three cells. An example of an update rule is shown the table 1.1.

Figure 1.5: A state of one dimensional cellular automaton

The three columns represent the state of a cell a_t^i and its left and right neighbor, a_t^{i-1} and a_t^{i+1} respectively. A living cell is denoted by 1, a dead cell is denoted by 0. The last column denotes the state of the middle cell a_i in the next step $t + 1$. The sequence of *one*s and *zero*s in the last column is the binary representation of a rule. In this particular case, of the Rule 90. Since there is $2^8 = 256$ combinations for the last columns, there is 256 rules for this most basic cellular automaton.

According to Wofram [2], these automata can be classified by their correspondence to the dynamical systems into three classes [2]

(a) **Limit point:**
The final configuration is homogeneous.
Rules number $0, 4, 16, 32, 36, 48, 54, 60, 62$.

(b) **Limit cycles:**
Simpe time-periodic patterns.
Rules number $8, 24, 40, 56, 58$.

(c) **Strange attractors:**

a_t^{i-1}	a_t^i	a_t^{i+1}	a_{t+1}^i
1	1	1	0
1	1	0	1
1	0	1	0
1	0	0	1
0	1	1	1
0	1	0	0
0	0	1	1
0	0	0	0

Table 1.1: Rule 90

Chaotic patterns, see the figure 1.6.

Rules number $2, 6, 10, 12, 14, 18, 22, 26, 28, 30, 34, 38, 42, 44, 46, 50$.

The figures were plotted by our own implementation of this automaton. They represent the evolution of cellular automata with some of the mentioned rules. The downer-most row is the initial configuration of the cellular automaton with one cell alive in the middle, all other cells are dead. The 2^{nd} row is the configuration after the 1^{st} update and so forth.

Formally, the update rule that we have described by the table, may be written in the form

$$a_i^{(t)} = f\big[\sum_{j=-r}^{j=r} \alpha_j a_{i+j}^{(t-1)}\big] \tag{1.1}$$

where a_i refer to the state of the j^{th} cell, αs are the integer weights, and f is the function that takes integer as the single argument, and r is the range of the neighborhood.

1.4 Rule 110

The rule 110 is special among them.b As Cook has proved [1], the rule 110 is special among, that this rule is equivalent to the Turing machine, so depending on the initial conditions, it could be classified in any of the mentioned classes.

In his visionary book New kind of Science [2], Wolfram suggest possibility, that in the infinitely large world of cellular automata, there is an automaton that

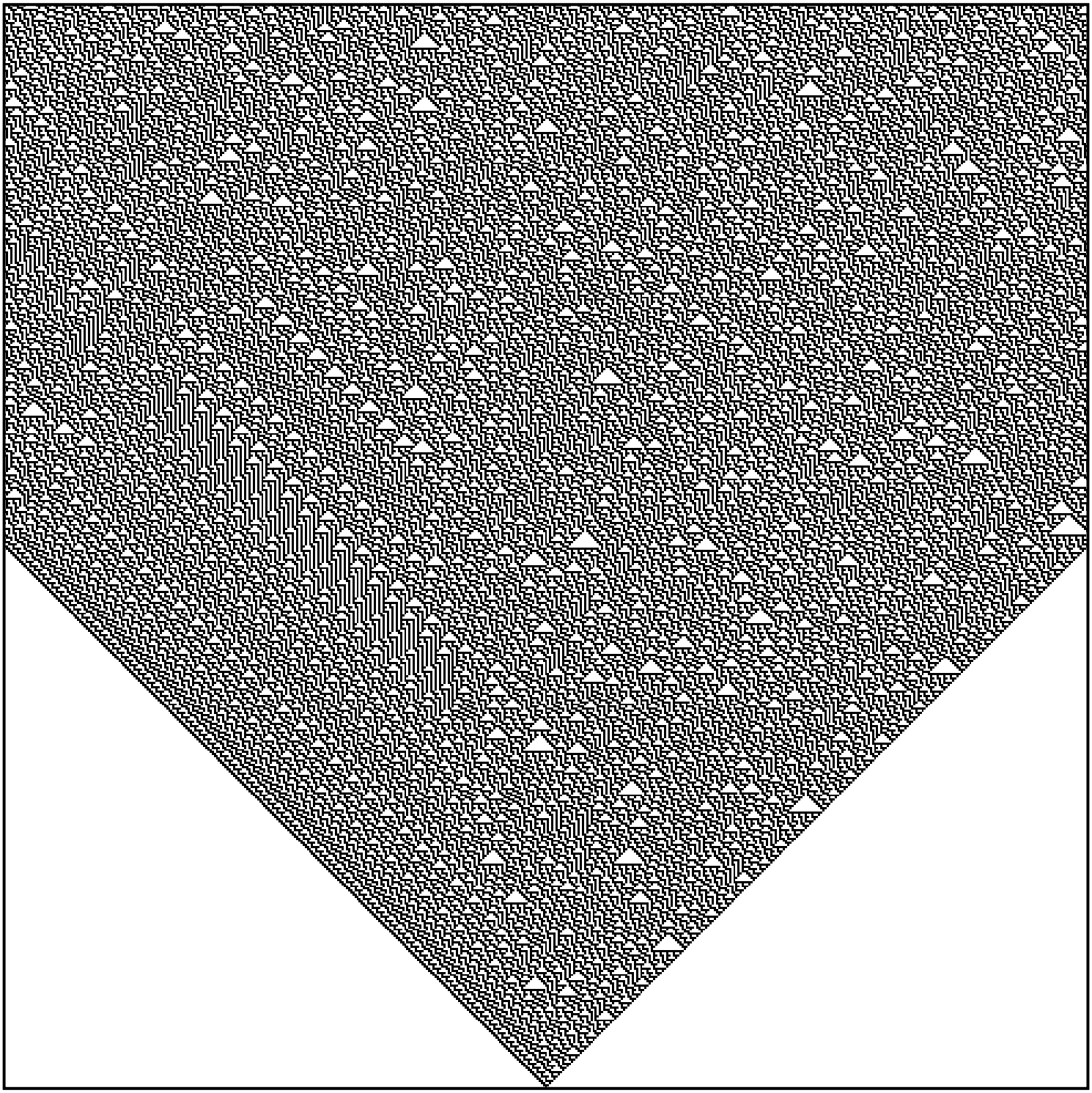

Figure 1.6: Rule 30

constitute a unified theory of the fundamental physics. Although the details of his idea met with rejection(see [9]), many notable physicists are attempting to construct such cellular automaton [10]).

However, focus of our work is much more modest that cellular automata describing universe. Our focus is on the cellular automata that model flows of the fluids.

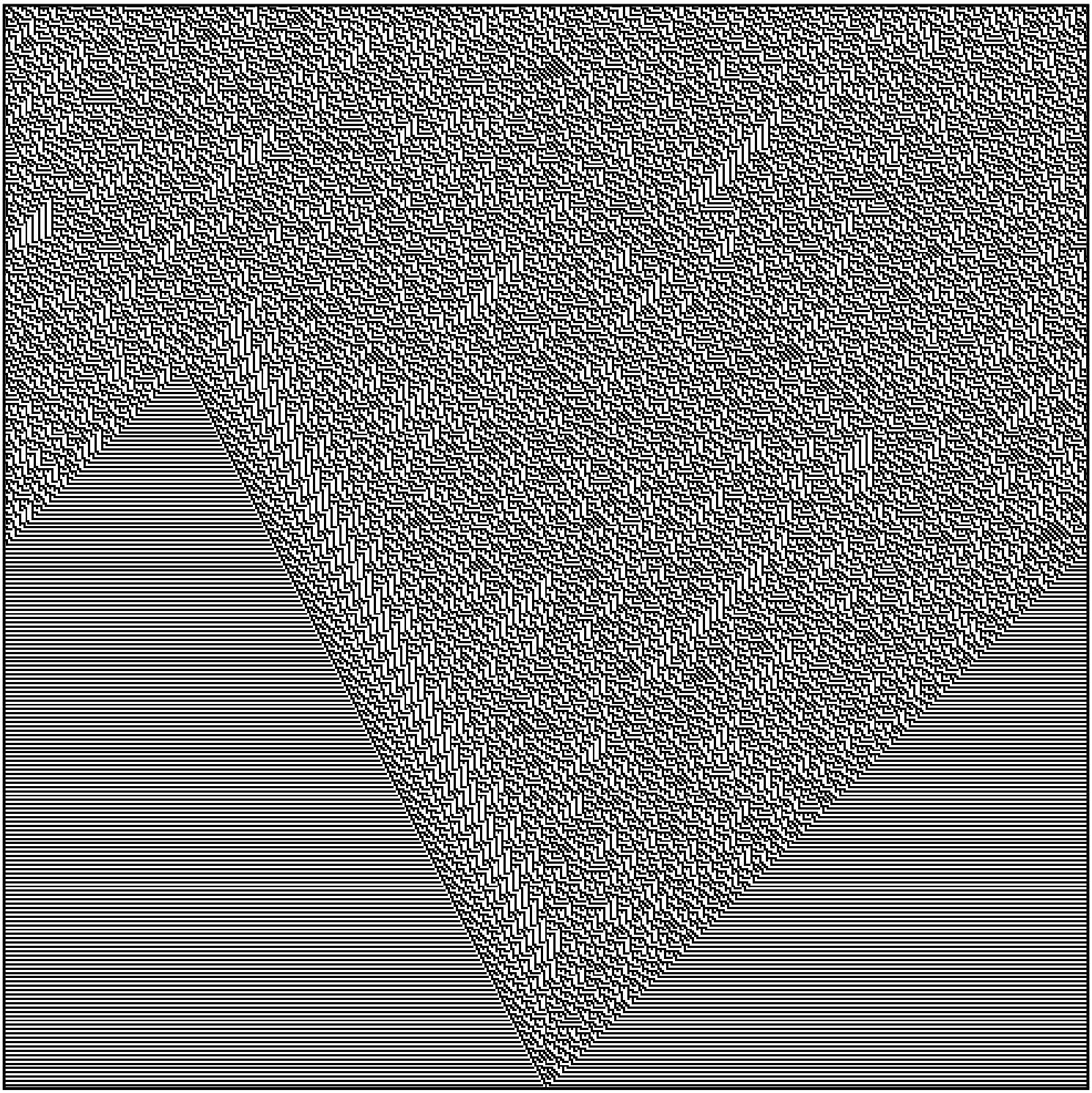

Figure 1.7: Rule 45

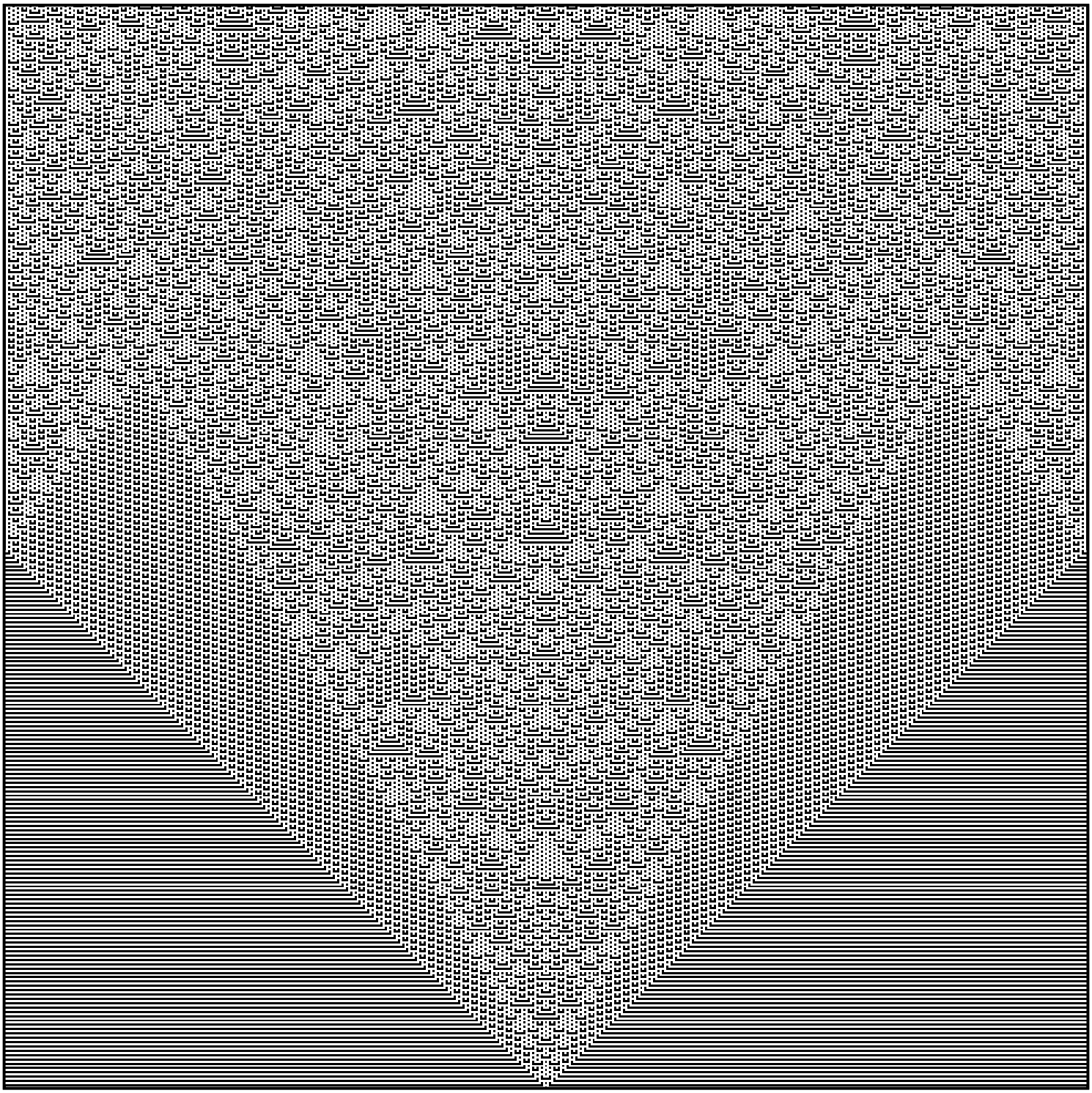

Figure 1.8: Rule 73

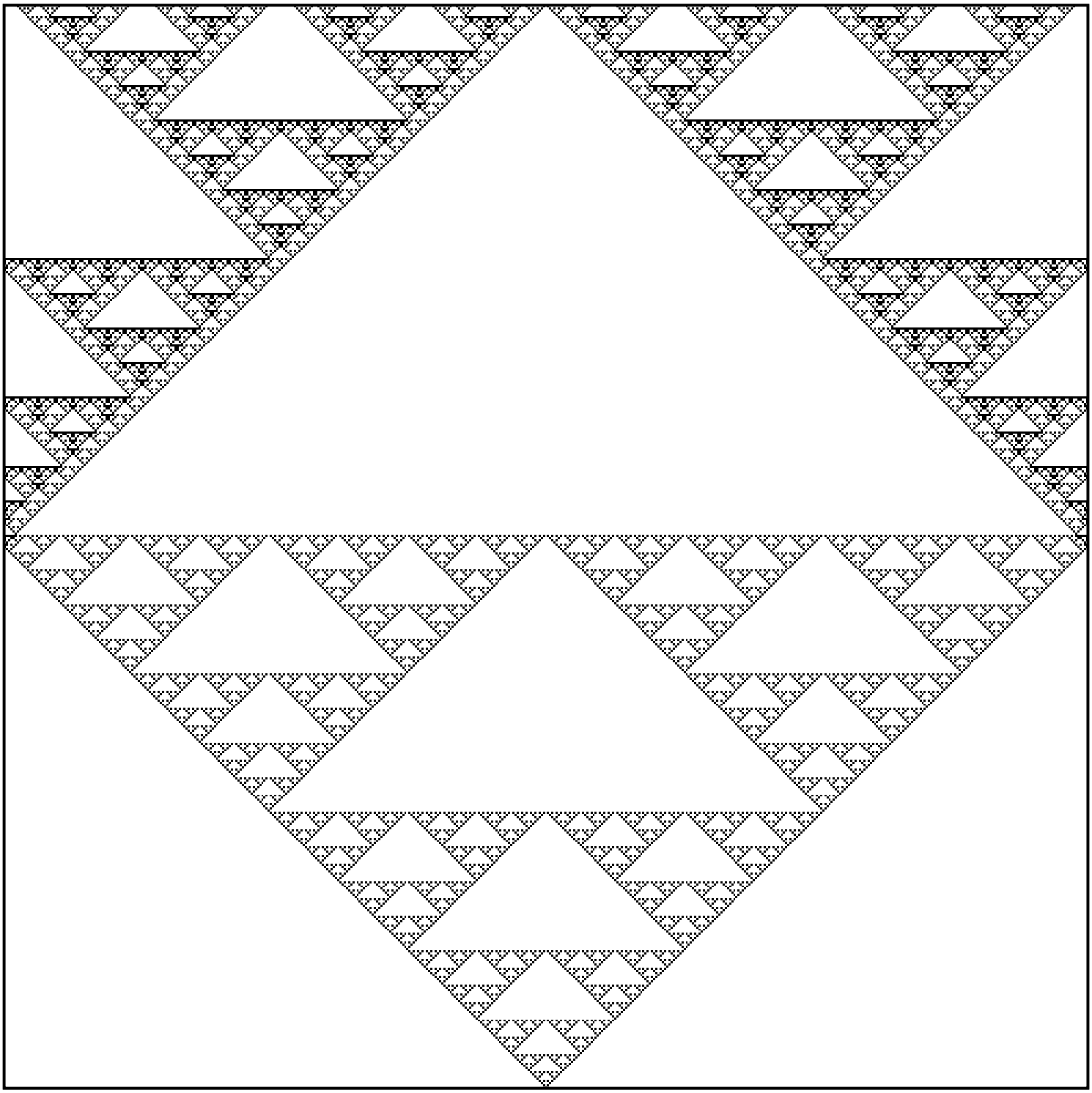

Figure 1.9: Sierpinski carpet - rule 90

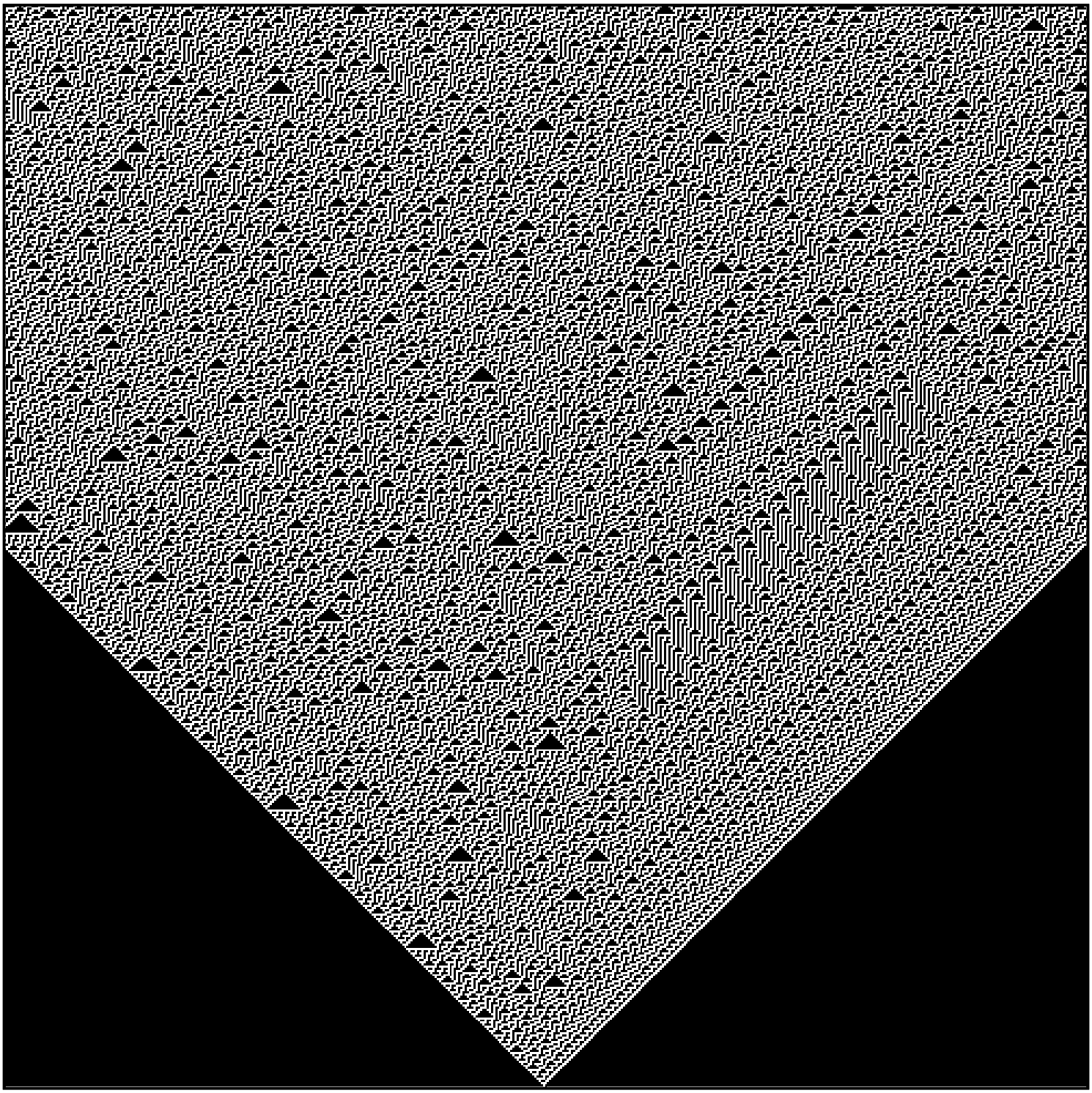

Figure 1.10: Rule 149

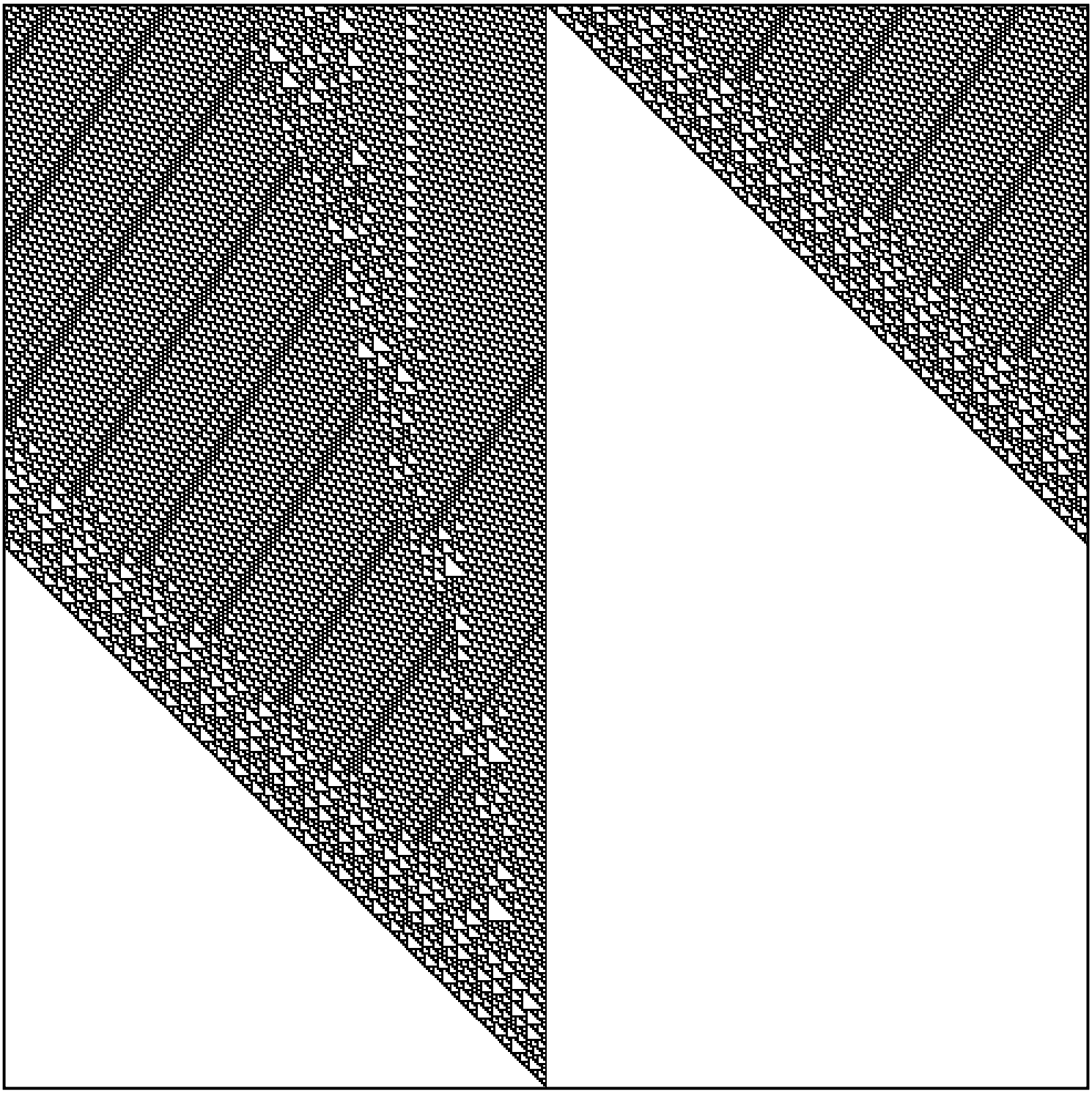

Figure 1.11: Rule 110

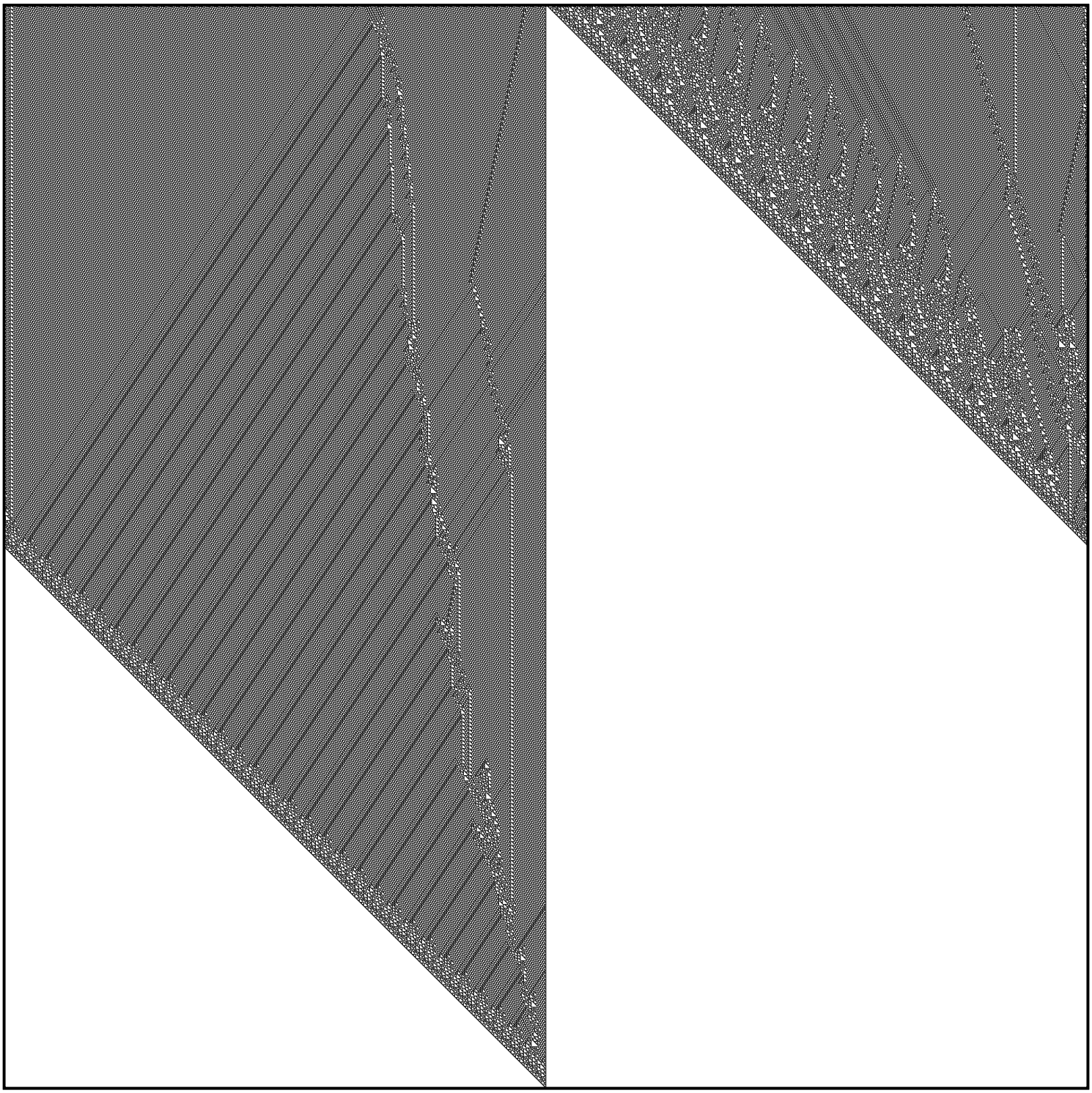

Figure 1.12: Rule 110 – 2000 × 2000

There is already a formal similarity between cellular automata we presented, and discrete partial differential equations. Consider the diffusion equation

$$\frac{\partial C}{\partial t} = \kappa \frac{\partial^2 C}{\partial x^2}.$$

By discretization forward in time, it is transformed to

$$C_i^{(t)} = f\big[\sum_{j=-1}^{j=1} \alpha_j \, C_{i+j}^{(t-1)}\big]$$

Formally, this equation corresponds to the rule of the one dimensional cellular automaton 1.1. However, C_i is not from discrete finite set, but it is a continuous value, the α_i are not integers, but reals, and this would cause instability of this cellular automaton, as discussed in [2] and the formal similarity leads to the dead end.

The connection of the cellular automata with the fluid mechanics is not straight-forward or formal, but it is grounded in the symmetries and conservation laws found in the hydrodynamic equations and the special class of cellular automata - the lattice gas cellular automata.

In these symmetries lies not only beauty of this method and their attractiveness for physicists, but their principal advantage over the better-established CFD methods.

2. Lattice gass cellular automata

The first lattice gass cellular automaton was proposed in 1973 by Hardy, Pomeau and de Pazis, who named it – the HPP model.

Unfortunately, it could not do its job sufficiently well. For the reasons that we will sketch in this chapter, its macroscopic limit does not converge to Navier-Stokes equations close enough.

In the subsequent chapters we will explore two different approaches how to make functional LGCA. They both build on the ideas behind this imperfect HPP.

Therefore, it is worthwhile to explain the basic principles of HPP first, and later on, we will upgrade it - either to FHP, Pair-interaction or their multi-dimensional variants.

2.1 From CA to LGCA

Lattice of HPP is the simple rectangular 2D grid. At every point of a grid, there is a node sitting in, and this node is composed of 4 cells, see Figure 2.1.

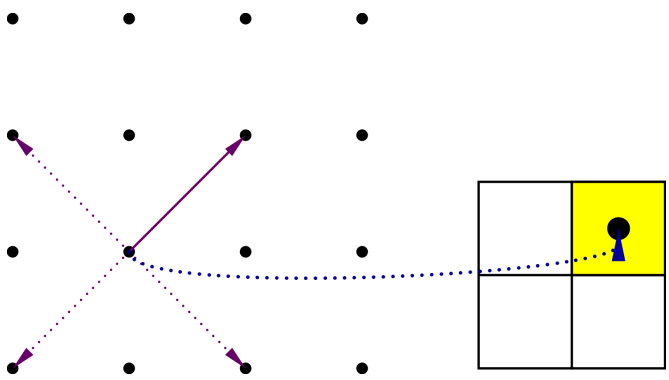

Figure 2.1: Rectangular grid

Each cell of the node can be in two states – empty (white square) or occupied by the particle (yellow square). The particle in this cell is heading to the diagonal node along the corresponding lattice vector.

2.2 Update rule

So far we have the grid full of particles. For all LGCA models, update is done in two subsequent steps – collision and propagation.

In the collision step, particles are swapped inside the node respecting two constraints - conservation of mass and conservation of momentum in the node.

In HPP, there are only two collision configurations, and one collision rule that guides them, see Figure 2.3.

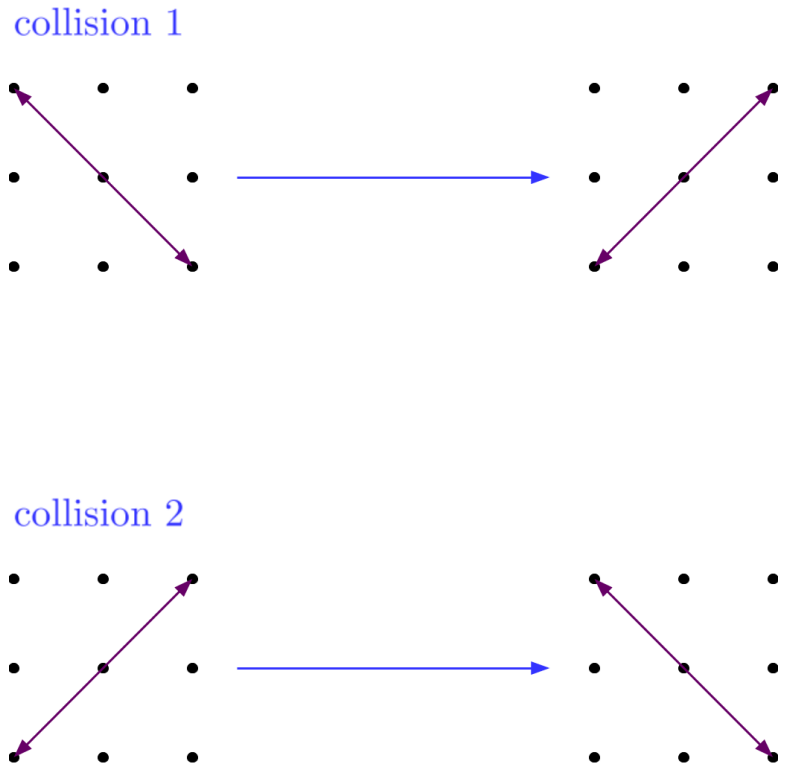

Figure 2.2: HPP colisions

These collision configurations are symmetric – the first configuration is resolved to the other and vice versa.

It is easy to understand that there are no other collision configurations and collision rules. If any other state gets changed, it would break the conservation of momentum and would be physically unrealistic.

2.3 Propagation:

After the collision is resolved, propagation follows – figure 2.3. During propagation, the particle moves from the nodes to nodes, along the lattice vectors that corresponds to the cells they occupied.

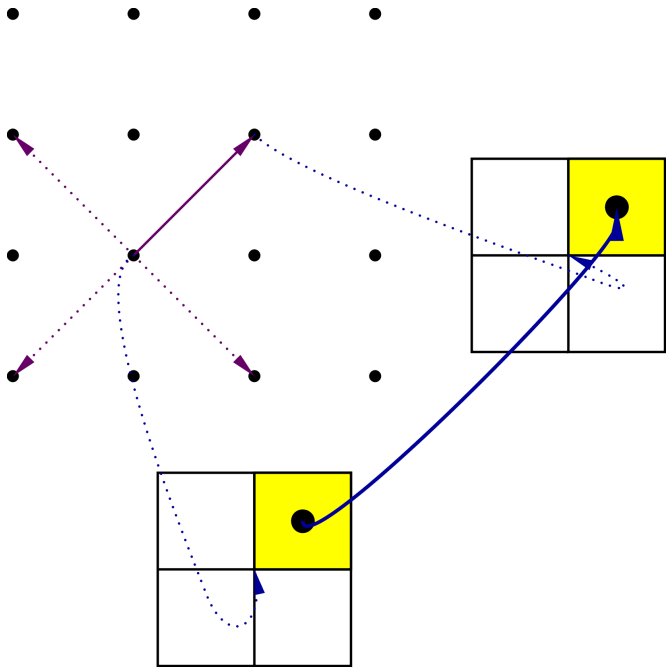

Figure 2.3: Propagation of particle from upper-left cell

2.4 Conservation laws

We already noted that collision and propagation conserve momentum, and they obviously conserve mass, since particles are neither created, nor anihilated during update. Let us inspect these conservation laws in the more depth by considering symmetries of this model.

Suppose we are using periodic boundary condition. Then, the finite rectangular grid of HPP is actually a torus. It is easy to imagine that if we shift the grid by the lattice vector, we get the very same torus. So this rectangular grid of HPP is symmetric with respect to translation. As we know by Norther's theorems, translational symmetry implies conservation of momentum.

Also, the grid possesses a rough rotational symmetry - rotating the grid by 90 degrees, we get the same grid.

However, this rotation by 90 degrees is too crude. In the following chapter, when we derive the hydrodynamic equations for this type of LGCA, we could see that four lattice vectors with rectangular symmetry leads to unrealistic equations, comparing to the better models.

Another implication of insufficient rotational symmetry are the non-physical quantities, that are conserved nevertheless – so called spurious invariant [1].

Consider orientation of particles in the figure 2.3 before the collision. One particle heads to north-east, the other south-west. After the collision, one particle

[1]The later LGCAs also posses the spurious invariants - so-called Zanetti's invariants, but they are under level of noise, due to higher rotational symmetry or additional degrees of freedom in the node

heads to north-west, other particle to south-east. So the number of particles heading to the south, east, north and west do not change by collision (and neither by propagation).

To assert it more rigorously, let us decompose the total momentum into the cardinal directions:

$$P = P_N + P_S + P_E + P_W. \tag{2.1}$$

This total momentum P is correctly conserved by HPP, but also quantities

$$P_{spur1} = P_N + P_E - P_S - P_W \tag{2.2}$$

and

$$P_{spur2} = P_N + P_W - P_S - P_E \tag{2.3}$$

are conserved, although these quantities have no physical counterparts.

To conclude this chapter and finish-off the HPP, it is physically implausible because

1. angular momentum is not conserved due to insufficient rotational symmetry,
2. other non-physical quantities, so called *spurious invariants* are conserved.

Although it is a flawed model, it sparked interest of the wider community and various successful LGCAs evolved from HPP. In the next chapter, we will introduce the first physically relevant branch of LGCAs – the FHP model.

3. FHP

Again, his improved lattice gas cellular automaton is named after its inventors – Frisch, Humpfrey and Pomeu. They proposed it in 1986 together with its three dimensional variant - the FCHC. Now that we presented the setting of FHP in two dimensions rather intuitively, let us explore the microdynamics of FHP in a more formal way. The formal treatment provides that the hydrodynamic equations that we derive are valid for FHP in arbitrary dimension (although finding an appropriate multidimensional lattice is non-trivial and possible only in 4 dimensions, as we will see). In following section, we will graphically explain the basic principles of FHP, the other sections will be more general and the obtained results will be valid for arbitrary dimensional FHP-like automaton (most importantly FCHC).

3.1 The lattice of FHP

The whole improvement of FHP is one simple change - instead of square grid, FHP builds on a hexagonal grid. All other properties are implied by the increased symmetry of the hexagonal grid.

On the figure 3.1, we have a part of the hexagonal grid, and from one of the nodes, six lattice vectors point to the neighboring nodes. Let us denote the set of the lattice vectors by $c_i,\ i = 1, 2, 3, 4, 5, 6$.

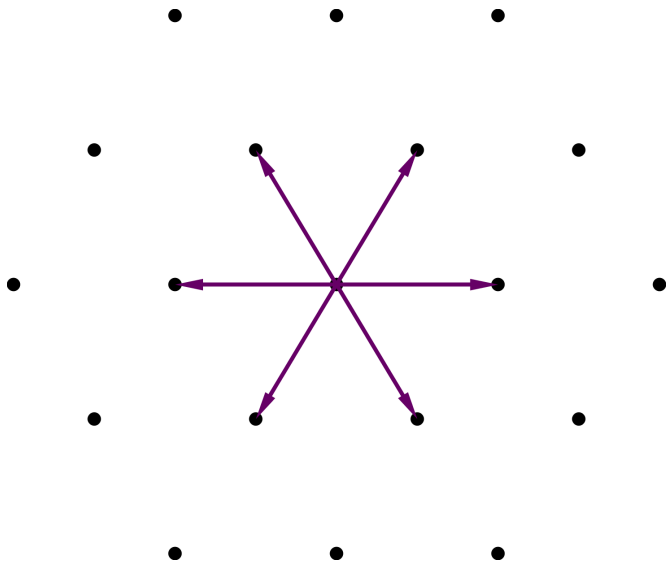

The node is nothing else then a set of the six cells and each of the cells corresponds to one of the lattice vectors. Let us denote the state of the node by $\boldsymbol{n} = (n_1, n_2, n_3, n_4, n_5, n_6)$, where $n_i = 0$ stands form empty i^{th} cell, and $n_i = 1$ implies that there is a particle in the i^{th} cell.

State of a node with the position $\mathbf{r}$ on lattice will be denoted by $\mathbf{n}(\mathbf{r})$, whereas the state of the *whole lattice* will be denoted by $\mathbf{n(.)}$.

3.2 Update rule

As we know, the update happens in discrete time steps ($t = 1, 2, 3...$) and consists of two subsequent steps - collision and propagation. Both of these steps are local, so they can be treated node by node.

3.2.1 Propagation

Propagation is the straight-forward phase and can be captured by the simple equation

$$Sn_i(\mathbf{r}) = \mathbf{n_i}(\mathbf{r} + \mathbf{c_i}).$$

If the cell is occupied by a particle – $n_i(\mathbf{r}) = \mathbf{1}$, it propagates along the corresponding lattice vector to the neighboring node, see the figure 3.1.

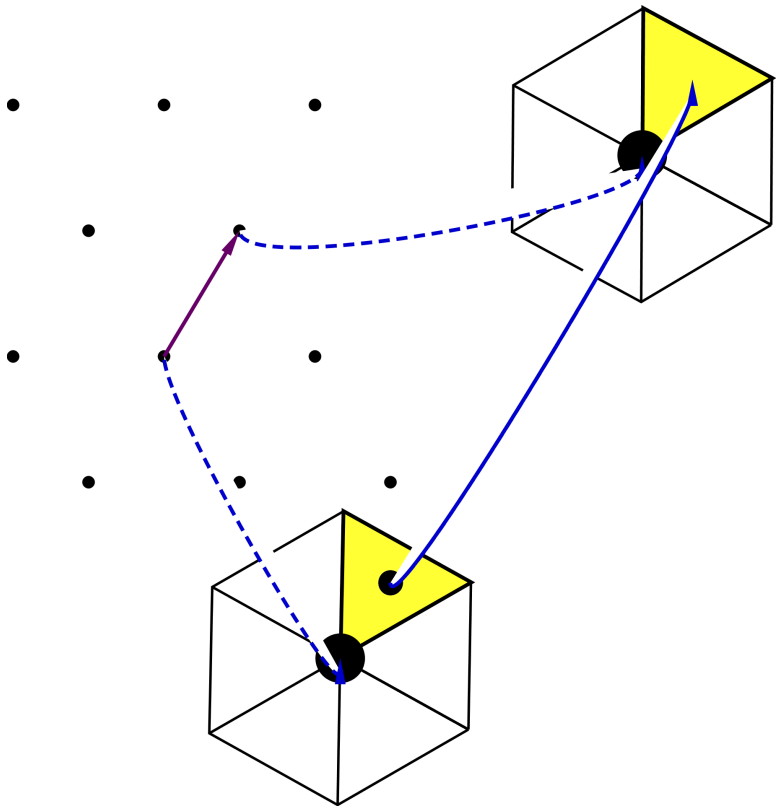

Figure 3.1: FHP collisions without rest particle.

The propagation, however, is preceded by the more interesting step – the collision.

3.2.2 Collision

The purpose of the collision is to swap as many particles in the node as possible. The only constraint on the collision rule is to preserve the number of particles (conservation of the mass) and to preserve the total momentum in the node.

These requirements lead only to a handful of collision configurations, see figure 3.2. For the simplicity, we are considering the FHP-I model, that does not included the "rest particles", otherwise we would have few more rules to add.

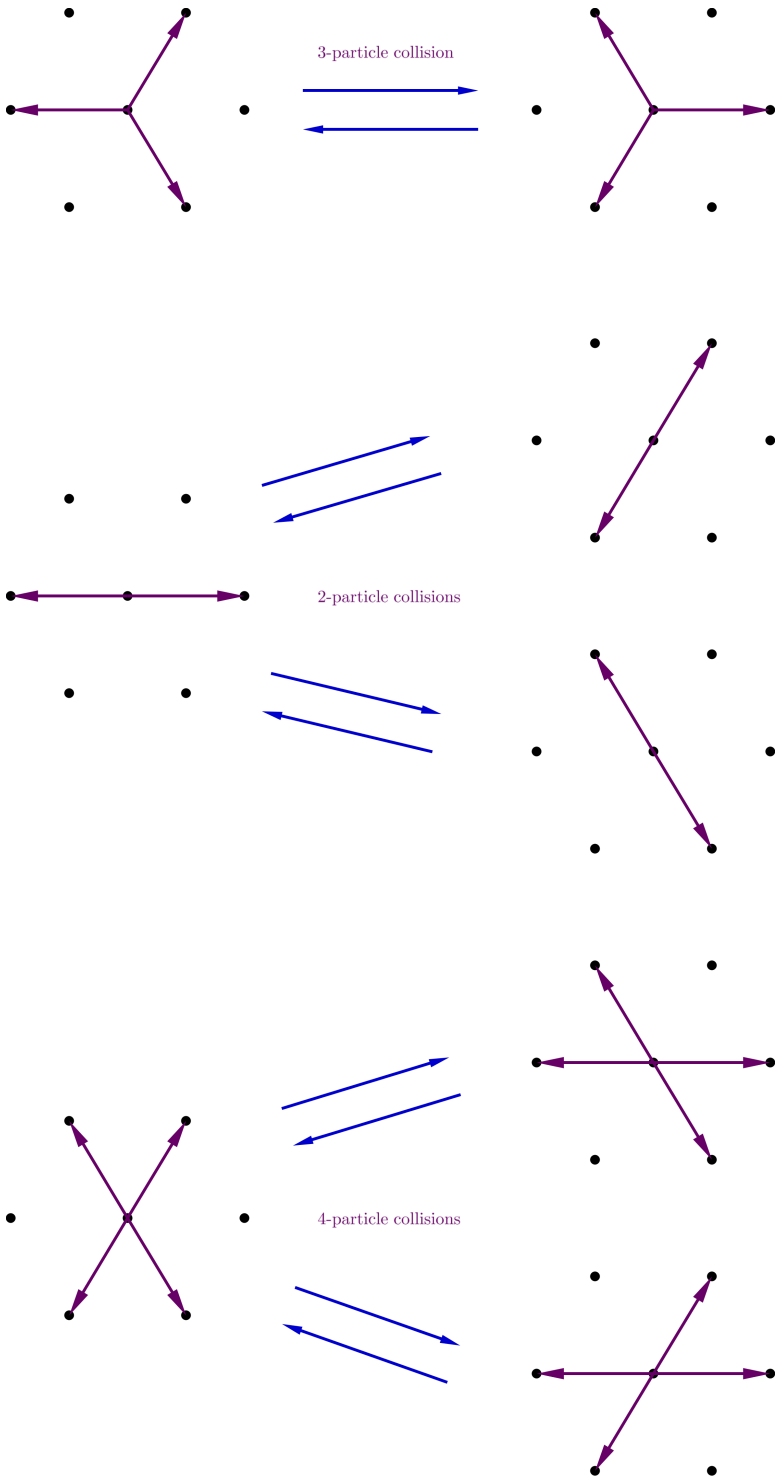

Figure 3.2: FHP collisions without rest particle.

We see that two and four particle configurations can be resolved in two different configurations. The resulting state need to be chosen randomly, with probability 1/2 for each state to preserve the parity symmetry of the model. If we were systematically choosing only one of them, we would introduce additional, non-physical invariant - chirality. Hence, we need to introduce non-determinism to the model.

We will express the probabilities of transition from state n to state n' by probability matrix:

$$A(n \to n') \geq 0$$

As we have 64 possible states of the node, matrix A is of dimension 64×64. For example, the cell of matrix A that governs the head-on collisions looks like this:

$$A' = \begin{bmatrix} 0 & \frac{1}{2} & \frac{1}{2} \\ \frac{1}{2} & 0 & \frac{1}{2} \\ \frac{1}{2} & \frac{1}{2} & 0 \end{bmatrix}$$

Since the collisions are symmetric, matrix A is symmetric as well.

Also, collisions are invariant to rotations and reflections of the node:

$$A(g(n) \to g(n')) = A(n \to n')$$

where $g \in G$, and G is the symmetry group of the node.

3.3 Collision operator

Interestingly, we can express the whole update step in one simple equation using collision operator Δ_i:

$$n_i(t+1, r+c_i) = n_i(t,r) + \Delta_i(t,r) \tag{3.1}$$

where Δ_i is

1. $\Delta_i = 0$ if no collision is happening in $n(t,r)$. Then state of the cell $n_i(t,r)$ only propagates to $n_i(t+1, r+c_i)$.
2. $\Delta_i = 1$ if there is not particle in $n_i(t,r)$ yet, but gets there after collision.
3. $\Delta_i = -1$ if there is particle in the $n_i(t,r)$, but after the collision, cell gets empty.

By this reasoning, we obtain the form of collision operator for FHP-I model

$$\begin{aligned} \Delta_i = {} & n_{i+1}n_{i+3}n_{i+5}(1-n_i)(1-n_{i+2})(1-n_{i+4}) \\ & -n_i n_{i+2} n_{i+4}(1-n_{i+1})(1-n_{i+3})(1-n_{i+5}) \\ & +\xi n_{i+1}n_{i+4}(1-n_i)(1-n_{i+2})(1-n_{i+3})(1-n_{i+5}) \\ & +(1-\xi)n_{i+2}n_{i+5}(1-n_i)(1-n_{i+1})(1-n_{i+3})(1-n_{i+4}) \\ & -n_i n_{i+3}(1-n_{i+1})(1-n_{i+2})(1-n_{i+4})(1-n_{i+5}). \end{aligned} \tag{3.2}$$

3.4 Microscopic conservation laws

We can easily prove that

$$\sum_i \Delta_i(t,r) = 0,$$
$$\sum_i c_i \Delta_i(t,r) = 0.$$

by substituting 3.2 into these equations. Combining with 3.1, these equations imply the conservation of mass and momentum

$$\begin{aligned} \sum_i n_i(t+1, r+c_i) &= \sum_i n_i(t,r), \\ \sum_i c_i n_i(t+1, r+c_i) &= \sum_i c_i n_i(t,r). \end{aligned} \tag{3.3}$$

By employing the aparatus of the statistical physics we will show that these microscopic conservation laws lead to physically realistic macroscopic description.

3.5 Conservation of probabilities

Let us define the phase space Γ as the set of all possible states of the lattice $n(.)$. Imagine we want to initialize cellular automaton with some macroscopic velocity $\boldsymbol{v_0}$, macroscopic pressure p_0, and macroscopic density ρ_0. We can realize this macrostate by very many microstates of lattice $n(.)$. We assign initial probability to each of these microstates:

$$P(0, s(.)) \geq 0.$$

Of course, probabilities over whole lattice are normalized so $\sum_s(.)P(0,s(.)) = 1$.

In the statistical mechanics, Liouville's space state theorem postulates that the density of the phase space is constant. Microdynamics of our model implies equivalent theorem for LGCA:

$$P(t+1, \mathcal{E}s(.)) = P(t, s(.))$$

It is obtained directly by applying the update formula

$$\mathcal{E}s(t,.) = s(t+1,.)$$

However, for indeterministic model such as FHP, the conservation of probability is governed by the more general formula

$$P(t+1, \mathcal{S}n'(.)) = \sum_{n(.)\in\Gamma} \prod_{n(.)} A(n(\boldsymbol{r} \to n'(\boldsymbol{r}))P(t, n(.)), \tag{3.4}$$

that constitutes the LGCA version of Chapman-Kolmogorov equation.

3.6 Mean occupation numbers

Motivated by the ensemble formalism of statistical physics, we define mean occupation numbers

$$N_i = \langle n_i \rangle = \sum_{s(.)\in\Gamma} n(s(.))P(t, s(.)).n$$

This formula naturally suggests definition of the mean mass density

$$\rho(t, r) = \sum_i N_i(t, r) \tag{3.5}$$

and the momentum density

$$j(t, r) = \sum_i c_i N_i \tag{3.6}$$

Due to conservation of probabilities, the conservation laws 3.3 implies conservation of the mean quantities

$$\sum_i N_i(t + 1, r + c_i) = \sum_i N_i(t, r) \tag{3.7}$$

$$\sum_i c_i N_i(t + 1, r + c_i) = \sum_i c_i N_i(t, r) \tag{3.8}$$

3.7 Equilibrium occupation numbers

After laborious definitions in previous sections, we are ready for one of the central theorems for FHP. It states that the equilibrium occupation numbers are given by Fermi-Dirac distribution. Its implications will haunt us until the last chapter.

We state it without the lengthy proof, but we recommend [2] or [5] for the non-believers.

Since the formalism that we were using in previous section is independent of the dimension of FHP, we can state this theorem for the FHP-like automaton in arbitrary dimension D with the lattice vectors $c_i \in R^D,\ i = 1...b$.

Theorem 1: The following statements are equivalent:

1. N_i^{eq}s are solutions of Chapman-Kolmogorov equation (reference)

2. N_i^{eq}s are solutions of set of b equations:

$$\Delta_i(N) = \sum_{nn'} (n'_i - n_i) A(n \to n') \prod_j N_j^{n_j} (1 - N_j)^{1-n_j} \tag{3.9}$$

3. N_i are given by Fermi-Dirac distribution where h is real number and $\mathbf{q}$ is D-dimensional vector.

To express N_i^{eq} explicitly as function of ρ and $\boldsymbol{u}$, we employ technique of Lagrange multipliers with natural constraints

$$\rho = \sum_i N_i = \sum_i \frac{1}{1 + exp(h + \boldsymbol{q}.\boldsymbol{c_i})} \tag{3.10}$$

$$\boldsymbol{u} = \sum_i \boldsymbol{c_i} \boldsymbol{N_i} = \sum_i \frac{\boldsymbol{c_i}}{1 + exp(h + \boldsymbol{q}.\boldsymbol{c_i})} \tag{3.11}$$

Explicit solutions are available only in few special cases. In general, we may use expansion for small Mach numbers ($\boldsymbol{u}/c_{\text{sound}}$). By expansion up to second order, equilibrium distribution for D-dimensional FHP-like automaton reads [1]

$$N_i^{eq}(\rho, \boldsymbol{u}) = \frac{\rho}{b} + \frac{D\rho}{c^2 b} \boldsymbol{c_i}.\boldsymbol{u} = \rho G(\rho) Q_{i\alpha\beta} u_\alpha u_\beta + O(u^3) \tag{3.12}$$

where

$$Q_{i\alpha\beta} = c_{i\alpha} c_{i\beta} - \frac{c^2}{D} \delta_{\alpha\beta} \tag{3.13}$$

and

$$G(\rho) = \frac{D^2}{2c^4 b} \frac{b - 2\rho}{b - \rho}. \tag{3.14}$$

3.8 Chapman-Enskog expansion

Because relaxation towards equilibrium values happens in a few updates of the automaton, it is standard procedure to expand the occupation numbers $N_i(t, r)$ around the equilibrium occupation numbers $N_i^{eq}(\rho, \boldsymbol{u})$:

$$N_i(t, r) = N_i^0(t, r) + \epsilon N_i^1(t, r) + \mathcal{O}(\epsilon^2) \tag{3.15}$$

The equations of mass and momentum conservation 3.7 and 3.8 can be equivalently stated in the form

$$\sum_i N_i(t + 1, r + c_i) - N_i(t, r) = 0, \tag{3.16}$$

$$\sum_i c_i (N_i(t + 1, r + c_i) - N_i(t, r)) = 0, \tag{3.17}$$

that is more suitable for our purpose.

Expansion of $N_i(t + 1, r + c_i)$ around $N_i(t, r)$ leads to

$$\begin{aligned} N_i(t + 1, r + c_i) = N_i(t, r) + \partial_t N_i(t, r) + c_{i\alpha} \partial_\alpha N_i(t, r) \\ + \frac{1}{2} \partial_t \partial_t N_i(t, r) + \frac{1}{2} c_{i\alpha} c_{i\beta} \partial_\alpha \partial_\beta N_i(t, r) + c_{i\alpha} \partial_t \partial_\alpha N_i(t, r) + \mathcal{O}(\partial^3). \end{aligned} \tag{3.18}$$

The expression above is the mixture of various physical phenomena – diffusion, advection, propagation of the sound waves or relaxation towards local equilibria. Each phenomena has its typical spatial and temporal scale, that corresponds to different powers of ϵ, see the tables below.

[1] The expansion is required up to the second order, because the non-linear term in Navier-Stokes equations will emerge from the quadratic term

TEMPORAL SCALES		
Scale	**Rescaling of time**	**Phenomena**
1 step	t	Relaxation towards local equilibrium
100 steps	$t_1 = \frac{1}{100}t = \epsilon t$	advection, sound waves (perturbation of mass and densi
10 000 steps	$t_2 = \frac{1}{10000}t = \epsilon^2 t$	diffusion

SPATIAL SCALES		
Scale	**Rescaling of length**	**Phenomena**
1 lattice unit	$\mathbf{r}$	Relaxation towards local equilibrium
100 lattice units	$\boldsymbol{r_1} = \frac{1}{100}\boldsymbol{r} = \epsilon\boldsymbol{r}$	diffusion, advection, sound waves

To derive the hydrodynamical equation that we long for, we will exploit the multi-scale technique. It starts by grouping-up the terms of hydrodynamical temporal and spatial scales.

Using to rescaled the length and time, we deduce the rescaled differential operators

$$\begin{aligned} \partial_t &= \epsilon\partial_t^{(1)} + \epsilon^2\partial_t^{(2)} \\ \partial_\alpha &= \epsilon\partial_\alpha^{(1)} \end{aligned} \tag{3.19}$$

Now, we are ready to expand the conservation laws 3.16 and 3.17 by Chapman-Enskog. We insert expansion 3.18 of $N_i(t+1, r+c_i)$, then we insert expansion of $N_i(t, r)$ according to 3.15. Finally, we substitute differential operators according to 3.19.

We do not present the whole monstrous expansion, only the terms of order ϵ, that we are interested in.

From conservation of mass 3.16 we get

$$\partial_t^{(1)} \sum_i N_i^{(0)} + \partial_\beta \sum_i c_{i\beta} N_i^{(0)} = 0, \tag{3.20}$$

and from conservation of momentum 3.17 we get

$$\partial_t^{(1)} \sum_i c_{i\alpha} N_i^{(0)} + \partial_\beta \sum_i c_{i\alpha} c_{i\beta} N_i^{(0)} = 0. \tag{3.21}$$

Using definition of mass density, and the following definition of the *momentum flux tensor*

$$P_{\alpha\beta}^{(0)} := \sum_i c_{i\alpha} c_{i\beta} N_i^{(0)} = \sum_i c_{i\alpha} c_{i\beta} N_i^{eq}(\rho, \boldsymbol{u}). \tag{3.22}$$

we can write the conservation laws in the shorter form

$$\begin{aligned} \partial_t^{(1)}\rho + \nabla^{(1)}(\rho\boldsymbol{u}) &= 0, \\ \partial_t^{(1)}(\rho u_\alpha) + \nabla^{(1)} P_{\alpha\beta}^{(0)} &= 0 \end{aligned} \tag{3.23}$$

In the first equation, we recognize the famous continuity equation, but we have some work to do with the second equation.

Substituting 3.12 for N_i^{eq} into momentum flux tensor, its components read (after some algebraic simplification)

$$\begin{aligned} P_{xx}^{(0)} &= \frac{\rho}{2} g(\rho)(u_x^2 - u_y^2) + \frac{\rho}{2}, \\ P_{yy}^{(0)} &= \frac{\rho}{2} g(\rho)(u_x^2 - u_y^2) + \frac{\rho}{2}, \\ P_{xy}^{(0)} &= P_{yx}^{(0)} = \rho g(\rho) u_x u_y, \end{aligned} \tag{3.24}$$

where we defined $g(\rho) = \frac{3-\rho}{6-\rho}$.

Unfortunately, it does not match the momentum flux tensor of Navier-Stokes equation

$$\begin{aligned} P_{xx} &= \rho\, u_x^2 + p \\ P_{yy} &= \rho\, u_y^2 + p \\ P_{xy} &= P_{yx} = \rho u_x u_y \end{aligned} \tag{3.25}$$

Let us examine why are these tensors different.

For low values of $\boldsymbol{u}^2$, pressure p is given by isothermal relation [**?**] $p = \frac{\rho}{2} = \rho c_s^2$, where $c_s = \frac{1}{\sqrt{2}}$ is the speed of sound.

What about $g(\rho)$?

The disease of FHP, FCHC and all lattice-gas cellular automata to follow is, that $g(\rho)$ is never equal to 1, as it is in Navier-Stokes equations.

The reason lies in the broken *Galilei invariance* of LGCA,as they all have discrete rotational symmetry (by 60° in FHP and between 60° and 45° in FCHC).

In the final chapter on theory of LGCA, we will show the fundamental treatment of this flaw. Symptomatic treatment, such as rescaling the time

$$t \to \frac{t}{g(\rho)}, \tag{3.26}$$

does not solve all the associated problems (D'Humier et al. 1987).

However, using this rescaled time, and setting density to be constant ($\rho = \rho_0$ except for the pressure term 3.28), we get the familiar incompressible Euler equation

$$\frac{\partial \boldsymbol{u}}{\partial t} + (\boldsymbol{u}\boldsymbol{\nabla})\boldsymbol{u} = -\boldsymbol{\nabla} P, \tag{3.27}$$

where we used

$$P = (\frac{\rho}{2\rho_0 g(\rho_0)} - \boldsymbol{u}^2). \tag{3.28}$$

.

This is as far as we can get in the first approximation. The derivation of the Navier-Stokes equations

$$\begin{aligned} \boldsymbol{\nabla}.\boldsymbol{u} &= 0, \\ \partial_t \boldsymbol{u} + (\boldsymbol{u}\boldsymbol{\nabla})\boldsymbol{u} &= -\boldsymbol{\nabla} P + \nu\, \nabla^2 \boldsymbol{u} \end{aligned} \tag{3.29}$$

would require terms of the order ϵ^2 from the Chapman-Enskog expansion to add in the equations 3.16 and 3.17, as done by Frisch [5].

4. FCHC

In two dimensions, we are lucky to find hexagon – a symmetric polygon that covers whole 2D plane and possesses sufficient rotational symmetry to make a good lattice for FHP.

In three dimensions, we have five symmetric candidates for LGCA but none of them works. They are so-called Plato solids. Out of them, dodecahedron or icosahedron might have sufficient rotational symmetry (interestingly, they have the same group of symmetries) but they do not cover whole 3D space uniformly. Only the cube does but LGCA build on a cubic grid would suffer from the same problem as HPP – insufficient rotational symmetry and insufficient degrees of freedom in the nodes.

Short analysis would show (see [1] for example) that, in 5 and more dimensions, we have only three symmetric solids – simplex, hypercube and its dual solid. None of them fits.

Fortunately, in four dimensions, we have three extra symmetric solids and one of them actually works.

4.1 Face-centered hypercube

Face-centered hypercube (we will use the shortcut FCHC) is the suitable solid for LGCA in four dimensions. It can be defined by its 24 vertices with the Cartesian coordinates

$$\begin{array}{cccc}
(\pm 1, & \pm 1, & 0, & 0), \\
(\pm 1, & 0, & \pm 1, & 0), \\
(\pm 1, & 0, & 0, & \pm 1), \\
(0, & \pm 1, & \pm 1, & 0), \\
(0, & \pm 1, & 0, & \pm 1), \\
(0, & 0, & \pm 1, & \pm 1).
\end{array}$$

These 24 vertices correspond to 24 lattice vectors in four dimensions but if we project them into three dimensions (by "deleting" the fourth coordinate q_4) we get only 18 lattice vectors

$$\begin{array}{ccc}
(\pm 1, & \pm 1, & 0), \\
(\pm 1, & 0, & \pm 1), \\
(\pm 1, & 0, & 0), \\
(\ 0, & \pm 1, & \pm 1), \\
(\ 0, & \pm 1, & 0), \\
(\ 0, & 0, & \pm 1).
\end{array}$$

For $q_4 = 0$ we have 12 lattice vectors (red lines on the figure 4.1), each vector corresponds to the single cell only. Hence, at most one particle propagates along each of these vectors.

For both $q_4 = -1$ and $q_4 = 1$ we get the same set of six lattice vectors (blue lines on the figure 4.1). Each vector corresponds to the two cells, hence two

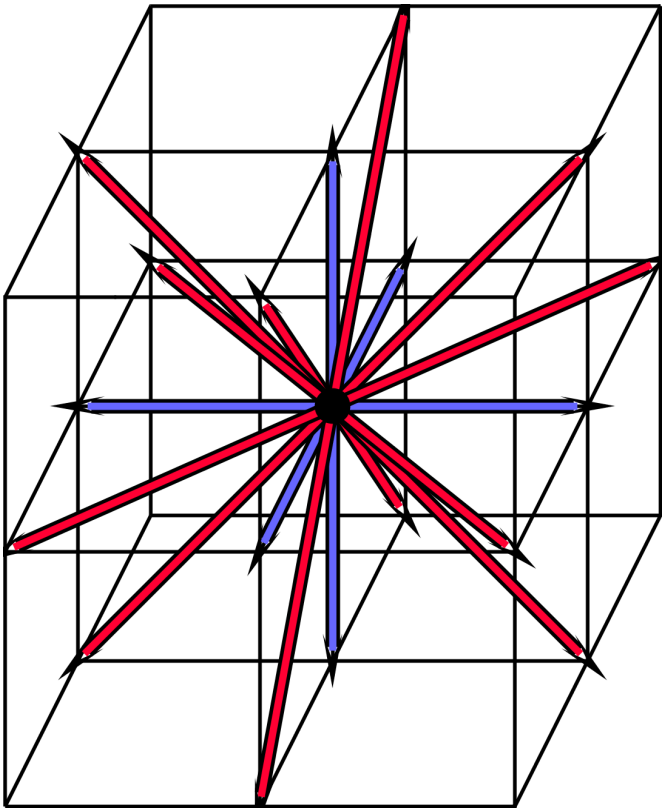

Figure 4.1: Projection of the lattice vectors into 3D. Red arrows are projections of vectors with $q_4 = 0$, blue arrows with $q_4 = \pm 1$.

particles can propagate along each vector.

It is efficient to denote each node of the lattice by 3 Cartesian integer coordinates.

In the resulting lattice, each node is connected to 18 neighbors by the lattice vectors of Fig. 4.1, and 24 particles can propagate along them in the single step.

4.2 Collision rules for FCHC

The FCHC lattice that we just described was proposed already by Frisch et. al. in 1986. However, they did not propose any recipe for a collision. It is easy to understand why it was not a simple task.

There are 24 cells in each node, hence the node can acquire $2^{24} = 16\ 777\ 216$ different states (that can be represented by 24 bits). It was easy to specify the collision rule for FHP in one simple table, but how do you specify rules for millions of states?

In the subsequent section we will show you how Henon answered to this challenge in his famous article [6].

4.2.1 Necessary conditions

Let us review what are the necessary conditions that collision rules must fulfill:

1. number of particles is preserved;

2. total momentum is preserved;

3. no other quantity is preserved;

4. exclusion principle – no two particles occupy one cell in the new state;

5. collision rules are invariant with respect to rotations and reflections of the node;

6. collisions satisfy the semi-detailed balance.

Henon proposed his own conditions on the collisions and showed that all conditions above are automatically fulfilled.

1. All collisions are isometries of FCHC – such transformations that preserve set of 24 lattice vectors above. It can be shown that this condition actually defines FHP collision set. For FCHC, this condition guarantees that conditions will be simple and leads us to the simple collision algorithm.

2. The choice of isometry is restricted by the momentum conservation only. There are 7009 possible values of momentum. But considering that collision rules are invariant under isometries of FCHC, and due to first restriction that collisions are isometries, we can consider 37 momenta only.

3. We want shear viscosity to be as low as possible, so that we can go to higher Reynolds numbers in our simulations. Suppressing the viscosity means is achieved by shortening the mean free path of the particles. In other words, we wish to change as many bits in the collision as possible. We will call such collisions "optimal isometries".

4. The isometry is randomly chosen among optimal isometries.

Having discussed the role of the isometries, let us define them properly.

4.3 Isometries of FCHC

By G we denote the group of isometries that preserve all 24 lattice vectors (or equivalently all vertexes of FCHC). Any isometry can be represented by 4×4 matrix

$$M = \begin{bmatrix} a_{11} & \dots & a_{14} \\ \dots & & \dots \\ a_{41} & \dots & a_{44} \end{bmatrix}. \tag{4.1}$$

Although the group G is of order 1152, it can be generated by five elements only, but it will be more comfortable to employ the generating set consisting of 12 elements to be described in the following section.

4.3.1 Generating set

Isometries $S_\alpha,\ \alpha = 1, 2, 3, 4$, are reflections over(?) plane $x_\alpha = 0$. For example, S_1 is represented by the matrix

$$S_1 = \begin{bmatrix} -1 & 0 & 0 & 0 \\ 0 & 1 & 0 & 0 \\ 0 & 0 & 1 & 0 \\ 0 & 0 & 0 & 1 \end{bmatrix} \tag{4.2}$$

that flips the sign of the first momentum coordinate q_1.

Another six isometries $P_{\alpha\beta}$ are reflections over plane $x_\alpha = x_\beta$. For example, P_{12} can be represented by matrix

$$P_{12} = \begin{bmatrix} 0 & 1 & 0 & 0 \\ 1 & 0 & 0 & 0 \\ 0 & 0 & 1 & 0 \\ 0 & 0 & 0 & 1 \end{bmatrix}. \tag{4.3}$$

that swaps the first and second coordinates of the momentum.

Another isometry Σ_1 is reflection over plane $x_1 + x_4 = x_2 + x_3$ represented by matrix

$$\Sigma_1 = \frac{1}{2} \begin{bmatrix} 1 & 1 & 1 & -1 \\ 1 & 1 & -1 & 1 \\ 1 & -1 & 1 & 1 \\ -1 & 1 & 1 & 1 \end{bmatrix}. \tag{4.4}$$

The last generating isometry Σ_2 is reflection over plane $x_1 = x_2 + x_3 + x_4$. In matrix representation it reads

$$\Sigma_2 = \frac{1}{2} \begin{bmatrix} 1 & 1 & 1 & 1 \\ 1 & 1 & -1 & -1 \\ 1 & -1 & 1 & -1 \\ 1 & -1 & -1 & 1 \end{bmatrix} \tag{4.5}$$

Any isometry of FCHC can be composed from these 12 isometries, so it can be uniquely expressed by

$$M = \begin{pmatrix} I \\ S_4 \end{pmatrix} \begin{pmatrix} I \\ S_3 \end{pmatrix} \begin{pmatrix} I \\ S_2 \end{pmatrix} \begin{pmatrix} I \\ S_1 \end{pmatrix} \begin{pmatrix} I \\ P_{34} \end{pmatrix} \begin{pmatrix} I \\ P_{23} \\ P_{24} \end{pmatrix} \begin{pmatrix} I \\ P_{12} \\ P_{13} \\ P_{14} \end{pmatrix} \begin{pmatrix} I \\ \Sigma_1 \\ \Sigma_2 \end{pmatrix} \tag{4.6}$$

where the brackets mean "one of the isometries inside the bracket".

4.3.2 Normalized momenta

Normalized momenta are such momenta that their components fulfill the following two conditions:

1. $q_1 \geq q_2 \geq q_3 \geq q_4 \geq 0$,

2. $q_0 = 0$ or $q_1 + g_4 = q_2 + q_3$.

Henon specified collision rules for normalized momenta only. There is 37 normalized momenta (out of 7009 total) so he significantly simplified the job.

If the state has normalized momentum (i.e. fulfilling 1), we just look into table and pick any isometry that is offered for that momentum. However, if the state doesn't have normalized momentum,

1. we normalize it by applying an appropriate isometry on the state. Let us denote this isometry by Γ. In fact, this isometry is equivalent to the change of the coordinate system.

2. Now that we have state with normalized momenta, search in the table and pick an optimal isometry.

3. We go back to the previous coordinate system by applying isometry Γ^{-1}.

4.3.3 Optimal isometries

However, in the step 2, we do not want to use all the isometries that conserve the momentum. Optimally, we would like to change as many bits as possible (that minimizes mean free path of particles, and that leads to desired low viscosity).

Although no further reduction then of 37 normalized momenta is possible, some of these momenta share same optimal isometries, that lead to minimal viscosity and preserve momentum.

Based on that, momenta can be divided into 12 classes, see the table below. First column specifies momentum, second column specifies isometries that we can apply to this momentum. Using this table is the effective way to resolve collisions in FCHC.

Normalized momenta	Optimal isometries
$q_1 = q_2 > q_3 > q_4 > 0$	P_{12}
$q_1 = q_2 = q_3 > q_4 > 0$	$P_{23}P_{12}$, $P_{23}P_{13}$
$q_1 > q_2 > q_3 > q_4 = 0$, $q_1 = q_2 + q_3$	$S_4\Sigma_1$, $S_4\Sigma_2$
$q_1 > q_2 > q_3 > q_4 = 0$, $q_1 \neq q_2 + q_3$	S_4
$q_1 = q_2 > q_3 > q_4 = 0$	S_4P_{12}
$q_1 > q_2 = q_3 > q_4 = 0$	$S_4\Sigma_1$, $S_4\Sigma_2$, $S_4P_{23}\Sigma_1, S_4P_{23}\Sigma_2$
$q_1 > q_2 = q_3 > q_4 = 0$, $q_q = 2q_2$	S_4P_{23}
$q_1 > q_2 = q_3 > q_4 = 0$, $q_1 \neq 2q_2$	$P_{23}P_{12}$, $P_{23}P_{13}$, $S_4P_{23}P_{12}$, $S_4P_{23}P_{12}$
$q_1 = q_2 = q_3 > q_4 = 0$	S_4S_3, S_3P_{34}, S_4P_{34}
$q_1 > q_2 = q_3 = q_4 = 0$	$S_3P_{34}P_{12}$, $S_4P_{34}P_{12}$, $S_4S_3\Sigma_1$, $S_4S_3P_{34}P_{12}\Sigma_1$, $S_4S_3\Sigma_2$, $P_{34}P_{12}\Sigma_2$
$q_1 > q_2 = q_3 = q_4 = 0$	$S_4S_2P_{23}$, $S_4S_3P_{23}$, $S_3S_2P_{24}$, $S_4S_3P_{24}$, $S_3S_2P_{34}$, $S_4S_2P_{34}$
$q_1 = q_2 = q_3 = q_4 = 0$	$S_3S_1P_{34}P_{12}$, $S_4S_1P_{34}P_{12}$, $S_3S_2P_{34}P_{12}$, $S_4S_2P_{34}P_{12}$, $S_2S_1P_{24}P_{13}$, $S_4S_1P_{13}P_{13}$, $S_3S_2P_{24}P_{13}$, $S_4S_3P_{24}P_{13}$, $S_2S_1P_{23}P_{14}$, $S_3S_1P_{23}P_{14}$, $S_4S_2P_{23}P_{14}$, $S_4S_3P_{23}P_{14}$

5. Pair Interaction LGCA

Pair-interaction automata (PI) constitute another branch that successfully evolved from HPP model, somewhat in contrast to FHP. To put it in a nutshell, FHP changed the rectangular grid for hexagonal, and thus obtained better rotational symmetry, increased the degree of freedom of the nodes and added new collision states.

The pair-interaction model preserves the HPP rectangular lattice, and the degrees of freedom in the node are incremented by the artificial definition of momentum. Momenta has no longer same direction as the lattice velocities, but they constitute another degree of freedom of the particle, that might change in the collision, independently of the lattice velocity. Although the differentiation in momentum and velocity might seem odd at the first glance, we will show that it leads to the physically correct microdynamics and offers us very efficient algorithm for implementation.

We will explore theory of Pair Interaction automaton in arbitrary dimension later on, but to get good understanding of the pair-interactions, we start with its 2D version, so we can explain the theory graphically.

5.1 User-friendly guide to Pair interactions

5.1.1 Pair-interactions automaton in two dimensions

Geometry of the lattice is same as for HPP model. It consists of nodes arranged in the rectangular grid:

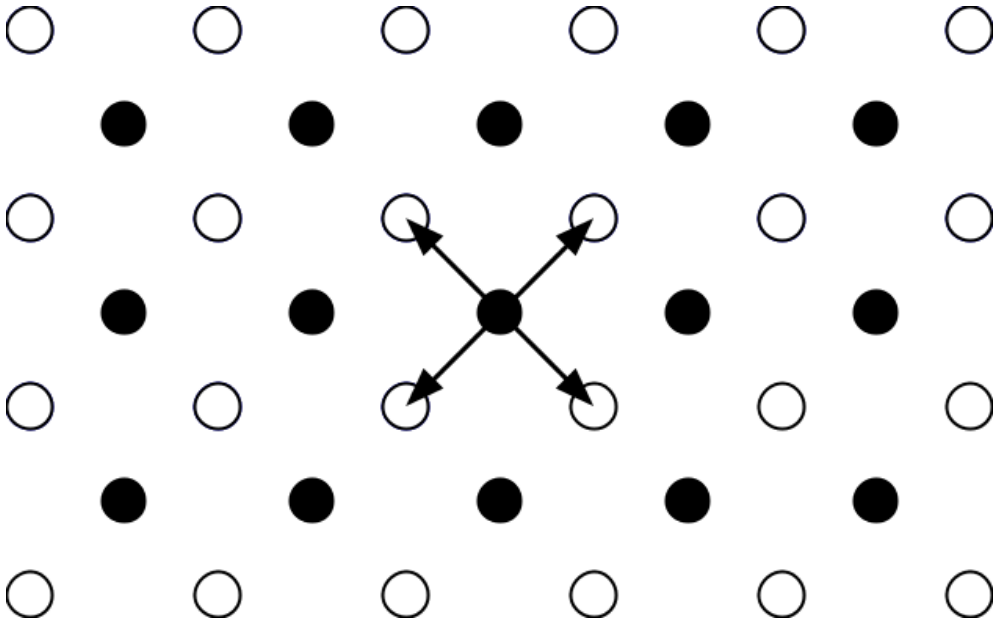

Figure 5.1: Lattice of 2D Pair Interaction automaton

Every node (the cirlce on the picture above) is connected to 4 diagonal neighbors. Let us consider that in the time-step t only the black nodes are occupied.

Then in the next step $t + 1$, only the white nodes are occupied. Without loss of generality we can assert that nodes with even Cartesian coordinates, e.g. [0,2], [2,4] are occupied at even time steps, and vice versa. This property of the grid offers very efficient implementation, as we need only one array for both even and odd time steps.

The node:
Let us look at the node in more detail:

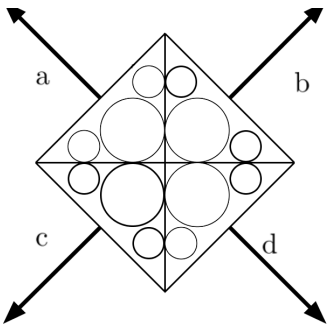

Figure 5.2: A node in detail

It consists of 4 cells (**a,b,c,d**) that are represented by 3 bits: one mass bit (a big circle) and two momentum bits (small circles).

The node on the picture above is empty (all bits are set to zero).

Here we have another example of a node:

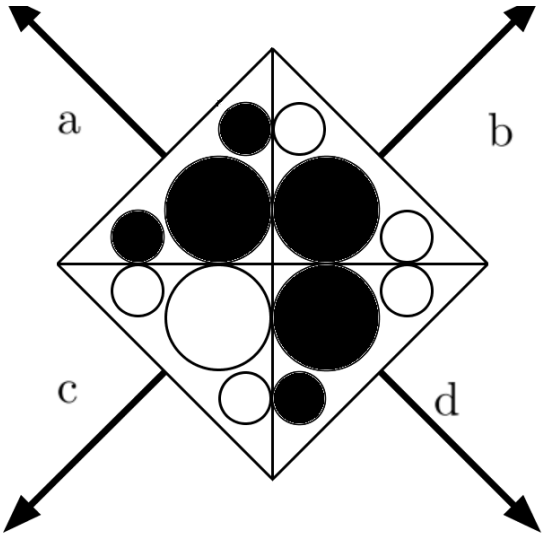

Figure 5.3: State of a node before collision

In this node, there are particles in the cells a,b,d (mass bit is set to 1 - the big circle is black).

Particle in the cell **a** is standing (both momentum bits are 0).

Particle in the cell **b** has momentum in direction [1,1] and particle in the cell **d** has momentum in direction [0,1].

5.1.2 Update rules

Following rules are true of every lattice-gas cellular automaton.

1. Lattice is changing in discrete time steps
2. Update rules are **local**. It means that state of the cell in the next step is determined by the current state of the cell itself and its four neighbors. Hence we can resolve update of the lattice node by node (suitable for parallel computing)
3. If this cellular automaton really simulates fluid dynamics and is physically realistic, update rule needs to conserve **mass, momentum and angular momentum**.

Update of the lattice is done in two steps, collision and propagation.

5.1.3 Collision

Collision changes configuration inside the single nodes. We require that momentum and mass is preserved in this step.

1) First, the cells are paired in X direction:

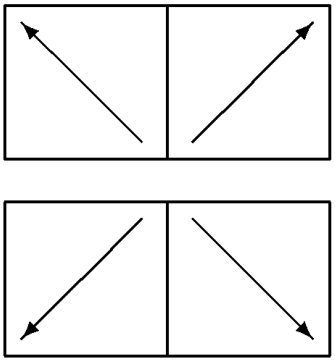

Figure 5.4: Pairs in X-direction

Then we swap the bits in the pairs so that total momentum in the pair is preserved. Therefore, node in 5.1.1 changes to

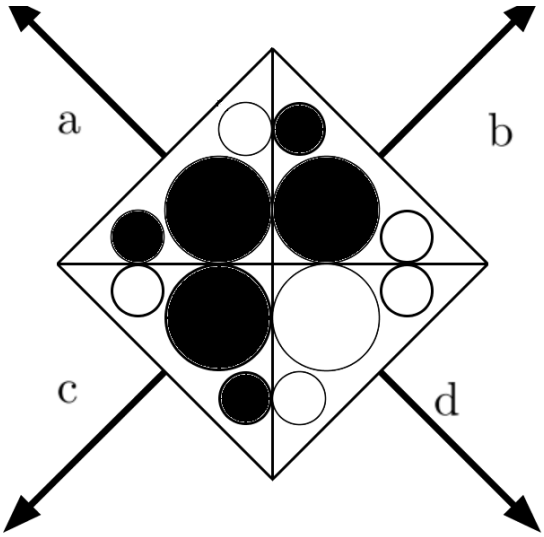

Figure 5.5: State of the node after pair-interaction in X direction

2) Then, the cells are paired in Y direction:

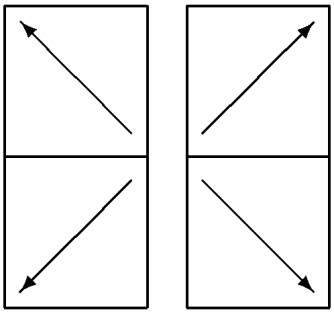

Figure 5.6: Pairs in Y-direction

Then we change the configuration in these pairs preserving mass and momentum in the node. Hence, the node in 5.1.3 changes into:

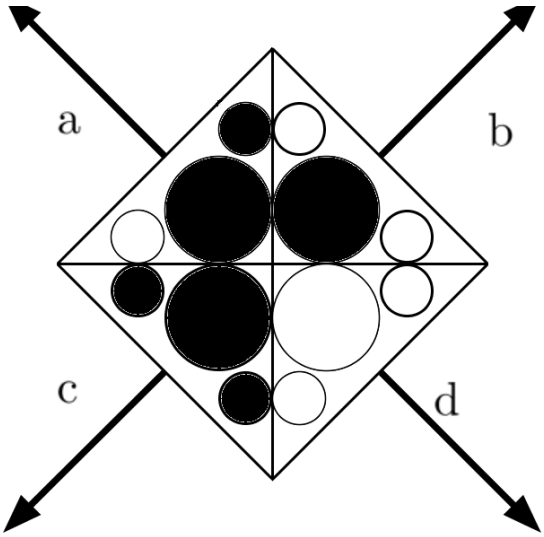

Figure 5.7: State of the node after pair-interaction in Y-direction

Actually, there is only 17 different configurations of the pairs. So instead of computing new configuration during every pair-interaction, we can just look in the table 13.2 below and change the configuration accordingly. We consider this to be the greatest practical advantage of PI comparing to other methods.

5.2 Propagation:

Particles propagates from a single node to the four neighboring nodes along the lattice vectors, see 5.1.1.

Particle from the cell **a** propagates to the node up-right, to the cell **a** as well.

Analogously, particle from cell **b** propagates to the node up-left, to the cell **b**.

Of course, particle carries all its bits (its momentum).

Generalization of this automaton to arbitrary dimension D is very straightforward. But we need to establish some mathematical formalism, as we haven't learned to draw D-dimensional pictures.

5.3 3D Pair-interaction cellular automaton

DIFFERENCES BETWEEN **2**D AND **N**D PAIR INTERACTION		
	2dim PI CA	**Ndim PI CA**
nodes	4 cells arranged into square	2^D cells arranged in hypercube
cells	1 mass bit, 2 momentum bits	1 mass bit, N momentum bits
neighbors	node has 4 neighbors	node has 2^D neighbors

In his famous paper, Nasilowski defined and used formalism that:

1. is more difficult then is necessary in our opinion (and in few cases he redefines it along the way)
2. therefore his arguments are more difficult then necessary

Instead, we will stick to the more modern formalism that we have been using. We consider it more brief and effective and reader should be already familiar with it.

In previous chapter, reader should get good understanding how 2D Pair-interaction works. believe that reader has already good idea how 2D Pair-interaction automaton works.

State of the node will be denoted by $\boldsymbol{n}(t, \boldsymbol{r})$, where $\boldsymbol{r}$ is its position on the lattice and t is the current time step. $\boldsymbol{n}(t, .)$ represents the whole lattice at time t, sometimes we can the time variable and use only $\boldsymbol{n}(.)$.

Each node consists of 2^D cells:

$$\boldsymbol{n} = (n_1, n_2, ..., n_{2^D}) \tag{5.1}$$

State of each node is given by $2^D(D+1)$ bits:

$$\boldsymbol{n} = \left\{ n_{i\alpha} \in \left\{0, 1\right\},\ i = 1..2^D,\ \alpha = 0, 1, ...D \right\} \tag{5.2}$$

where index i specifies cell of the node, and index α specifies the momentum bit of the cell. Actually, they are the Cartesian coordinates of the cell momenta.

Evolution of the lattice happens in discrete time steps - updates $\mathcal{U}$:

$$\mathcal{U}\boldsymbol{n}(t, .) = \boldsymbol{n}(t+1, .) \tag{5.3}$$

Update operator $\mathcal{U}$ can be further divided in two operations, collision $\mathcal{C}$ and propagation $\mathcal{P}$:

$$\mathcal{U} = \mathcal{P} \circ \mathcal{C} \tag{5.4}$$

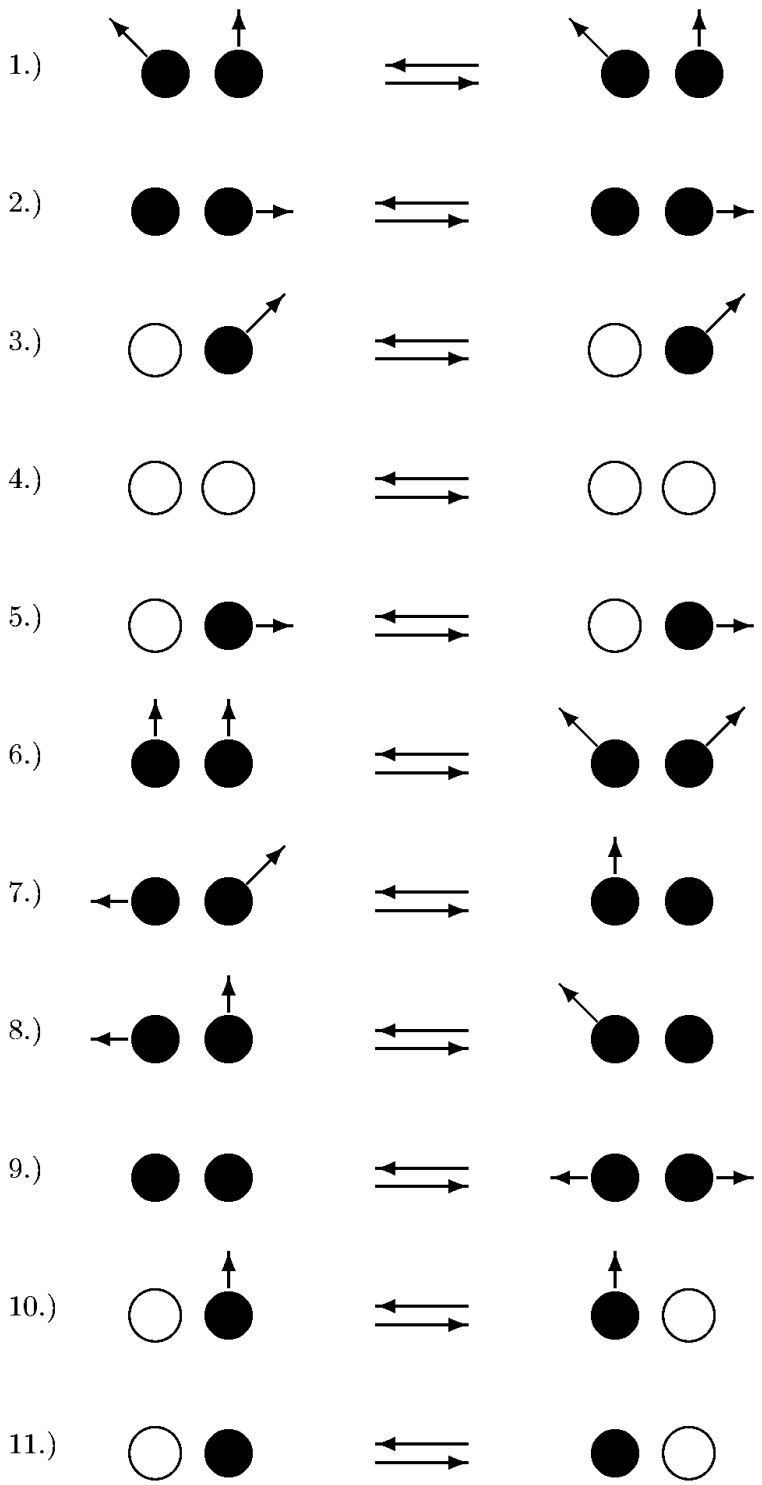

Figure 5.8: All admissible pair-interactions

5.4 Collision

The purpose of collision is to change the state of the node $\boldsymbol{n}$ into new state $\boldsymbol{n'}$ such that 2 conditions are fulfilled:

1. **Collision operator is one-to-one**:

   If $\mathcal{C} : \boldsymbol{n} \to \boldsymbol{n'}$, then $\mathcal{C} : \boldsymbol{n'} \to \boldsymbol{n}$.

   This reversibility condition allows us to apply Gibbs formalism later on.

2. **Collision preserves mass and momentum in the nodes**

   Mass and momentum are given by

$$m_0 = \sum_i n_{i0} \tag{5.5}$$

$$p_\alpha = \sum_i c_{i\alpha} n_{i\alpha}, \ \alpha = 1, 2, ...D \tag{5.6}$$

   Using these definitions, condition of mass and momentum conservation could be expressed by:

$$\begin{aligned} m_o = m'_o \quad &\Leftrightarrow \quad \sum_i n_{i0} = \sum_i n'_{i0}, \\ p_\alpha = p'_\alpha \quad &\Leftrightarrow \quad \sum_i c_{i\alpha} n_{i\alpha} = \sum_i c_{i\alpha} n'_{i\alpha}, \ \alpha = 1, 2, ...D \end{aligned} \tag{5.7}$$

   The easiest collision rule fulfilling these conditions would be identity

$$\mathcal{I} : \boldsymbol{n} \to \boldsymbol{n} \tag{5.8}$$

but this "non-collision" would lead to undesired, non-physical invariants. On the contrary, we want to change as many bits in the node as possible, or to say it physically, change directions to as many particles as conservation of momentum allows. Providing that, the mean free path of particles is reduced to minimum, and we can reach higher Reynold numbers in the simulations.

Such collision algorithm is surprisingly simple and was described in previous section graphically. Now we state collision rule more formally for arbitrary dimension D. The algorithm consists of D steps. In each step ($d = 1...D$), we create pairs of cells in d^{th} direction, or equivalently, we create pairs (n_i, n_j), such that $c_{id} = -c_{jd}$ and $c_{i\alpha} = c_{j\alpha}$ for $\alpha \neq d$. If $n_{id} = n_{jd}$ (it means that in direction d, momentum of the pair is zero), we swap the states of the cells n_i and n_j without changing the total momentum of the pairs. In the end of the collision, the total momentum of the node is conserved, because all the pair-interactions conserved the momentum.

5.5 Equilibrium statistics

We start by revoking the basic result of the microdynamics

$$\boldsymbol{n}(t+2,.) = \mathcal{U}^2\boldsymbol{n}(t,.) \tag{5.9}$$

In the odd and even time steps, the different parts of the hlattice are occupied, so it does not make sense to compare them. That is why we are comparing states of the lattice over the two time steps.

The microdynamical equation 5.9 implies conservation of probabilities

$$P(t,\boldsymbol{n}(.)) = P(t+2,\mathcal{U}^2\boldsymbol{n}(.)) \tag{5.10}$$

where $P(t,n(.))$ is the probability of occurrence of lattice in some state $n(.)$ from the statistical ensable of automata.

5.5.1 Gibbs distribution

Let's see if the Gibbs probability distribution fulfill the conservation law 5.10.

First we define the total momentum of the whole lattice $\mathcal{L}$:

$$m_\alpha(.) = \sum_{i,\boldsymbol{r}} c_{i\alpha} n_{i\alpha}(\boldsymbol{r}),\ \alpha = 0,1,..D \tag{5.11}$$

Now we can define Gibbs probability for our model:

$$P^E(n(.)) = \frac{W(n(.))}{Z} \tag{5.12}$$

where

$$W(n(.)) = exp(-\sum_{\alpha=0}^{D} \mu_\alpha m_\alpha(.)) \tag{5.13}$$

and Z is the partition function

$$Z = \sum_{n(.))} W(n(.)) \tag{5.14}$$

Conservation of local momenta 5.7 implies conservation of the total momentum

$$m_\alpha(.) = m'_\alpha(.),\ \alpha = 0,1,..D \tag{5.15}$$

that immediately implies conservation of Gibbs probability

$$P^E(t+2,\mathcal{E}^2 n(.)) = P^E(t,n(.)). \tag{5.16}$$

Additivity of the momentum cell by cell over the whole lattice (equation 5.11) implies that there is no statistical correlation between different cells:

$$P^E(n(.)) = \prod_{i,\boldsymbol{r}} P^E(n_i(\boldsymbol{r})) \tag{5.17}$$

Even further, if we consider, that

$$P(n_i(\boldsymbol{r})) = \frac{W(n_i(\boldsymbol{r}))}{Z} \tag{5.18}$$

where

$$W(n_i(\boldsymbol{r})) = exp(-\sum_{\alpha=0}^{D} \mu_\alpha c_{i\alpha} n_{i\alpha}(\boldsymbol{r})) = \prod_{\alpha=0}^{D} exp(-\mu_\alpha c_{i\alpha} n_{i\alpha}(\boldsymbol{r})) = \prod_{\alpha=0}^{D} W(n_{i\alpha}(\boldsymbol{r})) \tag{5.19}$$

we can see that bits of the cells $n_{i\alpha},\ \alpha = 1, 2, ...D$ are not statistically correlated.

For sure, they are correlated with n_{i0}, because $n_{i0} = 0 \Rightarrow n_{i\alpha} = 0\ for\ \forall\ \alpha = 1, 2, ...D$.

But for $\alpha = 1, 2, ...D$ we can write:

$$\sigma_{i\alpha} = prob(n_{i\alpha} = 1 | n_{i0} = 1) = \frac{W(n_{i\alpha})}{Z_{i\alpha}} \tag{5.20}$$

where

$$W(n_{i\alpha}) = exp(-\mu_\alpha c_{i\alpha} n_{i\alpha}) \tag{5.21}$$

and

$$Z_{i\alpha} = \sum_{n_{i\alpha}=0}^{1} W(n_{i\alpha}). \tag{5.22}$$

Hence

Little more laborious calculation would lead us to mean occupation numbers

$$\rho_i := < n_{i0} > = \frac{Z_i - 1}{Z_i} = \frac{e^{-\mu_0} \prod_{\alpha=1}^{D} (1 + e^{-\mu_\alpha c_{i\alpha}})}{1 + e^{-\mu_0} \prod_{\alpha=1}^{D} (1 + e^{-\mu_\alpha c_{i\alpha}})} = f\big(\mu_0 + \sum_{j=1}^{d} lnf(-\mu_j v_j)\big). \tag{5.23}$$

ρ_i can be interpreted as probability that cell n_i is occupied, but also as the equilibrium mass of the cell.

To define the density, we need to consider what is the volume of the node. Since lattice vectors $c_{i\alpha}$ span interval $[-1, 1]^D$, we can define volume V as

$$V = 2^D \tag{5.24}$$

Then the mass density reads

$$\rho = 2^{-D} \sum_i \rho_i \tag{5.25}$$

and the momentum density

$$q_a := 2^{-D} \sum_i c_{i\alpha} < n_{i\alpha} > = 2^{-D} \sum_i c_{i\alpha} \rho_i \sigma_{i\alpha}. \tag{5.26}$$

It is efficient to use only one quantity instead of mass and momentum density, and our formalism invites us to do so. We define the **hypermomentum** density

$$q_\alpha := 2^{-D} \sum_i c_{i\alpha} < n_{i\alpha} > \tag{5.27}$$

where q_0 is the mass density ρ, and $(q_1, q_2, ...q_D)$ is the momentum density.

Expanding formulas 5.23 and 5.20 in Taylor series and inserting to the last equation leads to rather lengthy calculation (Appendix B in [2]), that results in

$$\begin{aligned} \rho_i &= \rho + 2\frac{1-\rho}{2-\rho}\boldsymbol{v}.\boldsymbol{q} + 2\,\frac{(1-\rho)(1-2\rho}{(2-\rho)^2\rho}\left[(\boldsymbol{v}.\boldsymbol{q})^2 - q^2\right] + O(q^3), \\ \sigma_{ij} &= \frac{1}{2} + \frac{v_j q_j}{(2-\rho)\rho} + O(q^3) \end{aligned} \tag{5.28}$$

5.6 Hydrodynamic description

It is based on the assumption that the state of the cellular automaton is near its equilibrium. In that case, the whole state of the automaton can be specified by a few macroscopic order parameters q_α.

For example, expectation values $p_{i\alpha}$ are continuous differentiable functions of the parameter q

$$p_{i\alpha} = p_{i\alpha}(q, \nabla q, \nabla^2 q, ...) \tag{5.29}$$

and we can expand them in Chapman-Enskog series in terms of $p^{eq}_{i\alpha}$

$$p_{i\alpha} = p^{eq}_{i\alpha} + r_{i\alpha} + \mathcal{O}(\nabla^2) \tag{5.30}$$

with

$$r_{i\alpha} = \sum_{\beta j} R_{i\alpha\beta j} \nabla_j q_\beta. \tag{5.31}$$

We will use this expansion later on.

The resulting equations of this section will be the hydrodynamic equations for the pair-interaction automaton.

They are the set of evolution equations for the order parameters

$$\partial_t q_\alpha = \dot{q_\alpha}(q, \nabla q, \nabla^2 q, ...) \tag{5.32}$$

Due to conservation of the hypermomentum, the right hand side of 5.32 must be of the form

$$\dot{q_\alpha} = -\sum_k \nabla_k Q_{\alpha k}(q, \nabla q, \nabla^2 q). \tag{5.33}$$

Let us look back to the microdynamical propagation equation

$$n_{i\alpha}(t+1, \boldsymbol{r} + \boldsymbol{c_i}) = n'_{i\alpha}(t, \boldsymbol{r}), \tag{5.34}$$

that directly implies

$$p_{i\alpha}(t+1, \boldsymbol{r}+\boldsymbol{c_i}) = p'_{i\alpha}(t, \boldsymbol{r}). \tag{5.35}$$

If we expand $p_{i\alpha}(t+1, \boldsymbol{r}+\boldsymbol{c_i})$ in terms of $p_{i\alpha}(t, \boldsymbol{r})$, insert it to 5.35 and apply $2^{-D}\sum_i c_{i\alpha}$ on both sides, we get

$$2^{-D}\sum_i c_{i\alpha}\big[(\partial_t + c_{i\alpha}\nabla_\alpha) + \frac{1}{2}(\partial_t + c_{i\alpha}\nabla_\alpha)^2 + ...\big]p_{i\alpha} = 0 \tag{5.36}$$

The right-hand side disappeared because of the conservation of hypermomentum

$$2^{-D}\sum_i c_{i\alpha}p_{i\alpha} = 2^{-D}\sum_i c_{i\alpha}p'_{i\alpha}. \tag{5.37}$$

Analogously to FHP and FCHC model, we can define various temporal and spatial scales (see Table 3.8) and expand operator of time derivative and space derivative into modes

$$\begin{aligned} \partial_t &= \epsilon\partial_t^{(1)} + \epsilon^2\partial_t^{(2)} + ... \\ \partial_\alpha &= \epsilon\partial_\alpha^{(1)} \end{aligned} \tag{5.38}$$

Inserting 5.30 and 5.38 into 5.36 leads to

$$\begin{aligned} 0 = 2^{-D}\sum_i c_{i\alpha}(\epsilon\partial_t^{(1)} + c_i\nabla_i)p_{i\alpha}^{eq} \\ +2^{-D}\sum_i c_{i\alpha}\big[\epsilon^2\partial_t^{(2)}p_{i\alpha}^{eq} + \frac{1}{2}(\epsilon\partial_t^{(1)} + c_{i\alpha}\nabla_\alpha)^2 p_{i\alpha}^{eq} \\ +(\partial_t^{(1)} + c_{i\alpha}\nabla_\alpha)\sum_{j\beta} R_{\beta j\alpha i}\nabla_j q_\beta\big] + \mathcal{O}(\nabla^3) \end{aligned} \tag{5.39}$$

Each order of ϵ must vanish separately.
For the terms linear in ϵ we get

$$2^{-D}\sum_i c_{i\alpha}(\partial_t^{(1)} + c_{i\alpha}\nabla_\alpha)p_{i\alpha}^{eq} = 0 \tag{5.40}$$

or equivalently in terms of momentum density:

$$\partial_t^{(1)}q_\alpha + \sum_k \nabla_k Q^0_{\alpha k} = 0 \tag{5.41}$$

where we used definition of hypermomentum 5.27, and defined zeroth term of momentum flux tensor $Q^0_{\alpha k}$:

$$Q^0_{\alpha k} := 2^{-D}\sum_i c_{i\alpha}c_{ik}p_{i\alpha}^{eq} \tag{5.42}$$

We can split equation 5.6 into two - mass density conservation and momentum conservation:

$$\partial_t\rho + \boldsymbol{\nabla.g^0}(\rho, \boldsymbol{q}) = \mathcal{O}(\nabla^2) \tag{5.43}$$

$$\partial_t q_j + \sum_k \nabla_k Q^0_{jk}(\rho, \boldsymbol{q}) = \mathcal{O}(\nabla^2) \tag{5.44}$$

where we used $g_k := Q_{0k}$.

5.7 Hydrodynamic limiting cases

In this section, we will derive hydrodynamic limiting cases of our model, that corresponds to four physical approximations, namely

1. compressible Euler equation,
2. acoustic limit,
3. inviscid incompressible Euler equation,
4. incompressible Euler equation with viscosity.

Starting with equation 5.43, blabla dokonci
expand in $\epsilon \ll 1$, that is defined as the Knudsen number (ratio of mean free path and macroscopic scale).

1) Compressible Euler equation
For physical fluid, the equations read

$$\begin{aligned} \partial_t \rho + \boldsymbol{\nabla}.\boldsymbol{q} &= 0, \\ \partial_t q_j + \sum_k \nabla_k \big[p(\rho)\,\delta_{jk} + \frac{1}{\rho}\,q_j\,q_k = 0 \end{aligned} \tag{5.45}$$

For our model, we need to pick up terms of order

$$\partial_t = O(\epsilon^2),\ \boldsymbol{\nabla} = O(\epsilon^2),\ \rho = \frac{1}{2} + O(\epsilon), \boldsymbol{q} = O(\epsilon) \tag{5.46}$$

and we get

$$\begin{aligned} \partial_t \rho + \boldsymbol{\nabla}.\big[(\frac{10}{9} - \frac{8}{9}big)\boldsymbol{q}\big] &= 0, \\ \partial_t q_j + \sum_k \nabla_k \big[\frac{\rho}{2}\delta_{jk} + \frac{8}{9} q_j\,q_k\big] &= 0 \end{aligned} \tag{5.47}$$

As in case of FHP, the absence of Galilei invariance in our model caused the unphysical dependence of the pressure p on ρ.

2) Acoustic limit
Picking up the terms of order

$$\partial_t = O(\epsilon),\ \boldsymbol{\nabla} = O(\epsilon),\ \rho = \rho_0 + O(\epsilon),\ \boldsymbol{q} = O(\epsilon) \tag{5.48}$$

leads to linear equations of sound

$$\begin{aligned} \partial_t \rho + 2\frac{1-\rho_0}{2-\rho_0}\boldsymbol{\nabla}.\boldsymbol{q} &= 0, \\ \partial_t \boldsymbol{q} + \frac{1}{2}\nabla\rho &= 0\,. \end{aligned} \tag{5.49}$$

3) Inviscid incompressible Euler equations

For the ideal physical fluid (ideal fluid means inviscid and incompressible), the equations read

$$\begin{aligned} \boldsymbol{\nabla}.\boldsymbol{u} &= 0, \\ (\partial_t + \boldsymbol{u}.\boldsymbol{\nabla})\boldsymbol{u} + \nabla\Phi &= 0, \end{aligned} \tag{5.50}$$

with $\Phi = p/\rho_0 = 2p$ being the kinematic pressure.

For our model, taking terms of order

$$\partial_t = O(\epsilon^3), \qquad \boldsymbol{\nabla} = O(\epsilon^2), \qquad \rho = \frac{1}{2} + O(\epsilon^2), \qquad \boldsymbol{q} = O(\epsilon) \tag{5.51}$$

from the expansion (cislo) leads us to

$$\begin{aligned} \boldsymbol{\nabla}.\boldsymbol{q} &= 0, \\ (\partial_t + \frac{8}{9}\boldsymbol{q}.\boldsymbol{\nabla})\boldsymbol{q} + \frac{1}{2}\boldsymbol{\nabla}\rho &= 0. \end{aligned} \tag{5.52}$$

At last, our automaton got the hydrodynamic equations right, as we can easily transform then into 5.50 by setting

$$\Phi = \frac{4}{9}\rho, \qquad \boldsymbol{u} = \frac{8}{9}\boldsymbol{q}. \tag{5.53}$$

The $\boldsymbol{u}$ is the hydrodynamic velocity and

Notice that the hydrodynamic velocity $\boldsymbol{u}$ is the momentum convection velocity, and can not be interpreted as the mean velocity of particles

$$\boldsymbol{w} = \frac{\langle \sum_i v_i n_{i0} \rangle}{\langle \sum_i n_{i0} \rangle} = ... = \frac{2(1-\rho)}{(2-\rho)\rho}\boldsymbol{q}. \tag{5.54}$$

The reason behind this difference lies in the broken Galilean invariance of our model. The ratio between the velocities is called the "g-factor" ($g(\rho)$, and for our special case, it is equal to

$$\boldsymbol{w} = \frac{4}{3}\boldsymbol{q} = \frac{2}{3}\boldsymbol{u}. \tag{5.55}$$

It already arised in the FHP and FCHC model (where $g(\rho) \sim 1/2$ for small ρ).

The Navier-Stokes equations

For most applications, the inviscid incompressible approximation is too much idealized, and we would like to find an approximation of Navier-Stokes equations

$$\begin{aligned} \boldsymbol{\nabla}.\boldsymbol{u} &= 0, \\ (\partial_t + \boldsymbol{u}.\boldsymbol{\nabla}\boldsymbol{u} + \nabla\Phi &= \nu\nabla^2\boldsymbol{u} \end{aligned} \tag{5.56}$$

with the friction term on the right hand side, containing the shear viscosity ν.

For our model, the analogous set of equations is obtained by picking up terms

$$\partial_t = O(\epsilon^2), \qquad \nabla = O(\epsilon), \qquad , \rho = \frac{1}{2} + O(\epsilon), \qquad \boldsymbol{q} = O(\epsilon). \tag{5.57}$$

that leads to

$$\begin{aligned} \boldsymbol{\nabla}.\boldsymbol{q} &= 0, \\ (\partial_t + \frac{8}{9}\boldsymbol{q}.\boldsymbol{\nabla})q_j + \frac{1}{2}\nabla_j\rho &= \sum_{klm} T_{jklm}\nabla_l\nabla_m q_k. \end{aligned} \tag{5.58}$$

Is this set of equations equivalent to Navier-Stokes 5.56? If we could show that T_{jklm} is isotropic, the equations would be equivalent by the transformation 5.53. However, this is not the case, our model do not posses symmetries that forces T_{jklm} to be isotropic. We need to go to the second approximation to get more information of the tensor T_{jklm}.

Lengthy calculation that can be found in [7] leads to

$$\begin{aligned} T_{00km} &= \frac{1}{9}\delta_{kl}, \\ T_{jklm} &= \frac{1}{6}(3\delta_{jl}\delta_{km} + \delta_{jm}\delta_{lk}(1+\gamma_{mk}) - 2\delta_{jklm}). \end{aligned} \tag{5.59}$$

To see if it is isotropic or not, let us consider simple example of two-dimensional flow in $x_1 - direction$

$$q_1 = q_1(t, x_2), \qquad q_2 = 0. \tag{5.60}$$

Then, the Navier-Stokes equations 5.56 reduces to

$$\partial_t q_1 = \nu(\nabla_2)^2 q_1, \tag{5.61}$$

where $\nu = T_{1122}$ is the shear viscosity coefficient.

Let us rotate the flow by the angle α. We get

$$\partial_t q_1' = \nu'(\nabla_2')^2 q_1' \tag{5.62}$$

where the prime quantities are obtained by transformation

$$\begin{aligned} \boldsymbol{x} &= R\,\boldsymbol{x'}, \\ \boldsymbol{\nabla} &= R\boldsymbol{\nabla}, \\ \boldsymbol{q} &= R\boldsymbol{q'} \\ T'_{j'k'l'm'} &= \sum_{jklm} T_{jklm}R_{jj'}R_{kk'}R_{ll'}R_{mm'} \end{aligned} \tag{5.63}$$

with the orthogonal matrix

$$R = \begin{pmatrix} cos(\alpha) & sin(\alpha) \\ -sin(\alpha) & cos(\alpha) \end{pmatrix}. \tag{5.64}$$

The viscosity transformed into rotated coordinate system reads

$$\begin{aligned} \nu' = T'_{1122} = T_{1122}cos^4(\alpha) + T_{2211}sin^4(\alpha) \\ +(T_{1111} + T_{2222} - T_{1212} - T_{2121} - T_{1221} - T_{2112})cos^2(\alpha)sin^2(\alpha). \end{aligned} \tag{5.65}$$

The viscosity tensor in original coordinate system reads

$$\begin{aligned} T_{1122} = T_{2211} &= \frac{1}{2}, \\ T_{1111} = T_{2222} &= \frac{1}{3}, \\ T_{1212} = T_{2121} &= 0, \\ T_{1221} &= \frac{1}{6}, \\ T_{2112} &= \frac{1}{2}. \end{aligned} \tag{5.66}$$

Inserting these components into 5.65yields

$$\nu' = \frac{1}{2}(cos^4(\alpha) + sin^4(\alpha)), \tag{5.67}$$

which clearly shows that the shear viscosity is angle-dependent in contrast with the physical fluid and proves anisotropy of the viscosity tensor 5.59.

6. Hydrodynamic equations

Let us start by invoking hamiltonian for the N particle system

$$H = \frac{1}{2m}\sum_{i=1}^{N} p_i^2 + \sum_{i=1}^{N} V(r_i) + \sum_{i<j} U(r_i - r_j)$$

where V is the potential of the force $F = -\nabla V$, that effects all the particles equally, and U is the potential of the 2-particle interactions. We require that U is short-ranged, meaning $U(r) \approx 0$ for r of order much larger then is the atomic distance scale.

As usual in the framework of continuum mechanics, N is a ridiculously large number, something like $N \approx 10^{23}$.

Hence, we represent the state of the system by the probability density function $f(\boldsymbol{x}, \boldsymbol{u}, t)$. It specifies the probability that the system is found in the vicinity of point $(\boldsymbol{x}, \boldsymbol{u})$.

As usual, the probability is normalized:

$$\int f(\boldsymbol{x}, \boldsymbol{u}, t)\,\mathrm{d}\boldsymbol{x}\,\mathrm{d}\boldsymbol{u}$$

Since the microdynamics under consideration is deterministic, the probability density function is locally conserved and we may write its continuum equation

$$\frac{\partial f}{\partial t} + \frac{\partial}{\partial \boldsymbol{x}}(\dot{\boldsymbol{x}} f) + \frac{\partial}{\partial \boldsymbol{u}}(\dot{\boldsymbol{u}} f) = 0 \tag{6.1}$$

Notice that this equation can be written using the material derivative

$$\frac{D}{D\,t} = \frac{\partial}{\partial t} + \nabla$$

By inserting the Hamilton's equations

$$\frac{\partial \vec{p_i}}{\partial t} = -\frac{\partial H}{\partial \vec{r_i}},\ \frac{\partial \vec{r_i}}{\partial t} = \frac{\partial H}{\partial \vec{p_i}}$$

into the equation 6.1, we obtain the Liouville's equation

$$\frac{\partial f}{\partial t} + \frac{\partial f}{\partial \boldsymbol{x}}\frac{\partial H}{\partial \boldsymbol{u}} - \frac{\partial f}{\partial \boldsymbol{u}}\frac{\partial H}{\partial \boldsymbol{x}} = 0.$$

It is often written using the Poisson brackets

$$\frac{\partial f}{\partial t} = \{H,\, f\}. \tag{6.2}$$

6.1 The BBGKY hierarchy

So far, the transition to probability description did not simplified the problem much – we are still dealing with the function of $N \approx 10^{23}$ variables.

We need to limit our ambitions and we will focus on the one-particle distribution, defined by

$$f_1(\boldsymbol{x}, \boldsymbol{u}, t) = N \int \prod_{i=2}^{N} \mathrm{d}\, x_i \mathrm{d}\, u_i f(\boldsymbol{x}, \boldsymbol{u}, t). \tag{6.3}$$

The choice of index 1 was arbitrary, because all the particles are identical. This is also the reason why f_1 is normalized to N:

$$\int f_1(\boldsymbol{x}, \boldsymbol{u}, t) \mathrm{d}\boldsymbol{x} \mathrm{d}\boldsymbol{u} = N$$

For many purposes, the function f_1 captures all we need to know. The average density of particles in the real space is

$$n(\boldsymbol{x}, t) = \int f_1(\boldsymbol{x}, \boldsymbol{u}, t) \mathrm{d}\boldsymbol{u}, \tag{6.4}$$

the average velocity of the particle is

$$(\boldsymbol{x}, t) = \int \boldsymbol{u} f_1(\boldsymbol{x}, \boldsymbol{u}, t) \mathrm{d}\boldsymbol{u},$$

and the energy flux is

$$\varepsilon(\boldsymbol{x}, t) = \int \boldsymbol{u} E(\boldsymbol{u}) f_1(\boldsymbol{x}, \boldsymbol{u}, t) \mathrm{d}\boldsymbol{u}.$$

To derive the equation governing the evolution of f_1, let us see how it varies in time:

$$\frac{\partial f_1}{\partial t} = N \int \prod_{i=2}^{N} \mathrm{d}\, x_i \mathrm{d}\, u_i \frac{\partial f}{\partial t} = N \int \prod_{i=2}^{N} \mathrm{d}\, x_i \mathrm{d}\, u_i \{H,\, f\}.$$

After some non-trivial arrangements we put the equation to the form

$$\frac{\partial f_1}{\partial t} = \{H_1, f_1\} + \Big(\frac{\partial f_1}{\partial t}\Big)_{coll}, \tag{6.5}$$

where

$$H_1 = \frac{p^2}{2m} + V(\boldsymbol{x}).$$

and

$$\Big(\frac{\partial f_1}{\partial t}\Big)_{coll} = N(N-1) \int \mathrm{d}\boldsymbol{x_2} \mathrm{d}\boldsymbol{u_2} \frac{\partial U(\boldsymbol{x} - \boldsymbol{x_2})}{\partial \boldsymbol{x}} . \frac{\partial}{\partial \boldsymbol{u}} \int \prod_{i=3}^{N} \mathrm{d}\boldsymbol{x_i} \mathrm{d}\boldsymbol{u_i} f(\boldsymbol{x}, \boldsymbol{u}, t).$$

We see that the evolution of f_1 is governed by the Liouville's equation plus the extra term, the *collision integral*.

Not surprisingly, it is not determined by one-particle distribution, because that does not contain the relation of one particle to the other particles. Some of that information is carried by the *two-particle distribution*

$$f_2(\boldsymbol{x}, \boldsymbol{u}, t) := N(N-1) \int \prod_{i=3}^{N} f(\boldsymbol{x}, \boldsymbol{u}, t) \mathrm{d}\boldsymbol{x_i} \mathrm{d}\boldsymbol{u_i}.$$

Using the two-particle distribution, the collision integral can be written as

$$\Big(\frac{\partial f_1}{\partial t}\Big)_{coll} = \int \mathrm{d}\boldsymbol{x_2} \mathrm{d}\boldsymbol{u_2} \frac{\partial U(\boldsymbol{x} - \boldsymbol{x_2})}{\partial \boldsymbol{x}} . \frac{\partial f_2}{\partial \boldsymbol{u}}.$$

We can see that to follow the evolution of one-particle distribution f_1, we also need to know something about the two-particle distribution. And again, to know the evolution of the two-particle distribution, we repeat the same procedure as before and find the Liouville-like equation for f_2 with additional term containing the three-particle distribution.

In general, the evolution of *n-particle distribution* is described by

$$\frac{\partial f_n}{\partial t} = \big\{H_n, f_n\big\} + \sum_{i=1}^{n} \int \mathrm{d}\boldsymbol{u_{n+1}} \mathrm{d}\boldsymbol{x_{n+1}} \frac{\partial U(\boldsymbol{x_i} - \boldsymbol{x_{n+1}}}{\partial \boldsymbol{x_i}} . \frac{\partial f_{n+1}}{\partial \boldsymbol{u_i}}, \tag{6.6}$$

where the Hamiltonian

$$H_n = \sum_{i=1}^{n} \Big(\frac{\boldsymbol{u_i}}{2m} + V(\boldsymbol{u_i})\Big) + \sum_{i<j\leq n} U(\boldsymbol{x_i} - \boldsymbol{x_j})$$

includes external forces V and interactions between the n particles.

The set of equations 6.6 is called the *BBGKY hierarchy*. Instead of the Liouville's equation governing the function of $N \approx 10^{23}$ variables, we have now the set of 10^{23} functions.

But it is truly more advantageous to work with the hierarchy of equations 6.6, as it is ready to be approximated. Depending on the particular problem at hands, we decide which terms are important and which terms can be ignored, thus truncating the problem to something manageable.

The most simple and useful of these truncations is the Boltzmann equation

$$\frac{\partial f_1}{\partial t} = \big\{H_1, f_1\big\} + \Big(\frac{\partial f_1}{\partial t}\Big)_{coll},$$

OPRAVIT that we already saw. The collision integral depends on the f_2. We would like to get rid of this dependence. , the closed equation for the f_1 alone.

We already saw its general form but the collision integral was dependent on f_2.

To proceed, let us define the two time scales: the time between particle collisions τ, and the time of collision itself, τ_{coll}. In a dilute gas, we have

$$\tau >> \tau_{coll},$$

so most of the time, f_1 follows the Hamiltonian evolution, with occasional, but abrupt perturbations by the collision.

What is the rate at which the collision happens?

Let the two particle with velocities $\boldsymbol{u_1}$ and $\boldsymbol{u_2}$ collide at the point $\boldsymbol{r}$, and during the collision, they gain velocities $\boldsymbol{u_1'}$ and $\boldsymbol{u_2'}$. Let us define the rate of the collision by

$$Rate = \omega(\boldsymbol{u_1}, \boldsymbol{u_2}|\boldsymbol{u_1'}, \boldsymbol{u_2'}) f_2(\boldsymbol{r}, \boldsymbol{r}, \boldsymbol{u_1}, \boldsymbol{u_2},$$

where ω carries information of the about the dynamics of the collision, and can be computed from the inter-atomic potential U.

Next, we focus on the particle with the momentum p_1. In the collision, particle with p_1 gains a different momentum p_1', or a particle with some momentum p_1' gains the momentum p_1. Hence ,the collision integral contains two terms:

$$\Big(\frac{\partial f_1}{\partial t}\Big)_{coll} = \int \big[\omega(\boldsymbol{u_1'}, \boldsymbol{u_2'}|\boldsymbol{u_1}, \boldsymbol{u_2}) f_2(\boldsymbol{r}, \boldsymbol{r}, \boldsymbol{u_1'}, \boldsymbol{u_2'}) - \omega(\boldsymbol{u_1}, \boldsymbol{u_2}|\boldsymbol{u_1'}, \boldsymbol{u_2'}) f_2(\boldsymbol{r}, \boldsymbol{r}, \boldsymbol{u_1}, \boldsymbol{u_2})\big] \mathrm{d}\boldsymbol{u_2} \mathrm{d}$$

Considering the symmetries of the process (invariance under time reversal and parity), we have

$$\omega(\boldsymbol{u_1'}, \boldsymbol{u_2'}|\boldsymbol{u_1}, \boldsymbol{u_2}) = \omega(\boldsymbol{u_1}, \boldsymbol{u_2}|\boldsymbol{u_1'}, \boldsymbol{u_2'}) \tag{6.7}$$

. Finally, in order to express the collision integral in terms of f_1 instead of f_2, we make a non-trivial assumption, that velocities of colliding particles are uncorrelated:

$$f_2(\boldsymbol{r}, \boldsymbol{r}, \boldsymbol{u_1}, \boldsymbol{u_2}) = f_1(\boldsymbol{r}, \boldsymbol{u_1})\, f_1(\boldsymbol{r}, \boldsymbol{u_2}). \tag{6.8}$$

This assumption is known as a *molecular chaos hypothesis*, and seems quite reasonable. However, by supposing that particles are uncorrelated before the collision, but they become correlated by colliding, we introduce the arrow of time on the scene, that is far from being innocent.

Finally, using 6.7 and 6.8, we can write the collision integral in the form

$$\Big(\frac{\partial f_1}{\partial t}\Big)_{coll} = \int \omega(\boldsymbol{u_1'}, \boldsymbol{u_2'}|\boldsymbol{u_1}, \boldsymbol{u_2}) \big[f_1(\boldsymbol{r}, \boldsymbol{u_1'}) f_1(\boldsymbol{r}, \boldsymbol{u_2'}) - f_1(\boldsymbol{r}, \boldsymbol{u_1}) f_1(\boldsymbol{r}, \boldsymbol{u_2})\big] \mathrm{d}\boldsymbol{u_2} \mathrm{d}\boldsymbol{u_1'} \mathrm{d}\boldsymbol{u_2'} \tag{6.9}$$

and we can express the *Boltzmann equation*

$$\frac{\partial f_1}{\partial t} = \big\{H_1, f_1\big\} + \Big(\frac{\partial f_1}{\partial t}\Big)_{coll} \tag{6.10}$$

in the closed form.

6.2 Equilibrium and detailed balance

The *equilibrium distribution* is defined such that it does not explicitly depend on the time

$$\frac{\partial f_1^{eq}}{\partial t} = 0.$$

Using the Boltzmann equation, we can express this condition equivalently as

$$\{f_1, H_1\} + \Big(\frac{\partial f_1}{\partial t}\Big)_{coll} = 0.$$

If we restrict ourselves to the case where external force is not present,

$$V(\boldsymbol{r}) = 0,$$

any function of momentum commutes with Hamiltonian and the streaming term vanishes. According to 6.9, to make the collision integral vanish, we need to satisfy the *detailed balance* condition

$$f_1^{eq}(\boldsymbol{r}, \boldsymbol{u_1}) f_1^{eq}(\boldsymbol{r}, \boldsymbol{u_2}) = f_1^{eq}(\boldsymbol{r}, \boldsymbol{u_1'}) f_1^{eq}(\boldsymbol{r}, \boldsymbol{u_2'}), \tag{6.11}$$

or equivalently

$$\log(f_1^{eq}(\boldsymbol{r}, \boldsymbol{u_1})) + \log(f_1^{eq}(\boldsymbol{r}, \boldsymbol{u_2})) = \log(f_1^{eq}(\boldsymbol{r}, \boldsymbol{u_1'})) + \log(f_1^{eq}(\boldsymbol{r}, \boldsymbol{u_2'})).$$

The last equation tells us, that the sum of terms on the left is conserved in the collision.

As we know, such quantities are either momenta or energy, hence the terms in this equation are the linear combination of energy and momenta

$$log(f_1^{eq}(\boldsymbol{r}, \boldsymbol{u})) = \beta(\mu - E(\boldsymbol{u}) + \boldsymbol{v}.\boldsymbol{u}),$$

where

$$E(\boldsymbol{u}) = \frac{1}{2} m u^2$$

and β, μ and $\boldsymbol{v}$ are constants. Setting the constant μ such that normalization of f_1 is satisfied, we can write the solution

$$f_1^{eq} = \frac{N}{V} \Big(\frac{\beta}{2\pi m}\Big)^{3/2} e^{-\beta m (\boldsymbol{v}-\boldsymbol{u})^2/2}. \tag{6.12}$$

Supposing that β is the inverse temperature, this is the Maxwell-Boltzmann distribution.

If we forget about the streaming term $\{H_1, f_1\}$, then the detailed balance condition 6.11 leads to the much larger class of solutions, so called *local equilibrium distributions*

$$leq \tag{6.13}$$

where μ, β and $\boldsymbol{v}$ are promoted to the functions. Using these distributions, the collision integral vanishes, but the streaming term lives on.

6.3 Hydrodynamics

Just like the termodynamics describes systems in the equilibrium, hydrodynamics describes systems in the local equilibrium, with the parameters that vary slowly in space and time. These are quantities that do not relax to their equilibrium

values immediately, but change on the much slower scale. In this section we will show that these quantities are density $\rho(\boldsymbol{r}, t)$, temperature $T(\boldsymbol{r}, t)$ and velocity $\boldsymbol{u}(\boldsymbol{r}, t)$.

Let us have a function $A(\boldsymbol{r}, \boldsymbol{u})$. To see how does the function A vary in space, let us integrate over the momentum

$$\langle A(\boldsymbol{r}, t)\rangle = \frac{\int A(\boldsymbol{r}, \boldsymbol{u}) f_1(\boldsymbol{r}, \boldsymbol{u}, t)\mathrm{d}\boldsymbol{u}}{\int f_1(\boldsymbol{r}, \boldsymbol{u}, t)\mathrm{d}\boldsymbol{u}}.$$

We are already familiar with the denominator – it is the particle density function, so we can write

$$\langle A(\boldsymbol{r}, t)\rangle = \frac{1}{n(\boldsymbol{r}, t)} \int A(\boldsymbol{r}, \boldsymbol{u}) f_1(\boldsymbol{r}, \boldsymbol{u}, t)\mathrm{d}\boldsymbol{u}.$$

Note that the resulting function is a function of space and time, since we computed average only over the momentum variables.

We are interested in the functions A that vanish, when integrated against the collision integral

$$\int A(\boldsymbol{r}, \boldsymbol{u}) \Big(\frac{\partial f_1}{\partial t}\Big)_{coll} \mathrm{d}\boldsymbol{u} = 0.$$

Intuitively, this condition is required because we are interested in the quantities that vary slowly, but the collisions are abrupt processes, and the term involving collision integral vary very fast.

Substituting the expression for the collision integral 6.9 to the last equation, we get

$$\int A(\boldsymbol{r}, \boldsymbol{u_1}) \omega(\boldsymbol{u_1'}, \boldsymbol{u_2'} | \boldsymbol{u_1}, \boldsymbol{u_2}) \big[f_1(\boldsymbol{r}, \boldsymbol{u_1'}) f_1(\boldsymbol{r}, \boldsymbol{u_2'}) - f_1(\boldsymbol{r}, \boldsymbol{u_1}) f_1(\boldsymbol{r}, \boldsymbol{u_2})\big] \mathrm{d}\boldsymbol{u_1} \mathrm{d}\boldsymbol{u_2} \mathrm{d}\boldsymbol{u_1'} \mathrm{d}\boldsymbol{u_2'} = 0.$$

Considering the symmetries of ω, this condition is equivalent to

$$\begin{aligned} \int \omega(\boldsymbol{u_1'}, \boldsymbol{u_2'} | \boldsymbol{u_1}, \boldsymbol{u_2}) \big[f_1(\boldsymbol{r}, \boldsymbol{u_1'}) f_1(\boldsymbol{r}, \boldsymbol{u_2'}) - f_1(\boldsymbol{r}, \boldsymbol{u_1}) f_1(\boldsymbol{r}, \boldsymbol{u_2})\big] \\ \times \big[A(\boldsymbol{r}, \boldsymbol{u_1}) + A(\boldsymbol{r}, \boldsymbol{u_2}) - A(\boldsymbol{r}, \boldsymbol{u_1'}) - A(\boldsymbol{r}, \boldsymbol{u_2'})\big] \mathrm{d}\boldsymbol{u_1} \mathrm{d}\boldsymbol{u_2} \mathrm{d}\boldsymbol{u_1'} \mathrm{d}\boldsymbol{u_2'} = 0 \end{aligned},$$

which holds if

$$A(\boldsymbol{r}, \boldsymbol{u_1}) + A(\boldsymbol{r}, \boldsymbol{u_2}) = A(\boldsymbol{r}, \boldsymbol{u_1'}) + A(\boldsymbol{r}, \boldsymbol{u_2'}).$$

So A is a quantity that is conserved during the collision, which is true for the energy, momenta, and trivially, for a constant function, e.g. $A = 1$. These are the *collision invariants* of our interest.

If we plug any collision invariant to the Boltzmann equation 6.10 and integrate over the momenta variables, the term involving collision integral vanishes

a

Because A do not explicitly depend on time, we can put it in the time derivative, and by integrating other terms by part, we get

b.

Finally, using the notation for the average, we can rewrite it as

$$c \tag{6.14}$$

which is the master equation telling the evolution of the collisional invariant.

Substituting the trivial collisional invariant $A = 1$ into this equation yields

$$\frac{\partial n}{\partial t} + \frac{\partial}{\partial \boldsymbol{r}}.(\overline{\boldsymbol{u}}).$$

Multiplying by particle mass m, this is the continuity equation. In the last equation, we introduced notation

$$\overline{u} = \langle \boldsymbol{u} \rangle,$$

that we will use from now on.

Substituting the next collisional invariant, the momentum $A = m\boldsymbol{u}$, yields

$$\frac{\partial}{\partial t}(mn\langle u_i \rangle) + \frac{\partial}{\partial r_j}\langle mnu_i u_j \rangle - \langle nF_i \rangle = 0 \tag{6.15}$$

If we expand the middle term like

$$\langle u_i u_j \rangle = \langle$$

and we define the pressure tensor

$$P_{ij} = P_{ji} = \rho$$

we can write the equation 6.15 in the usual form

$$aa$$

It is the equation of momentum conservation. We can interpret it according to the Newton's law – the left-hand side is the accelartion of the fluid element, and the right-hand involves the external force $\boldsymbol{F}$ and the internal pressure of the fluid

Let us pause at the pressure tensor for a moment. We can evaluate it on the equilibrium distribution and find out that it is proportional to the temperature

$$P_{ij} = nk_B T\delta_{ij}$$

that truly corresponds to the ideal gas law.

The last collisional invariant is the kinetic energy of particles. Instead of absolute kinetic energy, we shall use the relative kinetic energy

$$A = \frac{1}{2}m(\overline{\boldsymbol{u}} - \boldsymbol{u})^2,$$

so we will get rid off some terms when we substitute it into our master equation 6.14

$$a \tag{6.16}$$

Using the idea of equipartition, we can define the temperature for the non-equilibrium system

$$\frac{3}{2}k_B T(\boldsymbol{r},t) = \frac{1}{2}m\langle(\overline{\boldsymbol{u}} - \boldsymbol{u})^2\rangle$$

Let us define another quantity, the *heat flux*

$$\frac{1}{2}m\rho\langle(u_i - \overline{u_i})(\boldsymbol{u} - \overline{\boldsymbol{u}})^2\rangle.$$

Using the definition of heat flux and pressure tensor, we can rewrite the equation 6.16

aa

Since the pressure tensor is symmetric, we can replace $\partial u_j/\partial r_i$ with the symmetric *rate of strain*

$$U_{ij} = \frac{1}{2}\left(\frac{\partial u_j}{\partial r_i} + \frac{\partial u_i}{\partial r_j}\right)$$

Further, using the continuity equation, we obtain the conservation of energy in its usual form

aa

Finally, we have the three equations, describing the time evolution of the particle density n, momentum $\boldsymbol{u}$ and the temperature T. Although they hold for any distribution f_1, they are not the closed set of equations – equation for n depends on $\boldsymbol{u}$, equation for momentum depends on the pressure tensor P_{ij} and the equation for temperature depends on the heat flux q. To determine any of these, we need compute the distribution f_1 from the Boltzmann equation, which is not easy.

Since we are looking for the solution that varies slowly, the first approximation would be the local equilibrium distribution, for which $col = 0$.

Using the distribution do compute the P_{ij} and q, we obtain new form the conservation laws:

However, we are still missing dissipation in these equations. To show it, we can combine the equations refANDref to obtain

$$\left(\frac{\partial}{\partial t} + u_j\frac{\partial}{\partial r_j}\right)(\rho T^{-2/3}) = 0$$

This implies that $\rho T^{-2/3}$ is constant along the streamlines, which means that the motion of the fluid is adiabatic – not increasing entropy. Hence we have no mechanism for the fluid to return to the equilibrium yet.

It is easy to see what we are missing. We chose local equilibrium as an approximation for the distribution f_1, so that the collision integral vanish, but it does not solve the streaming term. However, if we stick to the long wave-length variations in the velocity, we need to add only little correction term

$$f_1 = f_1^{(0)} + \delta f_1. \tag{6.17}$$

The correction δf_1 contributes to the collision integral

$$\Big(\frac{\partial f_1}{\partial t}\Big)_{coll} = \int \omega(\boldsymbol{u_1'}, \boldsymbol{u_2'}|\boldsymbol{u_1}, \boldsymbol{u_2})\big[f_1(\boldsymbol{u_1'})f_1(\boldsymbol{u_2'}) - f_1(\boldsymbol{u_1})f_1(\boldsymbol{u_2})\big]\mathrm{d}\boldsymbol{u_2}\mathrm{d}\boldsymbol{u_1'}\mathrm{d}\boldsymbol{u_2'}$$

where we neglected the quadratic terms $O(\delta f_1^2)$ and used the fact that $f_1^{(0)}$ vanish in the collision integral.

To proceed further, the proper way would be to use *Chapman-Enskog expansion* of δf_1 to treat the collision operator properly, but there is an easier way to progress, the so called BGK [1] approximation. We simply set the collision integral to be

$$\Big(\frac{\partial f_1}{\partial t}\Big)_{coll} = -\frac{\delta f_1}{\tau}, \tag{6.18}$$

where τ is the relaxation time, and we take it to be a constant (although in general, it might be function of momentum). With this replacement, the Boltzmann equation changes to

$$\frac{\partial(f_1^{(0)} + \delta f_1)}{\partial t} - \big\{H_1, f_1^{(0)} + \delta f_1\big\} = -\frac{\delta f_1}{\tau}$$

6.4 Where is the viscosity?

Let us consider the flow of the fluid with the velocity gradient $\partial u_x/\partial z \neq 0$. According to the Newton's law, the shear viscosity is associated with the flux of x-momentum to the z-direction:

$$\Pi_{xz} = -\eta\frac{\partial u_x}{\partial r_z}, \tag{6.19}$$

which is the off-diagonal component of the pressure tensor

$$P_{xz} = \rho\langle(v_x - u_x)(v_z - u_z)\rangle.$$

As we already know, the local equilibrium distribution gives us the diagonal pressure tensor, but if we use the corrected distribution, we have

$$P_{ij} = P\delta_{ij} + \Pi_{ij}, \tag{6.20}$$

with the additional term Π_{ij}, which is a non-diagonal *stress tensor*

$$\Pi_{ij} = somethingsomething.$$

In fact, the Π_{ij} is traceless, because

$$\langle v^2 v_k v_l\rangle_0 = \delta_{kl}\langle v_i v_j v^2\rangle.$$

and it depends linearly on the U_{kl}. These two properties determine the form of the tensor

$$\Pi_{ij} = -2\mu\big(U_{ij} - \frac{1}{3}\delta_{ij}\nabla.\boldsymbol{u}\big). \tag{6.21}$$

[1] Bhatnagar-Gross-Krook

For $\partial u_x/\partial z \neq 0$, we can evaluate

$$\Pi_{xz} = \frac{2m\tau\rho}{15k_BT} U_{xx} \langle v^4 \rangle_0.$$

Comparing it to the Newton's law 6.19, we get an expression for the shear viscosity

$$\eta = nk_BT\tau. \tag{6.22}$$

Note that this expression is just an estimation, as it relies on the relaxation time approximation τ.

6.5 Navier-Stokes equations

The corrected distribution 6.17 does not change the density equation

$$\frac{\partial \rho}{\partial t} + \nabla.(\rho \boldsymbol{u}) = 0,$$

but due to the non-diagonal stress tensor 6.21, the momentum equation transforms to the Navier-Stokes equation

$$aa. \tag{6.23}$$

Since $\nabla\kappa \approx 0$ and $U_{ij}\Pi_{ij} \approx 0$ are small at the order we are working at, we can drop them, so we are left with

$$aa$$

Although our derivation relied on the dilute gas approximation, the Navier-Stokes equation are more general then that. In fact, they can be considered to be the most general expression for the momentum transport.

7. Lattice Boltzmann method

In the previous chapter, we showed that Boltzmann equation is superior to the Navier-Stokes and hydrodynamic equations – if we solve the Boltzmann equation, we can indirectly obtain the solution for the Navier-Stokes (NSE).

But since the distribution $f(\boldsymbol{x}, \boldsymbol{u}, t)$ is the function of seven variables, it is even more difficult to solve the Boltzmann equation then NSE. Surprisingly, the numerical method for the Boltzmann equation turns out to be simple to implement and straight-forward to parallelise, and it results in the exact advection (as opposed to NSE solvers, that have major difficulty with the advection term).

This numerical scheme evolved from the lattice-gas cellular automata that are the primary focus of our thesis, so we will explain it along the lines with LGCA, although explanations from the various perspectives are possible.

7.1 Basics

The basic quantity for LBM is the velocity distribution $f_i(\boldsymbol{r}, t)$. Using the probability density function 6.3, it can be defined as

$$f_i(\boldsymbol{r}, t) = f_1(\boldsymbol{r}, \boldsymbol{c_i}, t).$$

and represents the density of the particles, but only at the discrete time steps and points of the lattice.

The LBM lattice is often denoted by the symbol $DdQq$, where d is the dimension of the lattice, and q is the number of lattice vectors, e.g. $D1Q3$, $D2Q9$ or $D3Q19$, which is the most common 3D variant with 19 lattice vectors. Interestingly, it is the projection of the four dimensional FCHC lattice that we already described, see figure 4.1.

The mass and momentum density at the discrete point $(\boldsymbol{r}, t)$ is given by

$$\rho(\boldsymbol{r}, t) = \sum_i f_i(\boldsymbol{r}, t) \tag{7.1}$$

and

$$\boldsymbol{j}(\boldsymbol{r}, t) = \sum_i c_i f_i(\boldsymbol{r}, t), \tag{7.2}$$

which correspond to 3.5 and 3.6, that we derived for the FHP model.

For isotermal lattice Boltzmann equation, the speed of sound is determined by the simple formula

$$p = c_s^2 \rho,$$

and for the lattice sets we introduced above, it is

$$c_s^2 = \frac{1}{3}\frac{\Delta x^2}{\Delta t^2},$$

It is a good custom to set the lattice spacing $\Delta x = 1$ and time step $\Delta t = 1$.

The Boltzmann equation, discretized in space, time and velocity space 6.10 reads

$$f_i(\boldsymbol{x} + \boldsymbol{c_i}\Delta t, t + \Delta t) = f_i(\boldsymbol{x}, t) + \Omega_i(\boldsymbol{x}, t), \tag{7.3}$$

which states that particles from the population $f_i(\boldsymbol{x}, t)$ with the velocity $\boldsymbol{c_i}$ move to the point $\boldsymbol{x} + \boldsymbol{c_i}$ at the next time step. Before that, the particles are affected by the collision operator Ω that redistributes particles among the populations f_i. Notice that this corresponds to the equation 3.1 with one major difference – in FHP the respective quantities were boolean (empty cell or particle inside), in LBM, these are continuous values of particle densities that collide and propagate.

The LBM version of the BGK collision operator 6.18 is

$$\Omega_i(f) = -\frac{f_i - f_i^{eq}}{\tau}\Delta t,$$

and gives us a good intuition about what collisions do – the population numbers relax towards the equilibrium values at a rate given by τ. The equilibrium distribution is given by

$$f_i^{eq}(\boldsymbol{x}, t) = \tag{7.4}$$

where w_i are the weights specific to the LBM lattice used, $\boldsymbol{u} = \boldsymbol{j}/\rho$ with ρ and $\boldsymbol{j}$ are given by 7.1 and 7.2.

In the previous chapter, we established the link between Boltzmann and Navier-Stokes equations, and derived the expressions for the shear viscosity 6.22 and the stress tensor 6.21. Their discretized LBM variants are

$$\eta = c_s^2\big(\tau - \frac{\Delta t}{2}\big)$$

and

$$\Pi_{\alpha\beta} \approx -\big(1 - \frac{\tau}{2\tau}\big)\sum_i c_{i\alpha}c_{i\beta}(f_i - f_i^{eq}).$$

7.2 Collision and propagation

Analogously to lattice-gas cellular automata, the update given by the Boltzmann equation 7.3 can be decomposed in two subsequent steps:

1. **Collision**

   $$f_i^*(\boldsymbol{x}, t) = f_i(\boldsymbol{x}, t) - \frac{\Delta t}{\tau}\big(f_i(\boldsymbol{x}, t) - f_i^{eq}(\boldsymbol{x}, t)\big)$$

   where f_i^* is the particle distribution after the collision.

2. **Propagation**

   $$f_i(\boldsymbol{x} + \boldsymbol{c_i}\Delta t, t + \Delta t) = f_i^*(\boldsymbol{x}, t).$$

Less formally, the update step, which is the essence of the LBM computation, can be described in the few points:

1. Use f_i to compute ρ and $\boldsymbol{j}$ via 7.1 and 7.2.
2. Compute Maxwell-Boltzmann distribution f_i^{eq} via 7.4.
3. Carry out the collision and the propagation.

Part II

Implementation and applications

8. Practical part

In the theoretical part of the thesis, we have introduced the notion of cellular automaton and basic models of lattice-gas cellular automata by which it is possible to mimic the flow of physical fluids governed by the Euler equations and, to certain extent, the Navier-Stokes equations. We have described the algorithms behind the microdynamics of these models and emphasized the importance of the symmetries of the lattice for reproducing correct macroscopic behavior.

In this part, we implement the aforementioned algorithms in the language C++ and visualize the results using the *GNU*plot software. The original results of this thesis are summarized in the points to follow.

1. We implemented 1D and 2D cellular automata to show their interesting properties and motivate theoretical part. These results were already included in the theoretical part and will not be discussed further.

2. We implement FCHC and PI – the two distinct 3D LGCA introduced in theoretical part.

3. We inspect 3D flow around obstacles of various shapes.

4. We study fully-developed turbulent flow and compare its statistical properties to the Kolmogorov–Obuchov K41 theory. [2].

   Unfortunately, this most original and scientifically most interesting part is not concluded, but it provides the basis for future research.

9. General comments on the implementation

According to Wolf-Gladrow ([2], page. 2017), the most effective language for the implementation of LGCA is C (with slightly better performance than Fortran).

We listened to this advice and started the implementation in C language, but we could not resist to use some "shortcuts" of C++, but we stayed true to the C-style of programming.

The programs have substantially grew over the time, and we got on the crossroad how to efficiently develop our two models further. The current option number one (in the process while writing these lines) is to use the pure C, and pack it as *extension module* to Python, mainly for our own comfort in future applications, but we would be glad if it finds its way to some fellow out there.

9.1 Parallelization

Languages C and C++ offer us three popular and well documented interfaces for parallelization:

1. OpenMP
2. MPI
3. Cuda

We rather obey the old Chinese saying '谁闻起来像腋下汗湿的龙，不应该使用Cuda', so Cuda is obviously out of the question.

For a short time, MPI was a hot candidate, we have even used it on cellular automaton that is not included in this thesis. But after consulting the more experienced colleague, we concluded that minuses would overweight the pluses.

Since we have opporunity to use clusters at Metacenter (the network of clusters from academic institutions all over the Czech republic) we expected we could employ huge amount of processors, if we use MPI and compute on various clusters parallely. But we learnt that in the practice we can hardly employ more then two hundreds of processors. Using OpenMP, we can run the computation on SMP machine with 64 processors, that is not significantly lower.

The drawbacks of MPI are obvious, it requires vast modification of the code, comparing to OpenMP, that needs only few more lines of code to add (and sometimes, even that can be tricky).

Another aspect is that parallelization with OpenMP can be included to Python extension module, that we are considering to develop.

Therefore, OpenMP seemed like an appropriate choice.

In the following chapter, we offer brief discussion of the most important parts of our source code.

10. Implementation of FCHC

In the chapter blabla, we inspected FCHC automaton theoretically, you should be familiar with it before we start.

According to [**?**], (find idea on lack of implementation). And field of practical applications is ruled by Lattice Boltzmann model nowadays, so we really do not find many applications.

As the more advanced "lattice Boltzmann model" evolved from LGCA, it attracted And nowadays, the "lattice Boltzmann model" has taken over the application.

Due to huge number of state of the node and huge number of colli As state of the node is represented by 24 bits. Therefore, integer with its 32 bits is enough to represent both node and obstacle (24 bits + 1 bit).

Not so long ago, table that would specify collision rules for 2^{24} states was problematic - it would require approximately $2^{24} \times 10 \times 4bytes = 640$MB memory to manage.

Henon proposed algorithm for collision that would by-pass this obstacle, compute the possible set of states in reasonable time and chose optimal state.

However, the algorithm is quiet expensive on computation time, especially comparing to pair-interaction LGCA.

Therefore, we have chosen the following approach for resolving collisions:

1. At the beginning of the computation, before the simulation of the flow starts, we create table of 2^{24} entries. Integer index of the entry is the state of the node, and using Henon algorithm, we compute the optimal isometries for the state.

2. Collisions during simulation are resolved by choosing the resulting state from the table, instead of computing the optimal isometries again and again. We are not generating the random numbers to chose the resulting state, as it is expensive on resources and was significantly slowing the algorithm in the testing phase. However, we believe that choosing random states is not necessary and our solution for choosing the optimal isometries leads to the uniform distribution due to large number of nodes (around 10^8).

Excerpt of the source code relevant to the creation of the table and collision follows.

10.1 Algorithm for the creation of the table

```
/* The node is represented as the integer, first 24 bits corresponds
   to the cells. If the value of the cell is 1, it is occupied by
   particle, otherwise it is 0. */

#define C1 1
#define C2 (C1<<1)
#define C3 (C1<<2)
```

```
#define C4 (C1<<3)
#define C5 (C1<<4)
#define C6 (C1<<5)
#define C7 (C1<<6)
#define C8 (C1<<7)
#define C9 (C1<<8)
#define C10 (C1<<9)
#define C11 (C1<<10)
#define C12 (C1<<11)
#define C13 (C1<<12)
#define C14 (C1<<13)
#define C15 (C1<<14)
#define C16 (C1<<15)
#define C17 (C1<<16)
#define C18 (C1<<17)
#define C19 (C1<<18)
#define C20 (C1<<19)
#define C21 (C1<<20)
#define C22 (C1<<21)
#define C23 (C1<<22)
#define C24 (C1<<23)

/* We assigned the 25th bit to the obstacle. If it is 1, this node is
    part of the obstacle and is not occupied by the particles (thus if
    this bit is 1, all other bits are 0) */
#define OBS (C1<<24)

/* We create the array of the cells, so we can efficiently iterate
    over the cells */
int C[24] = {
   C1, C2, C3, C4,
   C5, C6, C7, C8,
   C9, C10, C11, C12,
   C13, C14, C15, C16,
   C17, C18, C19, C20,
   C21, C22, C23, C24
};


/* Array of the cells, such that Reverse[i] lies on the diagonal to
    the C[i] from above */
int Reverse[24] = {
   C4, C3, C2, C1,
   C8, C7, C6, C5,
   C12,C11,C10,C9,
   C16,C15,C14,C13,
   C20,C19,C18,C17,
   C24,C23,C22,C21
};
```

```
/* Lattice velocities. The lattice velocity c[i] corresponds to the
    cell C[i] */
const int c[24][4] = {
   { 1,1,0,0 },
   { 1,-1,0,0 },
   { -1,1,0,0 },
   { -1,-1,0,0 },

   { 1,0,1,0 },
   { 1,0,-1,0 },
   { -1,0,1,0 },
   { -1,0,-1,0 },

   { 1,0,0,1 },
   { 1,0,0,-1 },
   { -1,0,0,1 },
   { -1,0,0,-1 },

   { 0,1,1,0 },
   { 0,1,-1,0 },
   { 0,-1,1,0 },
   { 0,-1,-1,0 },

   { 0,1,0,1 },
   { 0,1,0,-1 },
   { 0,-1,0,1 },
   { 0,-1,0,-1 },

   { 0,0,1,1 },
   { 0,0,1,-1 },
   { 0,0,-1,1 },
   { 0,0,-1,-1 }
};

/* This function swap the i-th and j-th bit of the node n */
int switchBits(int n, int i, int j)
{
   int a, b;
   a = n & C[i];
   b = n & C[j];
   if (a > 0 && b == 0)
   {
      n ^= C[i];
      n |= C[j];
   }
   else if (b > 0 && a == 0)
   {
      n |= C[i];
      n ^= C[j];
   }
   return n;
```

```
}



/* Implementation of the isometries \Sigma_1 and \Sigma_2 on the node
   n*/
/* As all isometries that will follow, it is achieved by swapping the
   appropriate bits in the node */
/* It also transforms the momentum vector q */
/* The parameter j is dummy parameter, we need it so that all
   isometries have the same set of parameters */
int sigma(int n, int* q, int i, int j)
{
   int a = q[0];
   int b = q[1];
   int c = q[2];
   int d = q[3];

   if (i == 1)
   {
      q[0] = ( a + b + c - d ) / 2;
      q[1] = ( a + b - c + d ) / 2;
      q[2] = ( a - b + c + d ) / 2;
      q[3] = (-a + b + c + d ) / 2;

      n = switchBits(n, 1, 21);
      n = switchBits(n, 2, 22);
      n = switchBits(n, 5, 17);
      n = switchBits(n, 6, 18);
      n = switchBits(n, 8, 12);
      n = switchBits(n, 11, 15);
   }
   else
   {
      q[0] = ( a + b + c + d ) / 2;
      q[1] = ( a + b - c - d ) / 2;
      q[2] = ( a - b + c - d ) / 2;
      q[3] = ( a - b - c + d ) / 2;

      n = switchBits(n, 1, 20);
      n = switchBits(n, 2, 23);
      n = switchBits(n, 5, 16);
      n = switchBits(n, 6, 19);
      n = switchBits(n, 9, 12);
      n = switchBits(n, 10, 15);
   }
   return n;
}

/* Isometry S_i is the reflection over plane x_i */
int S(int n, int* q, int i, int j)
```

```
{
   switch (i)
   {
   case 1:
      q[0] = -q[0];
      n = switchBits(n, 0, 2);
      n = switchBits(n, 1, 3);
      n = switchBits(n, 4, 6);
      n = switchBits(n, 5, 7);
      n = switchBits(n, 8, 10);
      n = switchBits(n, 9, 11);
      break;
   case 2:
      q[1] = -q[1];
      n = switchBits(n, 0, 1);
      n = switchBits(n, 2, 3);
      n = switchBits(n, 12, 14);
      n = switchBits(n, 13, 15);
      n = switchBits(n, 16, 18);
      n = switchBits(n, 17, 19);
      break;
   case 3:
      q[2] = -q[2];
      n = switchBits(n, 4, 5);
      n = switchBits(n, 6, 7);
      n = switchBits(n, 12, 13);
      n = switchBits(n, 14, 15);
      n = switchBits(n, 20, 22);
      n = switchBits(n, 21, 23);
      break;
   case 4:
      q[3] = -q[3];
      n = switchBits(n, 8, 9);
      n = switchBits(n, 10, 11);
      n = switchBits(n, 16, 17);
      n = switchBits(n, 18, 19);
      n = switchBits(n, 20, 21);
      n = switchBits(n, 22, 23);
      break;
   default:
      break;
   }
   return n;
}

/* Isometry P_ij, reflecton over the plain x_i = x_j */
int P(int n, int*q, int i, int j)
{
   int a = i - 1;
   int b = j - 1;
   int qa = q[a];
```

```
q[a] = q[b];
q[b] = qa;

if (i == 1)
{
   if (j == 2)
   {
      n = switchBits(n, 1, 2);
      n = switchBits(n, 4, 12);
      n = switchBits(n, 5, 13);
      n = switchBits(n, 6, 14);
      n = switchBits(n, 7, 15);
      n = switchBits(n, 8, 16);
      n = switchBits(n, 9, 17);
      n = switchBits(n, 10, 18);
      n = switchBits(n, 11, 19);
   }
   else if (j == 3)
   {
      n = switchBits(n, 0, 12);
      n = switchBits(n, 1, 14);
      n = switchBits(n, 2, 13);
      n = switchBits(n, 3, 15);
      n = switchBits(n, 5, 6);
      n = switchBits(n, 8, 20);
      n = switchBits(n, 9, 21);
      n = switchBits(n, 10, 22);
      n = switchBits(n, 11, 23);
   }
   else if (j == 4)
   {
      n = switchBits(n, 0, 16);
      n = switchBits(n, 1, 18);
      n = switchBits(n, 2, 17);
      n = switchBits(n, 3, 19);
      n = switchBits(n, 4, 20);
      n = switchBits(n, 5, 22);
      n = switchBits(n, 6, 21);
      n = switchBits(n, 7, 23);
      n = switchBits(n, 9, 10);
   }
}
else if (i == 2)
{
   if (j == 3)
   {
      n = switchBits(n, 0, 4);
      n = switchBits(n, 1, 5);
      n = switchBits(n, 2, 6);
      n = switchBits(n, 3, 7);
      n = switchBits(n, 13, 14);
```

```
            n = switchBits(n, 16, 20);
            n = switchBits(n, 17, 21);
            n = switchBits(n, 18, 22);
            n = switchBits(n, 19, 23);
         }
         else if (j == 4)
         {
            n = switchBits(n, 0, 8);
            n = switchBits(n, 1, 9);
            n = switchBits(n, 2, 10);
            n = switchBits(n, 3, 11);
            n = switchBits(n, 12, 20);
            n = switchBits(n, 13, 22);
            n = switchBits(n, 14, 21);
            n = switchBits(n, 15, 23);
            n = switchBits(n, 17, 18);
         }
      }
      else if (i == 3 && j == 4)
      {
         n = switchBits(n, 4, 8);
         n = switchBits(n, 5, 9);
         n = switchBits(n, 6, 10);
         n = switchBits(n, 7, 11);
         n = switchBits(n, 12, 16);
         n = switchBits(n, 13, 17);
         n = switchBits(n, 14, 18);
         n = switchBits(n, 15, 19);
         n = switchBits(n, 21, 22);
      }
      return n;
   }

   /* Computes the total momentum of the node */
   int* momenta(int node)
   {
      int*q = new int[4]{ 0,0,0,0 };

      for (int i = 0; i < 24; ++i)
      {
         /* if the cell C[i] is occupied by particle, count its momentum */
         if (C[i] & node)
         {
            for (int j = 0; j < 4; ++j)
            {
               q[j] += c[i][j];
            }
         }
      }
      return q;
   }
```

```
/* We need to remember all the isometries that normalize the momentum,
   so we can transform it back to its original momentum */
/* We define this array so that we can reffer to the isometry by the
   single index */
int(*iso[])(int n, int*q, int i, int j) = { S,P,sigma };


/* This function does all isometries that normalized the node, but in
   the reverse order, so that original momentum is achieved */
void goBack(int**steps, int* nodes, int*q, int step, int length)
{
   for (int i = 1; i < length; i++)
   {
      for (int j = step - 1; j >= 0; --j)
      {
         nodes[i] = iso[steps[j][0]](nodes[i], q, steps[j][1],
             steps[j][2]);
      }
   }
}

/* Creates the entry for the state 'n' that we will insert into the
   table of collisions */
/* It is implementation of the Henon algorithm, that computes the set
   of optimal isometries */
int* newNode(int n, int**steps)
{
   int*q = momenta(n);

   int step = 0;

   // invert negative q[i]
   for (int i = 0; i < 4; i++)
   {
      if (q[i] < 0)
      {
         //S changes sign of q[i];
         n = S(n, q, i+1, 0);
         //we record each step to the array "steps" so we can go back
         steps[step][0] = 0;
         steps[step][1] = i+1;
         steps[step][2] = 0;
         ++step;
      }
   }
   // sort q[i] from high to low
   int highIndex;
   int highValue;
   for (int i = 0; i < 4; ++i)
   {
```

```
      highIndex = i;
      highValue = q[i];
      for (int j = i+1; j < 4; ++j)
      {
         if (q[j] > highValue)
         {
            highValue = q[j];
            highIndex = j;
         }
      }
      if (highIndex > i)
      {
         n = P(n, q, i + 1, highIndex + 1);
         steps[step][0] = 1;
         steps[step][1] = i + 1;
         steps[step][2] = highIndex + 1;
         ++step;
      }
   }
   // to fulfill second condition:
   if (q[3] > 0)
   {
      if (q[0] + q[3] == q[1] + q[2])
      {
         n = sigma(n, q, 2, 0);
         steps[step][0] = 2;
         steps[step][1] = 2;
         steps[step][2] = 0;
         ++step;
      }
      else if (q[0] + q[3] > q[1] + q[2])
      {
         n = sigma(n, q, 1, 0);
         steps[step][0] = 2;
         steps[step][1] = 1;
         steps[step][2] = 0;
         ++step;
      }
   }
   if (q[3] < 0)
   {
      n = S(n, q, 4, 0);
      //we record each step to the steps field, since we will go back
      steps[step][0] = 0;
      steps[step][1] = 4;
      steps[step][2] = 0;
      ++step;
   }


   int* nodes;
```

```
//class 12
if (q[0] == 0)
{
   int length = 13;
   nodes = new int[length];
   nodes[0] = length - 1;
   //S3 S1 P34 P12, S4 S1 P34 P12, S3 S2 P34 P12, S4 S2 P34 P12,
   //S2 S1 P24 P13, S4 S1 P24 P13, S3 S2 P24 P13, S4 S3 P24 P13,
   //S2 S1 P23 P14, S3 S1 P23 P14, S4 S2 P23 P14, S4 S3 P23 P14

   nodes[1] = P(n, q, 1, 2);
   nodes[1] = P(nodes[1], q, 3, 4);
   nodes[1] = S(nodes[1], q, 1, 0);
   nodes[1] = S(nodes[1], q, 3, 0);

   nodes[2] = P(n, q, 1, 2);
   nodes[2] = P(nodes[2], q, 3, 4);
   nodes[2] = S(nodes[2], q, 1, 0);
   nodes[2] = S(nodes[2], q, 4, 0);

   nodes[3] = P(n, q, 1, 2);
   nodes[3] = P(nodes[3], q, 3, 4);
   nodes[3] = S(nodes[3], q, 2, 0);
   nodes[3] = S(nodes[3], q, 3, 0);

   nodes[4] = P(n, q, 1, 2);
   nodes[4] = P(nodes[4], q, 3, 4);
   nodes[4] = S(nodes[4], q, 2, 0);
   nodes[4] = S(nodes[4], q, 4, 0);

   nodes[5] = P(n, q, 1, 3);
   nodes[5] = P(nodes[5], q, 2, 4);
   nodes[5] = S(nodes[5], q, 1, 0);
   nodes[5] = S(nodes[5], q, 2, 0);

   nodes[6] = P(n, q, 1, 3);
   nodes[6] = P(nodes[6], q, 2, 4);
   nodes[6] = S(nodes[6], q, 1, 0);
   nodes[6] = S(nodes[6], q, 4, 0);

   nodes[7] = P(n, q, 1, 3);
   nodes[7] = P(nodes[7], q, 2, 4);
   nodes[7] = S(nodes[7], q, 2, 0);
   nodes[7] = S(nodes[7], q, 3, 0);

   nodes[8] = P(n, q, 1, 3);
   nodes[8] = P(nodes[8], q, 2, 4);
   nodes[8] = S(nodes[8], q, 3, 0);
   nodes[8] = S(nodes[8], q, 4, 0);

   nodes[9] = P(n, q, 1, 4);
```

```
    nodes[9] = P(nodes[9], q, 2, 3);
    nodes[9] = S(nodes[9], q, 1, 0);
    nodes[9] = S(nodes[9], q, 2, 0);

    nodes[10] = P(n, q, 1, 4);
    nodes[10] = P(nodes[10], q, 2, 3);
    nodes[10] = S(nodes[10], q, 1, 0);
    nodes[10] = S(nodes[10], q, 3, 0);

    nodes[11] = P(n, q, 1, 4);
    nodes[11] = P(nodes[11], q, 2, 3);
    nodes[11] = S(nodes[11], q, 2, 0);
    nodes[11] = S(nodes[11], q, 4, 0);

    nodes[12] = P(n, q, 1, 4);
    nodes[12] = P(nodes[12], q, 2, 3);
    nodes[12] = S(nodes[12], q, 3, 0);
    nodes[12] = S(nodes[12], q, 4, 0);

    goBack(steps, nodes, q, step, length);

}
//class 11
else if (q[1] == 0)
{
    int length = 7;
    nodes = new int[length];
    nodes[0] = length - 1;
    //S4 S2 P23,  S4 S3 P23,  S3 S2 P24,
    //S4 S3 P24,  S3 S2 P34,  S4 S2 P34

    nodes[1] = P(n, q, 2, 3);
    nodes[1] = S(nodes[1], q, 2, 0);
    nodes[1] = S(nodes[1], q, 4, 0);

    nodes[2] = P(n, q, 2, 3);
    nodes[2] = S(nodes[2], q, 3, 0);
    nodes[2] = S(nodes[2], q, 4, 0);

    nodes[3] = P(n, q, 2, 4);
    nodes[3] = S(nodes[3], q, 2, 0);
    nodes[3] = S(nodes[3], q, 3, 0);

    nodes[4] = P(n, q, 2, 4);
    nodes[4] = S(nodes[4], q, 3, 0);
    nodes[4] = S(nodes[4], q, 4, 0);

    nodes[5] = P(n, q, 3, 4);
    nodes[5] = S(nodes[5], q, 2, 0);
    nodes[5] = S(nodes[5], q, 3, 0);
```

```
    nodes[6] = P(n, q, 3, 4);
    nodes[6] = S(nodes[6], q, 2, 0);
    nodes[6] = S(nodes[6], q, 4, 0);


    goBack(steps, nodes, q, step, length);

}
//class 10
else if (q[2] == 0 && q[0]==q[1])
{
    int length = 7;
    nodes = new int[length];
    nodes[0] = length - 1;
    //S3,P34,P12, S4,P34,P12, S4,S3,sigma1, S4,S3,P34,P12,sigma1
    //S4,S3,sigma2, P34,P12,sigma2
    nodes[1] = P(n, q, 1, 2);
    nodes[1] = P(nodes[1], q, 3, 4);
    nodes[1] = S(nodes[1], q, 3, 0);

    nodes[2] = P(n, q, 1, 2);
    nodes[2] = P(nodes[2], q, 3, 4);
    nodes[2] = S(nodes[2], q, 4, 0);

    nodes[3] = sigma(n, q, 1, 0);
    nodes[3] = S(nodes[3], q, 3, 0);
    nodes[3] = S(nodes[3], q, 4, 0);

    nodes[4] = sigma(n, q, 1, 0);
    nodes[4] = P(nodes[4], q, 1, 2);
    nodes[4] = P(nodes[4], q, 3, 4);
    nodes[4] = S(nodes[4], q, 3, 0);
    nodes[4] = S(nodes[4], q, 4, 0);

    nodes[5] = sigma(n, q, 2, 0);
    nodes[5] = S(nodes[5], q, 3, 0);
    nodes[5] = S(nodes[5], q, 4, 0);

    nodes[6] = sigma(n, q, 2, 0);
    nodes[6] = P(nodes[6], q, 1, 2);
    nodes[6] = P(nodes[6], q, 3, 4);

    goBack(steps, nodes, q, step, length);
}
//class 9
else if (q[2] == 0 && q[0] > q[1])
{
    int length = 4;
    nodes = new int[length];
    nodes[0] = length - 1;
```

```
   nodes[1] = S(n, q, 3, 0);
   nodes[1] = S(nodes[1], q, 4, 0);

   nodes[2] = P(n, q, 3, 4);
   nodes[2] = S(nodes[2], q, 3, 0);

   nodes[3] = P(n, q, 3, 4);
   nodes[3] = S(nodes[3], q, 4, 0);

   goBack(steps, nodes, q, step, length);
}
//class 8
else if (q[0]==q[1] && q[1] == q[2] && q[2] > q[3] && q[3]==0)
{
   int length = 5;
   nodes = new int[length];
   nodes[0] = length - 1;
   //1
   nodes[1] = P(n, q, 1, 2);
   nodes[1] = P(nodes[1], q, 2, 3);
   //2
   nodes[2] = P(n, q, 1, 3);
   nodes[2] = P(nodes[2], q, 2, 3);
   //3
   nodes[3] = P(n, q, 1, 2);
   nodes[3] = P(nodes[3], q, 2, 3);
   nodes[3] = S(nodes[3], q, 4, 0);

   //4
   nodes[4] = P(n, q, 1, 3);
   nodes[4] = P(nodes[4], q, 2, 3);
   nodes[4] = S(nodes[4], q, 4, 0);

   goBack(steps, nodes, q, step, length);
}
//class 6 or 7
else if (q[0]>q[1] && q[1]==q[2] && q[2] > q[3] && q[3] == 0)
{
   //class 6
   if (q[0] == 2*q[1])
   {
      int length = 5;
      nodes = new int[length];

      nodes[0] = length - 1;

      nodes[1] = sigma(n, q, 1, 0);
      nodes[1] = S(nodes[1], q, 4, 0);

      nodes[2] = sigma(n, q, 2, 0);
      nodes[2] = S(nodes[2], q, 4, 0);
```

```
            nodes[3] = sigma(n, q, 1, 0);
            nodes[3] = P(nodes[3], q, 2, 3);
            nodes[3] = S(nodes[3], q, 4, 0);

            nodes[4] = sigma(n, q, 2, 0);
            nodes[4] = P(nodes[4], q, 2, 3);
            nodes[4] = S(nodes[4], q, 4, 0);

            goBack(steps, nodes, q, step, length);

        }
        //class 7
        else
        {
            int length = 2;
            nodes = new int[length];

            nodes[0] = length - 1;

            nodes[1] = P(n, q, 2, 3);
            nodes[1] = S(nodes[1], q, 4, 0);

            goBack(steps, nodes, q, step, length);
        }

    }
    //class 5
    else if (q[0]==q[1] && q[1]>q[2] && q[2] > q[3] && q[4] == 0)
    {
        int length = 2;
        nodes = new int[length];

        nodes[0] = length - 1;
        //1
        nodes[1] = P(n, q, 1, 2);
        nodes[1] = S(nodes[1], q, 4, 0);

        goBack(steps, nodes, q, step, length);
    }
    //class 3,4
    else if (q[0]>q[1] && q[1]>q[2] && q[2] > q[3] && q[3] == 0)
    {
        //class 3
        if (q[0]==q[1]+q[2])
        {
            int length = 3;
            nodes = new int[length];

            nodes[0] = length - 1;
```

```
      nodes[1] = sigma(n, q, 1, 0);
      nodes[1] = S(nodes[1], q, 4, 0);

      nodes[2] = sigma(n, q, 2, 0);
      nodes[2] = S(nodes[2], q, 4, 0);

      goBack(steps, nodes, q, step, length);

   }
   //class 4
   else
   {
      int length = 2;
      nodes = new int[length];

      nodes[0] = length - 1;

      nodes[1] = S(n, q, 4, 0);

      goBack(steps, nodes, q, step, length);
   }
}
//class 2
else if (q[0]==q[1] && q[1]==q[2] && q[2]>q[3] && q[3]>0)
{
   int length = 3;
   nodes = new int[length];

   nodes[0] = length - 1;

   nodes[1] = P(n, q, 1, 2);
   nodes[1] = P(nodes[1], q, 2, 3);

   nodes[2] = P(n, q, 1, 3);
   nodes[2] = P(nodes[2], q, 2, 3);

   goBack(steps, nodes, q, step, length);
}
//class 1
else if (q[0]==q[1] && q[1]>q[2] && q[2] > q[3] && q[3] > 0)
{
   int length = 2;
   nodes = new int[length];

   nodes[0] = length - 1;

   nodes[1] = P(n, q, 1, 2);

   goBack(steps, nodes, q, step, length);
}
else
```

```
      nodes = nullptr;
   return nodes;
}

/*  This is the high-level function that creates the table of
    isometries */
/* For all 2^24 possible states of the node, it calls the function
    newNode and save the set of new states */
void fillTable(int** table)
{
   int n;

   int ** steps = new int*[20];
   for(int i = 0; i<20; ++i)
      steps[i] = new int[3];

   for ( n = 0; n < OBS; ++n)
      table[n] = newNode(n, steps);
}
```

10.2 Algorithm for collision

Once we have the table specifying optimal isometrical states ready (by the function *fillTable* above), the algorithm for collision is to implement. The only non-trivial task is to achieve uniform distribution of chosen isometries without generation of the random numbers, as it is expensive on CPU time.

```
/* For all nodes 'n' on the grid, this function looks in the table and
    choose from optimal final states */

void Collision(int***grid, int**table, int t, int X, int Y, int Z)
{
   int x,y,z;

   int n;
   int k;
#pragma omp parallel for private (x,y,z,n,k)
   for (x = 0; x < X; ++x)
      for (y = 0; y < Y; ++y)
         for (z = 0; z < Z; ++z)
         {
            //We find that node with position [x][y][y] on the grid is
                in the state n
            n = grid[x][y][z];
            // If there is obstacle in the node, we skip it.
            if (n & OBS)
               break;
            /* k is initialized by the external parameter t,
                and k is moduled by number of optimal isometries for the
                   state n */
```

```
            k = (t % table[n][0]) + 1;

            // we assign the k-th optimal state to the node
            grid[x][y][z] = table[n][k];

            //every step, we increment the external parameter, so we
               hopefully achieve the uniform distribution of k (there
               is huge number of nodes on the grid)
            ++t;
         }
}
```

10.3 Propagation in FCHC

Although the collisions are resolved in the four dimensional space (and the particles are the four dimensional objects), for the purpose of propagation, we can simply 'forget' its four-dimensional nature.

The nodes and particles are sitting on the three dimensional grid and propagate along the 3D projection of lattice vectors 4.1.

```
/* The propagation is happening in all the nodes at once, but in the
   computer simulation, it is happening sequentially, so we need to
   use to grids (propagation happening on the one grid would overwrite
   some nodes by new particles before the old particles propagated
   away). */
/* Hence, we are using the two grids, 'int***even' and 'int***odd'.
   'Even' grid is occupied at even times, 'Odd' grid is occupied at
   odd times. For example, in odd time, first parameter of Propagation
   (int***from) will be 'Odd' and second parameter (int***to) will be
   'Even' */

void Propagation(int***from, int***to, int**table, int X, int Y, int Z)
{
   int x,y,z;
   int i;
   int n;
   int new_x, new_y, new_z;

#pragma omp parallel for private (n, new_x, new_y, new_z, x, y, z, i)
   for ( x = 0; x < X; ++x)
      for ( y = 0; y < Y; ++y)
         for ( z = 0; z < Z; ++z)
         {
            // The current state of the node at [x][y][z]
            n = from[x][y][z];
            // We check every cell
            for ( i = 0; i < 24; ++i)
            {
               // If the cell C[i] is occupied by particle, we propagate
                  it to the corresponding node.
```

```
            if (n & C[i])
            {
               new_x = PeriodicBC(x + c[i][0], X);
               new_y = PeriodicBC(y + c[i][1], Y);
               new_z = PeriodicBC(z + c[i][2], Z);
               // If there is obstacle in the node, particle's
                  velocity is reversed.
               // e.g. particle with momentum [1,0,-1,0] gains
                  momentum [-1,0,1,0] by the reflection from the
                  obstacle
               if (to[new_x][new_y][new_z] & OBS)
                  to[new_x][new_y][new_z] |= Reverse[i];
               else
                  to[new_x][new_y][new_z] |= C[i];
            }
         }
         from[x][y][z] = 0;
      }
}
```

11. Implementation of the Pair-Interaction LGCA in 3D

"Programmers waste enormous amounts of time thinking about, or worrying about, the speed of noncritical parts of their programs, and these attempts at efficiency actually have a strong negative impact when debugging and maintenance are considered. We should forget about small efficiencies, say about 97% of the time: premature optimization is the root of all evil. Yet we should not pass up our opportunities in that critical 3%." Donald Knuth in "Structured programming with GoTo statement".

For sure, the implementation of the collision algorithm is in the critical 3%, as it is repeated more then 10^8 times per one update of the lattice.

With some knowledge of C compiler, we could do better, but for our own applications, this should be enough.

11.1 Implementation of the collision algorithm

```
// The node consists of 8 cells represented by single bits on the
    first, second, ... and eighth position.
#define A 1
#define B 2
#define C 4
#define D 8
#define E 16
#define F 32
#define G 64
#define H 128

/* To iterate over the cells, we arrange it in the char */
unsigned char cell[8] = {A, B, C, D, E, F, G, H};

/* The definition of the type Node. It consists of 8 mass bits (char
    m) and 3x8 momentum bits (char p[3]). It the node is part of the
    obstacle, node.o == 1. */
typedef struct
{
   unsigned char m;
   unsigned char p[3];
   int o;
} Node;
// Sure. char would be enough for and obstacle, but does not 64 bit
    processor prefer to manage 64 bit structures (m + p[3] + o = 64
    bits)?

// 3 directions (X, Y, Z), 4 pair-interactions in each direction, 2
    cells in each pair
unsigned char Pair[3][4][2] =
```

```
{
   {
      {A,E}, {B,F}, {C,G}, {D,H}
   },
   {
      {A,C}, {B,D}, {E,G}, {F,H}
   },
   {
      {A,B}, {C,D}, {E,F}, {G,H}
   }
};

// Finally we have have everything prepared for the collision
    algorithm.
Node collision(Node node)
{
   //mass
   unsigned char m = node.m;

   //momentum
    unsigned char * p = node.p;

   //d,u ... index for downer and upper momentum
   int d,u;

   // l, r ... left/right cell in the pair
   // ml, mr are non-zero, if there is a particle in the left/right
       cell of the pair (mass-left, mass-right)
   // lu, ld, ru, rd ... momenta of the particles (left-upper,
       left-downer, right-upper, right-downer)
   unsigned char l, r, ml, mr, lu, ld, ru, rd;

   for (int i = 0; i < 3; ++i)
   {
      d = (i+1) % 3;
      u = (i+2) % 3;
      for (int j = 0; j < 4; ++j)
      {
         l  = Pair[i][j][0];
         r  = Pair[i][j][1];

         ml = m&l;
         mr = m&r;
         ld = p[d]&l;
         lu = p[u]&l;
         rd = p[d]&r;
         ru = p[u]&r;

         /* PAIR INTERACTIONS */
         // case 6a
         if (ml && mr)
```

```
{
   if (lu && ru && !ld && !rd)
   {
      p[d] |= l;
      p[d] |= r;
   }
   //case 6b
   else if (lu && ru && ld && rd)
   {
      p[d] ^= l;
      p[d] ^= r;
   }
   //case 7a
   else if (ld && !lu && ru && rd)
   {
      p[d] ^= l;
      p[u] |= l;
      p[d] ^= r;
      p[u] ^= r;
   }
   else if (ld && lu && !ru && rd)
   {
      p[d] ^= l;
      p[d] ^= r;
      p[u] ^= l;
      p[u] |= r;
   }
   //case 7b
   else if (!ld && lu && !ru && !rd)
   {
      p[d] |= l;
      p[d] |= r;
      p[u] ^= l;
      p[u] |= r;
   }
   else if (!ld && !lu && ru && !rd)
   {
      p[d] |= l;
      p[d] |= r;
      p[u] |= l;
      p[u] ^= r;
   }
   //case 8a
   else if (ld && !lu && ru && !rd)
   {
      p[u] |= l;
      p[u] ^= r;
   }
   else if (!ld && lu && !ru && rd)
   {
      p[u] |= r;
```

```
            p[u] ^= l;
        }
        //case 8b
        else if (ld && lu && !ru && !rd)
        {
            p[u] |= l;
            p[u] ^= r;
        }
        else if (!ld && !lu && ru && rd)
        {
            p[u] |= r;
            p[u] ^= l;
        }
        //case 9a
        else if (!ld && !lu && !ru && !rd)
        {
            p[d] |= l;
            p[d] |= r;
        }
        //case 9b
        else if (ld && rd && !lu && !ru)
        {
            p[d] ^= l;
            p[d] ^= r;
        }
    }
    //case 10a
    else if (!ml && mr && ru && !rd)
    {
        m |= l;
        m ^= r;
        p[u] ^= r;
        p[u] |= l;
        if (p[i]&r)
        {
            p[i] ^= r;
            p[i] |= l;
        }
    }
    //case 10b
    else if (ml && !mr && lu && !ld)
    {
        m ^= l;
        m |= r;
        p[u] ^= l;
        p[u] |= r;
        if (p[i]&l)
        {
            p[i] ^= l;
            p[i] |= r;
        }
```

```
            }
            //case 11a
            else if (!ml && mr && !ru && !rd)
            {
               m |= l;
               m ^= r;
               if (p[i]&r)
               {
                  p[i] ^= r;
                  p[i] |= l;
               }
            }
            //case 11b
            else if (ml && !mr && !lu && !ld)
            {
               m |= r;
               m ^= l;
               if (p[i]&l)
               {
                  p[i] ^= l;
                  p[i] |= r;
               }
            }
         }
      }
      node.m = m;
      for(int i = 0; i < 3; ++i)
         node.p[i] = p[i];
      return node;
}

// This function resolves the collisions for all nodes on the lattice.
// This is the function we call from main().
void Collision(Node***array, int X, int Y, int Z, int start)
{
   int x,y,z;

#pragma omp parallel for private (x,y,z)
   for (x = start; x < X; x+=2)
   {
      for(y = start; y < Y; y+=2)
      {
         for(z = start; z < Z; z+=2)
         {
            if(array[x][y][z].o)
               break;
            array[x][y][z] = collision(array[x][y][z]);
         }
      }
   }
}
```

11.2 Implementation of the Propagation

Before we comment on the implementation, we want to emphasize one of the strong sides of PI automaton.

In FCHC, the lattice consisted of all the nodes with the discrete Cartesian coordinates (up to some upper boundary denoted by X, Y, Z). All of these nodes were interconnected and formed single lattice.

But the same lattice for Pair-Interaction automaton would contain 4 independent sub-lattices.

Let us consider node that has all Cartesian indices odd. It is connected to 8 nodes that have even Cartesian indices (because lattice vectors for PI are exclusively ± 1). These nodes create one of the four sub-lattices.

Another thing is, that we can avoid spurious Zannetti invariants if, for example, nodes with even indices are occupied at even time steps, and odd nodes at odd times. (for more on Zanneti invariants, see page blabla in [2]).

This gives us additional speed-up in computation, as we do not need two distinct lattices for FCHC (or FHP).

```
/* Group of cells that propagates in X-direction, Y-direction and
   Z-direction respectively. */
#define dirX (B+D+F+H)
#define dirY (E+F+G+H)
#define dirZ (A+B+E+F)
/* For example, because A & dirX == 0, particle in the cell A
   propagates in -X direction,
   but A & dirZ == 1, so it propagates in (positive) Z direction. */

// Implements periodic boundary condition.
// If index n flows under 0 or over upper boundary N, we assign it
   value from the other side of boundary.
int PeriodicBC(int n, int N)
{
   if (n<0) return N-1;
   else if (n<N) return n;
   // else n==N
   else return 0;
}

/* This function propagates particles among the nodes. */
/* If start == 0, we are at the even time step. Then it propagates
   from nodes with even indices (e.g. at position [0,2,124] on the
   lattice) to the nodes with odd indices (e.g. to the [1,1,123] etc).
   */
/* If start == 1, we are at the odd time step. Then it propagates from
   odd indices to the even indices. */

void Propagation(Node***array, int X, int Y, int Z, int start)
{
   Node node;
   unsigned char m;
   unsigned char*p;
```

```
    int x, y, z;
   int xN, yN, zN;
   int c, i;

#pragma omp parallel for private (m, p, x, y, z, xN, yN, zN, c, i)
   // Depending on start, we go through odd or even nodes
    for(x = start; x < X; x+=2)
   {
      for(y = start; y < Y; y+=2)
      {
         for(z = start; z < Z; z+=2)
         {
            // mass of the cells in the node (tells us which cells are
                occupied)
            m = array[x][y][z].m;
            // momentum of the particles in the node
            p = array[x][y][z].p;

            // we look at each cell in node
            for (c = 0; c < 8; ++c)
            {
               //if there is particle in the cell, we want to propagate
                   it to corresponding node
               if(m & cell[c])
               {
                  // if particle from cell[c] propagates in positive
                      direction of X
                  if (cell[c] & dirX)
                     xN = PeriodicBC(x+1,X);
                  // else particle propagates in negative direction of x
                  else
                     xN = PeriodicBC(x-1,X);
                  if (cell[c] & dirY)
                     yN = PeriodicBC(y+1,Y);
                  else
                     yN = PeriodicBC(y-1,Y);
                  if (cell[c] & dirZ)
                     zN = PeriodicBC(z+1,Z);
                  else
                     zN = PeriodicBC(z-1,Z);

                  // if there is obstacle in the new node,
                  // it stays in the old node, but we reflect it to
                      diagonal cell
                  if( array[xN][yN][zN].o )
                  {
                     array[xN][yN][zN].m |= cell[7-c];
                     for (i = 0; i < 3; ++i)
                     {
                        if(p[i] & cell[c])
                           array[xN][yN][zN].p[i] |= cell[7-c];
```

```
                    }
                    /*particles disappear on 0 and Z-1 */
                    // this holds in this particular computation

                    if(zN == 0 || zN == Z-1)
                    {
                       array[xN][yN][zN].m = 0;
                       for (int i = 0; i < 3; ++i)
                       {
                          array[xN][yN][zN].p[i] = 0;
                       }
                    }
                 }
                 else //if there is no obstacle in the new node, we
                     propagate particle to the new node
                 {
                    array[xN][yN][zN].m |= cell[c];
                    for(i = 0; i < 3; ++i)
                    {
                       if(p[i] & cell[c])
                          array[xN][yN][zN].p[i] |= cell[c];
                    }
                    /*particles disappear on the 0 and X-1 */

                    if (zN == 0 || zN == Z-1)
                    {
                       array[xN][yN][zN].m = 0;
                       for (i = 0; i < 3; ++i)
                          array[xN][yN][zN].p[i] = 0;
                    }
                 }
              }
           }
           //in the old array, we set the node to 0
           array[x][y][z].m = 0;
           for(i = 0; i < 3; ++i)
           {
              array[x][y][z].p[i] = 0;
           }
        }
     }
  }
}
```

---

h

12. Non-deterministic PI

Pair-Interaction that Nasilowski proposed is deterministic, and it might be considered to be its advantage. The collision (usually) leads to the maximal change of the state, that minimizes the viscosity (as we previously discussed). Moreover, it offers theoretical ground for using Gibbs distribution in derivation of macroscopic equations.

But let us explore following examples. First, consider node with one standing particle.

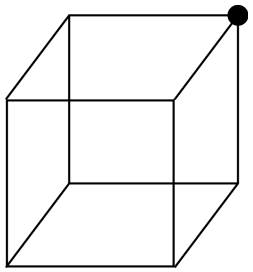

Figure 12.1: Node before collision

By deterministic pair-interactions in X,Y and Z direction, it is always resolved into the state

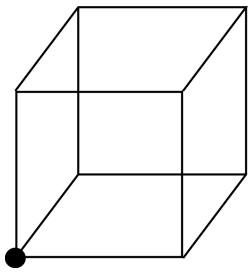

Figure 12.2: Node after deterministic collision

But it is no better then

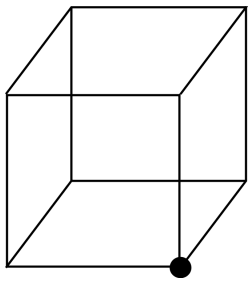

Figure 12.3: Another acceptable state after collision

or any other state with one standing particle.

Even better example is the node with two particles with momenta in X direction.

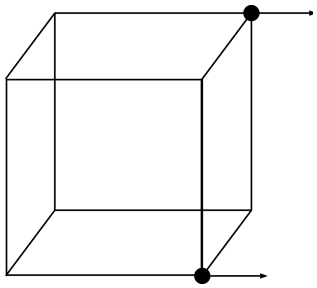

Figure 12.4: Node before collision, and after deterministic collision

The deterministic collision do not change its state (pair interaction in Y direction, followed by pair interaction in Z direction leads to the same state for this particular example).

However, collision that would be non-deterministic (let's say that pair interaction happens with probability 1/2) can lead to the following state

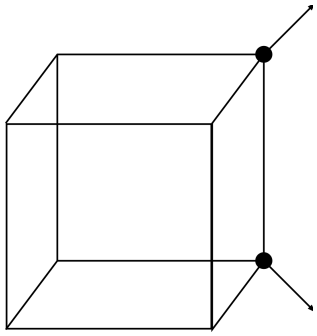

Figure 12.5: Node after non-deterministic collision

where both particles gained additional momenta, one in Z, and other in -Z direction. We could continue with the examples showing that deterministic PI do not realize all available states, even though some of them are more desirable.

Also, by chosing one of the many available states by non-deterministic PI, we believe that statistical avareging might work faster and lead to better results when statistical properties of the flow are inspected.

On the other hand, non-deterministic model, has one obvious drawback. Generation of random numbers is costy process and significantly slows down the collisions (although it might be cheated, we prefer to try honest non-deterministic model, then we can optimize).

The non-deterministic automaton was achieved by simple modification of the collision algorithm.

```
void Collision(Node***array, int X, int Y, int Z, int start)
{
  /* Rundom numbers are generated by Mersen-Twister pseudo-random
     generator */
  random_device rd;
```

```
   mt19937 rng(rd());

   /* As there are 12 pair interactions per one collision, we want to
      generate 12 random bits with uniform distribution */
   int upper = pow(2, 12);
   uniform_int_distribution<int> uni(0,upper - 1);

   int r;
   int x,y,z;

#pragma omp parallel for private (x,y,z)
   for (x = start; x < X; x+=2)
   {
      for(y = start; y < Y; y+=2)
      {
         for(z = start; z < Z; z+=2)
         {
               r =  = uni(rng);
               array[x][y][z] = collision(array[x][y][z], r);
         }
      }
   }
}

/*  Comparing to deterministic collision function, it has second
    parameter ran */
/* first 12 bi
Node collision(Node node, int ran)
{
   //mass
   unsigned char m = node.m;

   //momentum
    unsigned char *p = node.p;

   //d,u ... index for downer and upper momentum
   int d,u;

   // l, r ... left/right cell in the pair
   // ml, mr ... particle in left/right cell is present (mass-left,
      mass-right)
   // lu, ld, ru, rd ... momenta of particles (left-upper, left-downer,
      right-upper, right-downer)
   unsigned char l, r, ml, mr, lu, ld, ru, rd;

   // For first pair-interaction, first bit is set to one, other bits
      are zero
   int count = 1;
   for (int i = 0; i < 3; ++i)
   {
      d = (i+1) % 3;
```

```
u = (i+2) % 3;
for (int j = 0; j < 4; ++j)
{
   /* If the ran has corresponding bit equal to 1, the
      pair-interaction go on, else it is skipped */
   if (!( ran &count))
   {
      count <<= 1;
      break;
   }
   count <<= 1;
   ....
   ....
   /* The rest of the function is not modified */
```

12.1 Exploding cube

To demonstrate the difference of deterministic and non-deterministic automaton in the crystal form, we simulated the "explosion of the cube".

The simulations were performed on the lattice $240 \times 240 \times 240$ nodes for deterministic PI, and for the slower non-deterministic PI, size of the domain was $120 \times 120 \times 120$. Periodic boundary conditions were used.

Into the cube with the side of the length 3 times smaller then the lattice (hence the volume of the cube was 1/27 of the lattice), we put particles into all available cells, with maximal momenta in all directions. Therefore, the total momentum of the particles is 0.

The evolution of the system for both versions of PI is to be seen on the following pictures.

The is only short excerpt of the evolution of deterministic PI, but the patterns you will se were repeating in the infinite loop. We performed simulation up to 9000 steps and the pattern did not change.

On the other hand, the pattern in the non-deterministic PI broke after first explosion already - see Figure 12.1.

Although the inertia of the bulk flow is present in the non-deterministic PI after many periods, it exhibits the realistic "spilling" of the particles, in contrast to the perfect evolution of deterministic automaton.

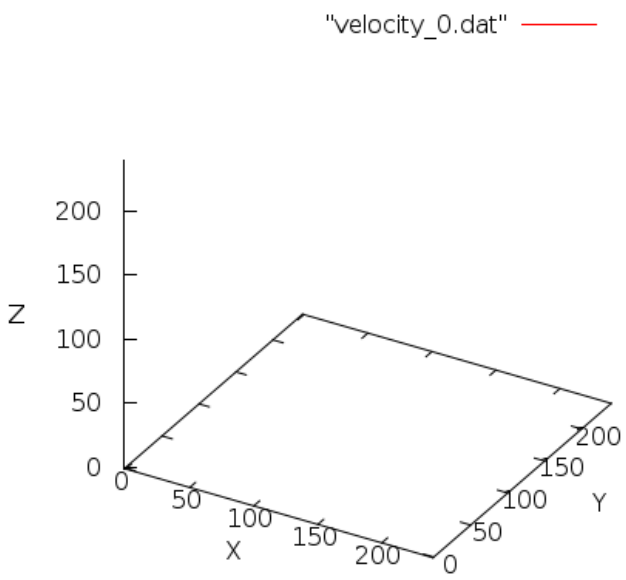

Figure 12.6: Deterministic PI - time 0

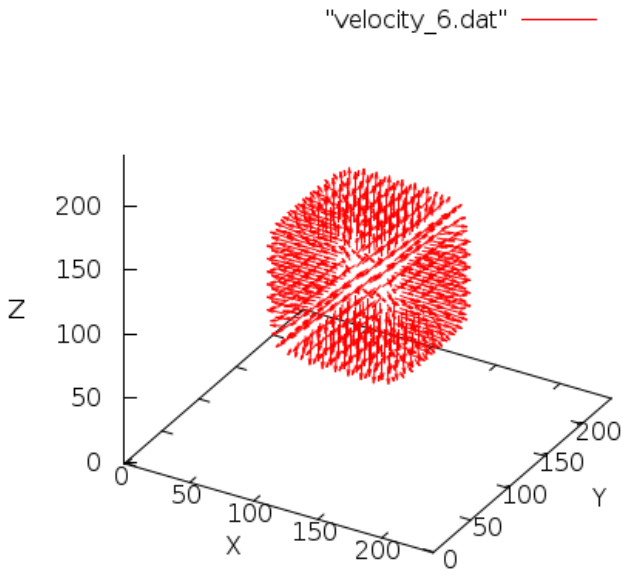

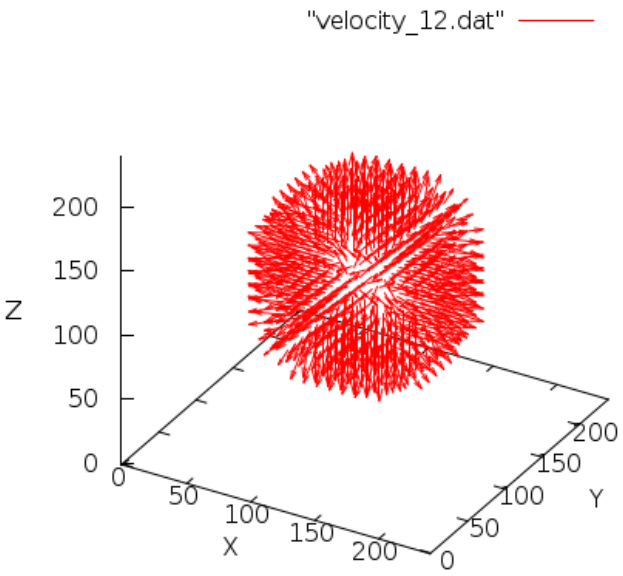

Figure 12.7: Deterministic PI - time 12

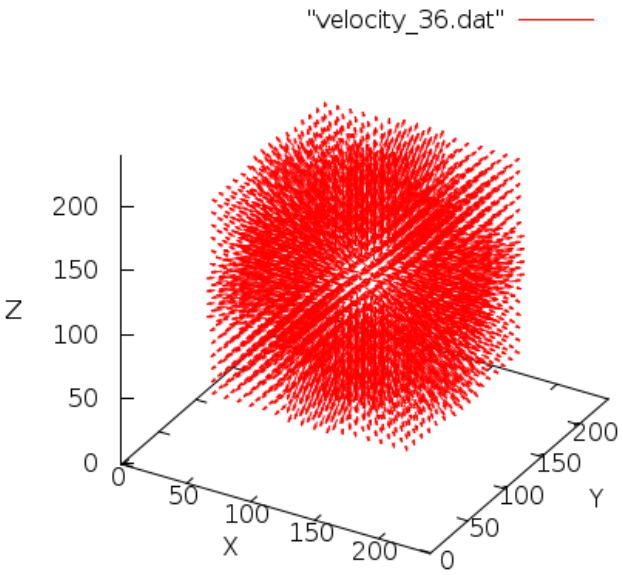

Figure 12.8: Deterministic PI - time 36

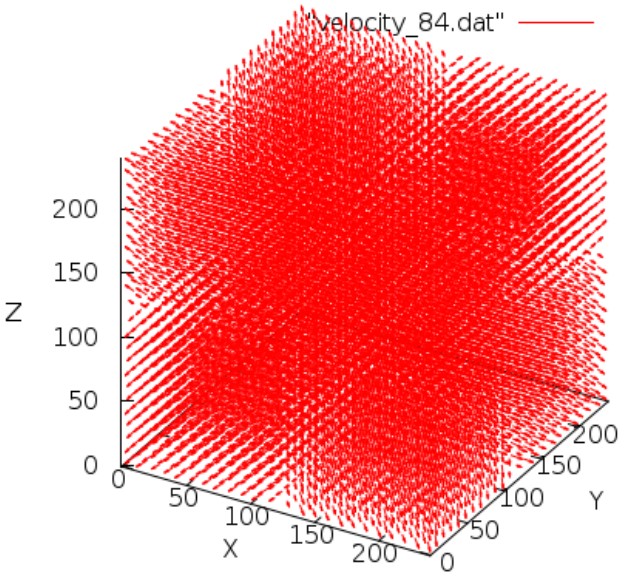

Figure 12.9: Deterministic PI - time 84

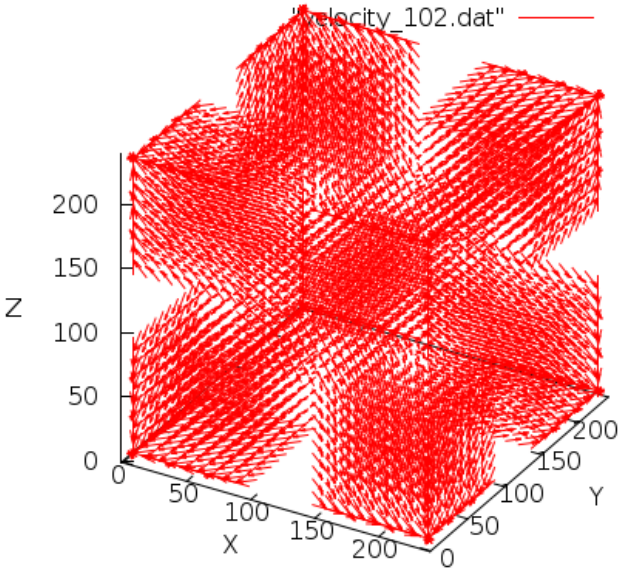

Figure 12.10: Deterministic PI - time 102

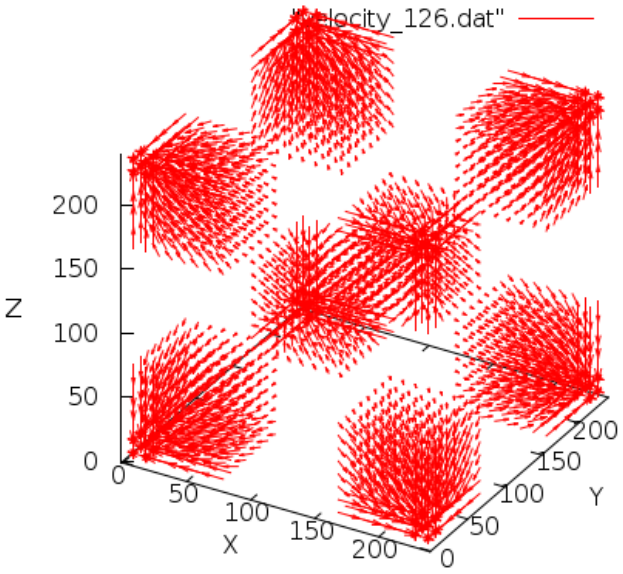

Figure 12.11: Deterministic PI - time 126

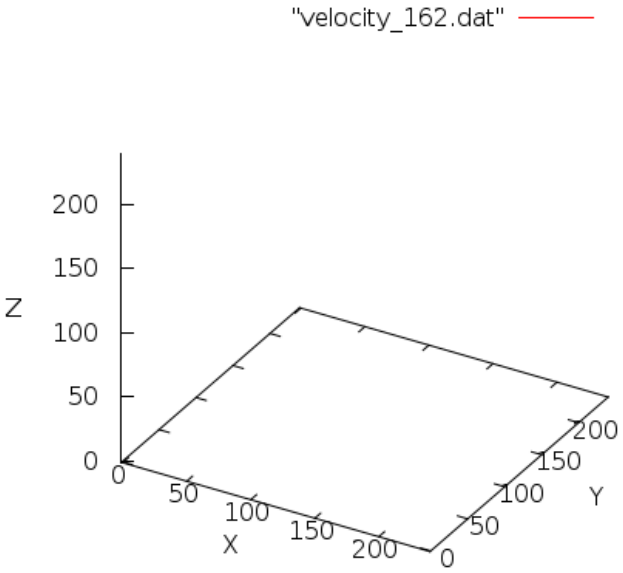

Figure 12.12: Deterministic PI - time 162

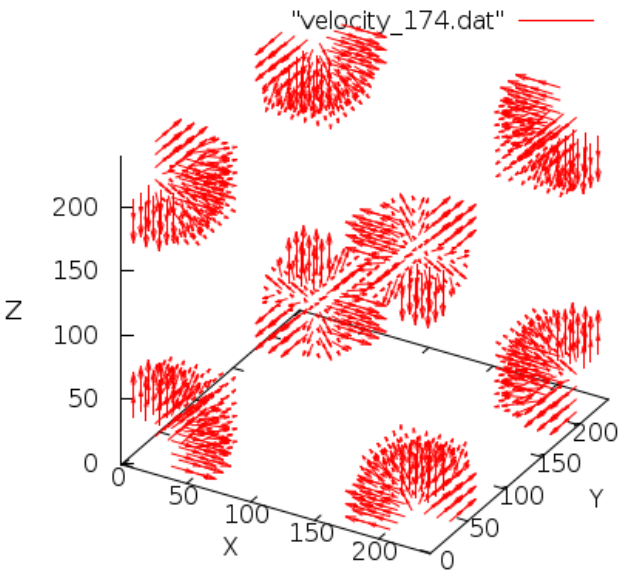

Figure 12.13: Deterministic PI - time 174

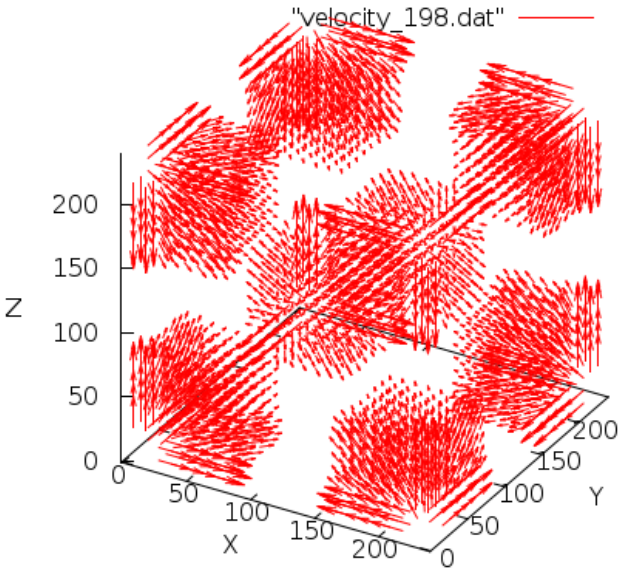

Figure 12.14: Deterministic PI - time 198

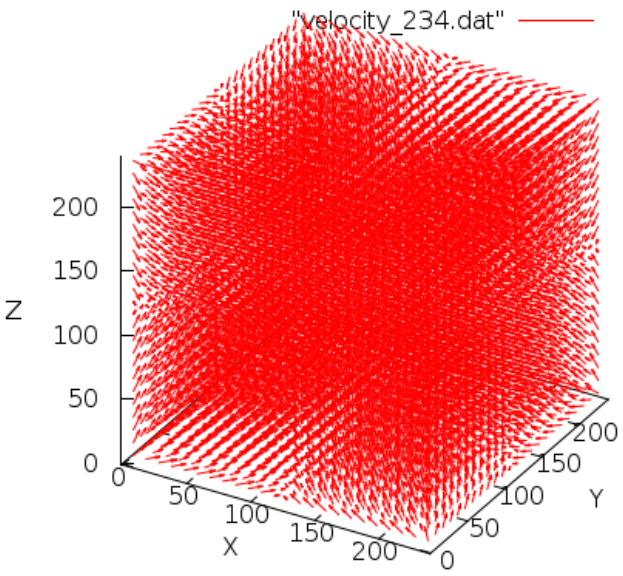

Figure 12.15: Deterministic PI - time 234

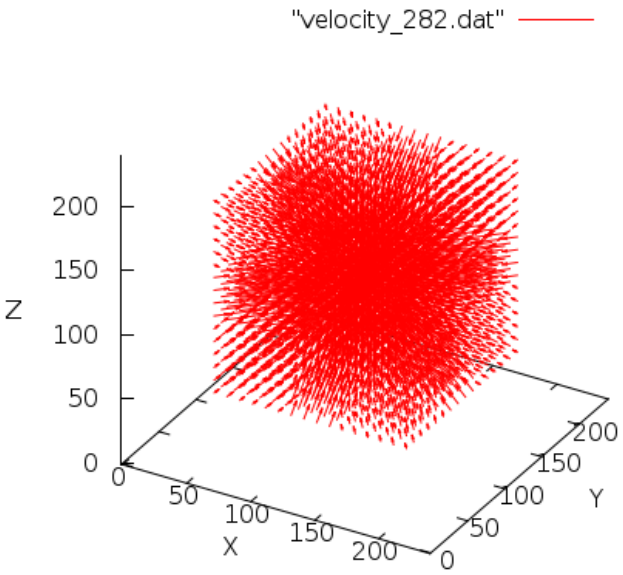

Figure 12.16: Deterministic PI - time 282

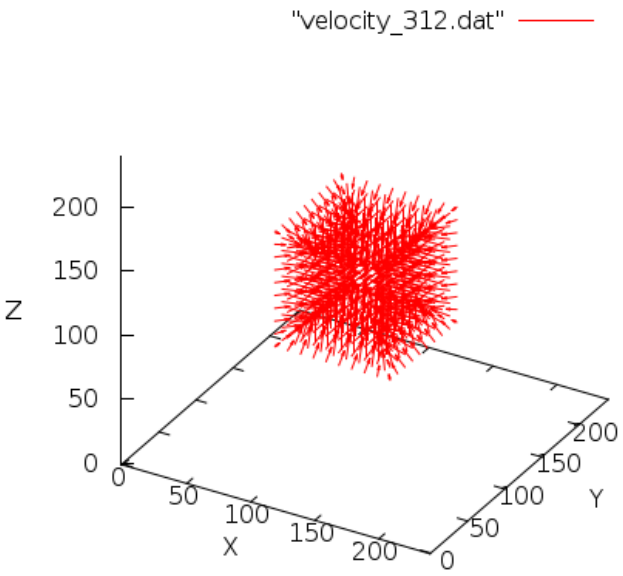

Figure 12.17: Deterministic PI - time 312

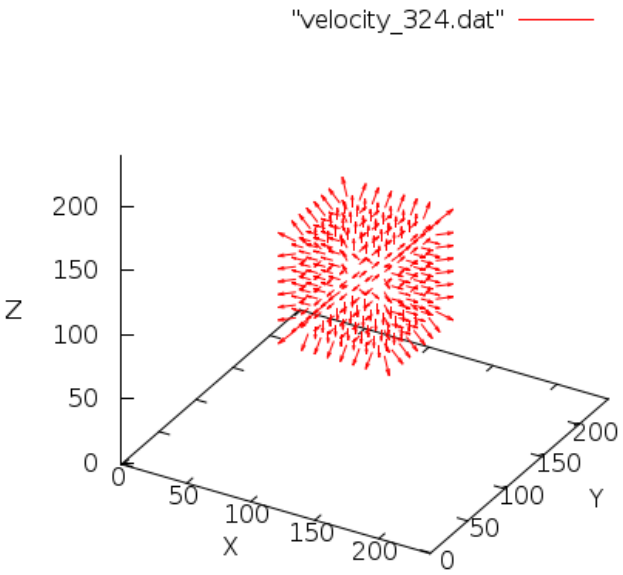

Figure 12.18: Deterministic PI - time 324

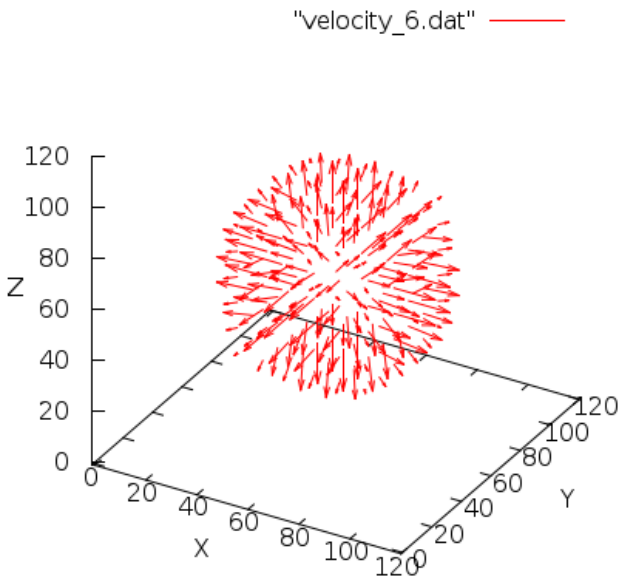

Figure 12.19: Non-deterministic PI - time 6

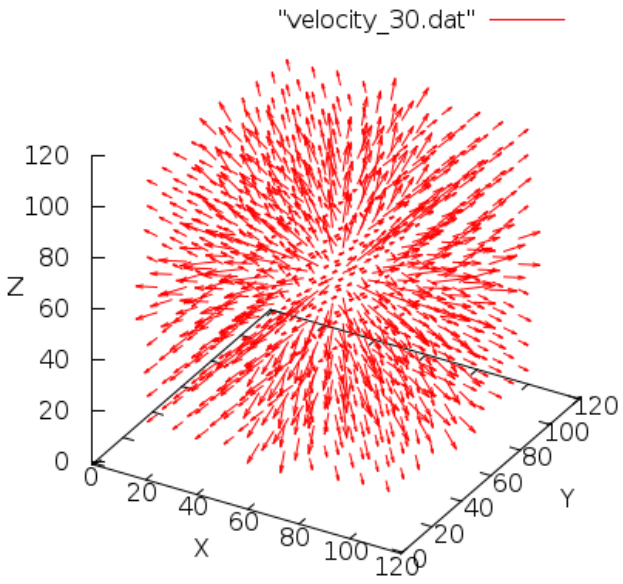

Figure 12.20: Non-deterministic PI - time 30

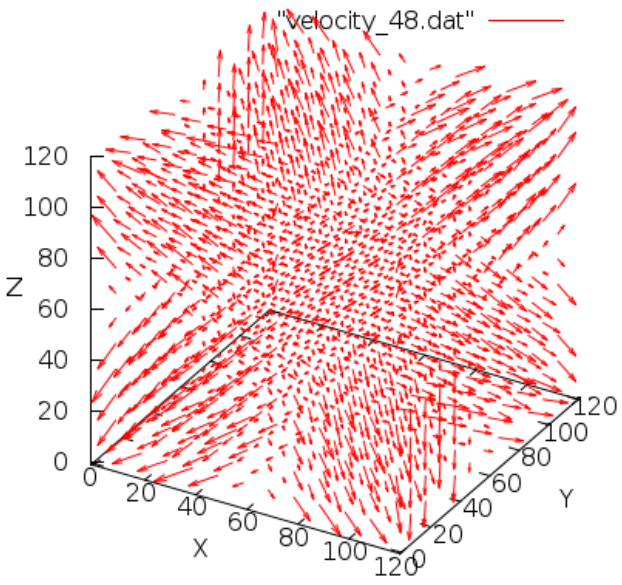

Figure 12.21: Non-deterministic PI - time 48

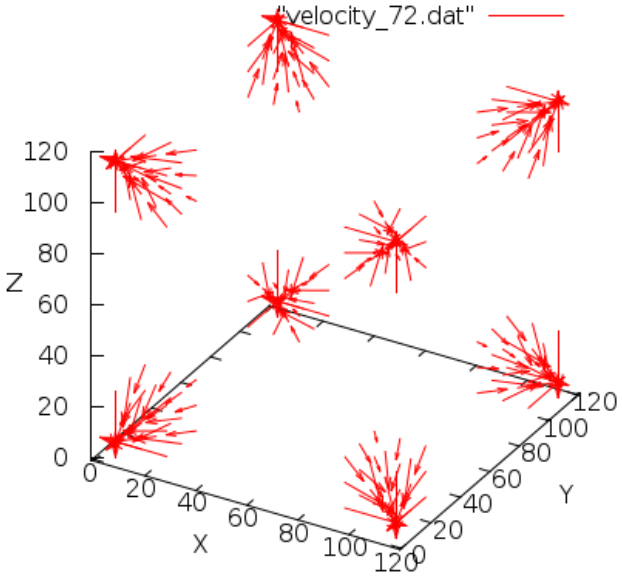

Figure 12.22: Non-deterministic PI - time 72

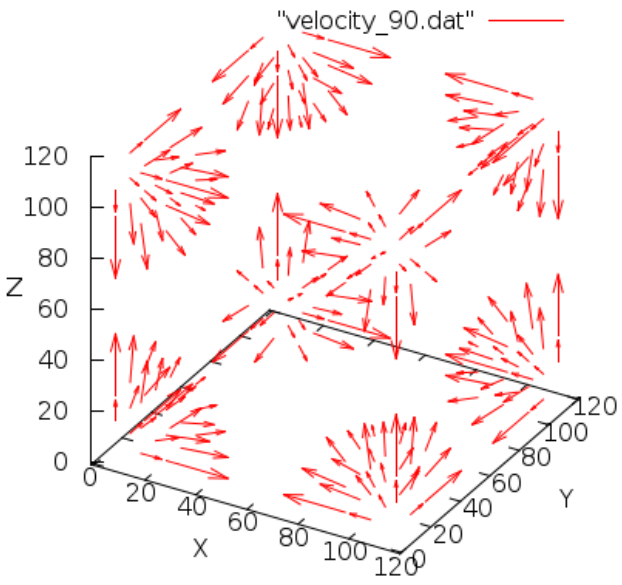

Figure 12.23: Non-deterministic PI - time 90

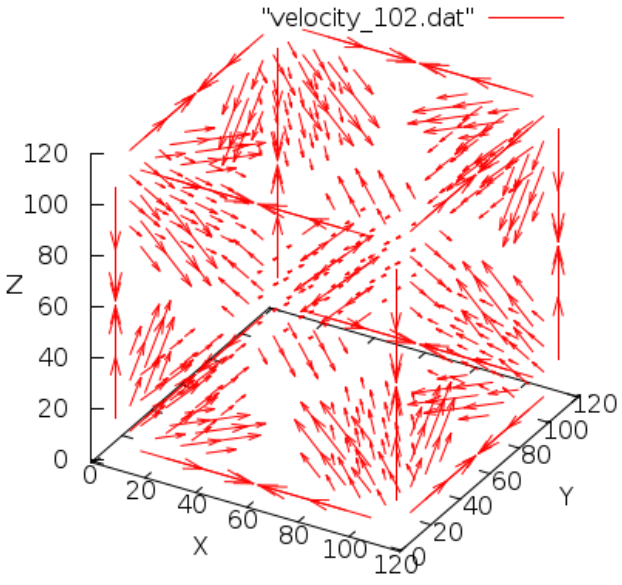

Figure 12.24: Non-deterministic PI - time 102

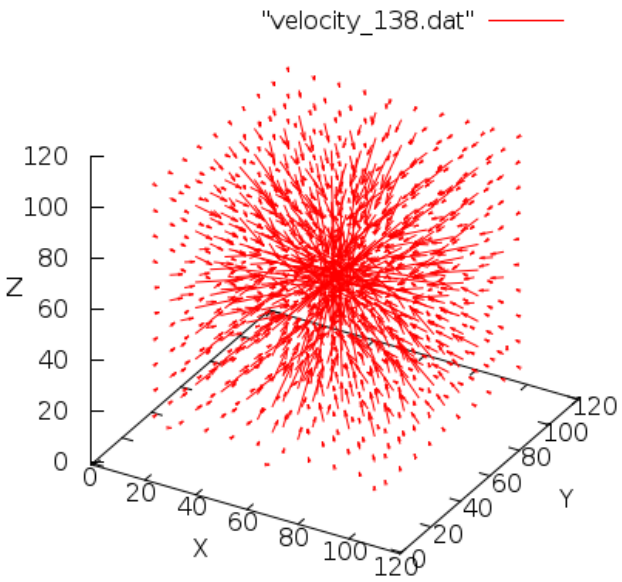

Figure 12.25: Non-deterministic PI - time 138

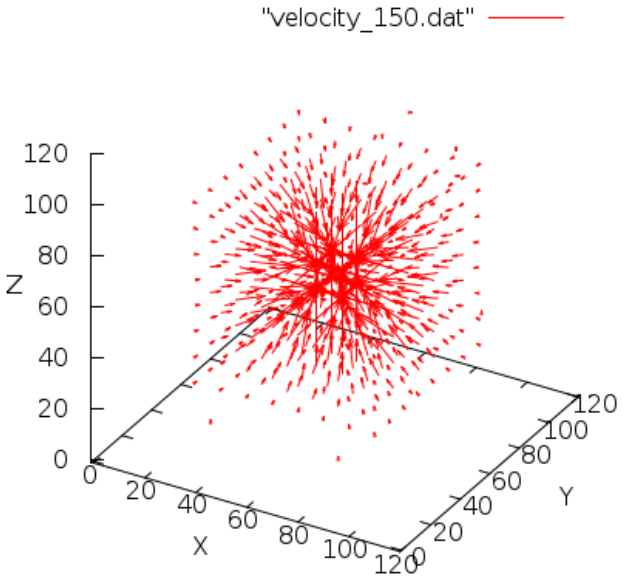

Figure 12.26: Non-deterministic PI - time 150

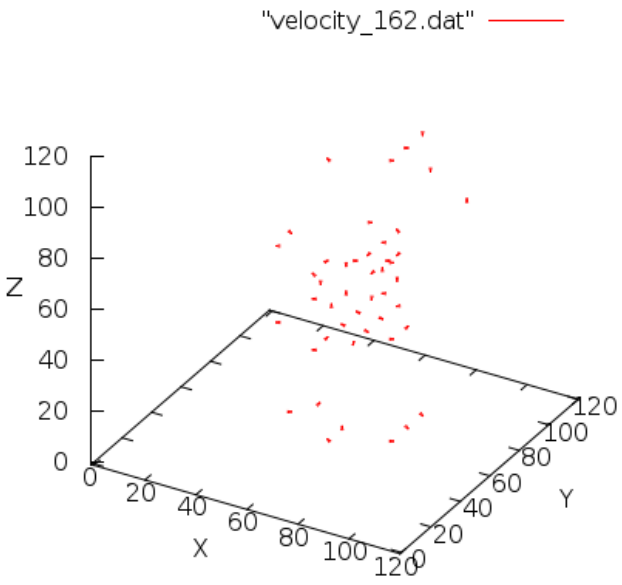

Figure 12.27: Non-deterministic PI - time 162

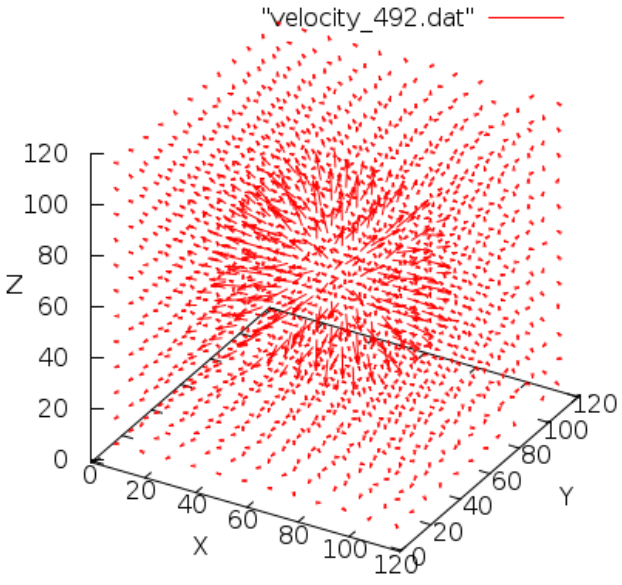

Figure 12.28: Non-deterministic PI - time 492

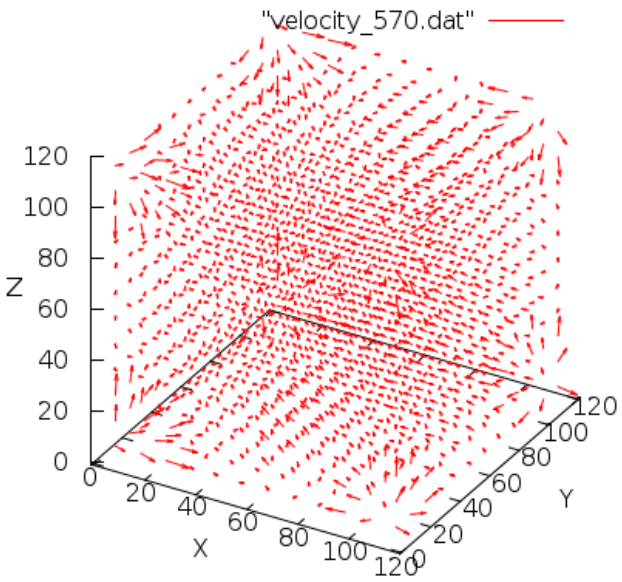

Figure 12.29: Non-deterministic PI - time 570

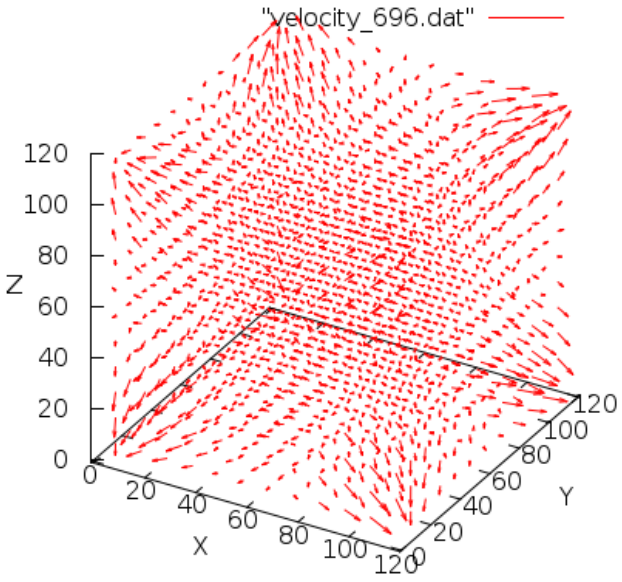

Figure 12.30: Non-deterministic PI - time 696

13. Study of the flow around the obstacles

In previous chapter, we explained microdynamics of FCHC and PI, that is non-physical. However, if we avarage velocities of the particles over sufficiently large region, we obtain physical velocity field.

The function that implements computation of velocity from LGCA lattice is simple and similar for FCHC and PI, so we comment only on FCHC implementation.

```
void compute_velocity(int***grid, double****v, int X, int Y, int Z,
    int side, int I, int J, int K)
{
   // We compute mean velocity over the cube with the side of length
      'side'.
   // N is the number nodes in this cube.
   double N = side*side*side;

   int i, j, k, l, m, n;

   int x, y, z;

#pragma omp parallel for private (i,j,k,l,m,n,x,y,z)

   for (i = 0; i < I; ++i)
   {
      for (j = 0; j < J; ++j)
      {
         for (k = 0; k < K; ++k)
         {
            for (x = i*side; x < (i + 1)*side; ++x)
            {
               for (y = j*side; y < (j + 1)*side; ++y)
               {
                  for (z = k*side; z < (k + 1)*side; ++z)
                  {
                     n = grid[x][y][z];
                     for (m = 0; m < 24; ++m)
                     {
                        if (n & C[m])
                        {
                           for (l = 0; l < 3; ++l)
                           {
                              v[i][j][k][l] += c[m][l];
                           }
                        }
                     }
                  }
```

```
            }
         }
         for (l = 0; l < 3; l++)
            v[i][j][k][l] /= N;
      }
   }
}
```

In the following section, we present the simulation of the flow around the spherical obstacle and round plate.

Particles with velocity in positive Z direction are created on a plain $z = 1$, and at the plain $z = Z - 1$ they propagate freely out of the tunnel.

The flow is actually happening in the tunnel with the square intersection. This tunnel is made of same 'material' as the obstacle, meaning that same no-slip condition holds at the tunnel and obstacle.

That no-slip condition holds at the obstacles can be seen from following excerpt of Propagation function (from FCHC, but same principle is applied in PI).

```
/* Particle at the cell C[i] propagates along the lattice vector c[i]
   to a new node. */
if (n & C[i])
{
   new_x = PeriodicBC(x + c[i][0], X);
   new_y = PeriodicBC(y + c[i][1], Y);
   new_z = PeriodicBC(z + c[i][2], Z);
   if (to[new_x][new_y][new_z] & OBS)
   /* However, if there is obstacle in that node, it gets to the cell
      Reverse[i], that is cell diagonal to the C[i]. Let's say it had
      velocity v1 = [1,0,-1,0], by reflection it gained velocity v2 =
      [-1,0,1,0]. In the next step, particle propagates back to the
      node where it came from. */
   /* Hence, the velocity at the obstacle is v1 + v2 = 0, so we really
      fulfilled no-slip condition. */
      to[new_x][new_y][new_z] |= Reverse[i];
   else
      to[new_x][new_y][new_z] |= C[i];
}
```

13.1 Flow around the sphere

We emphasize that the vector field is the physical velocity field. Each velocity vector is computed over $N = 80^3/8 = 64000$ nodes for PI and $N = 80^3 = 521000$ for FCHC (by the function $compute_velocity$ above).

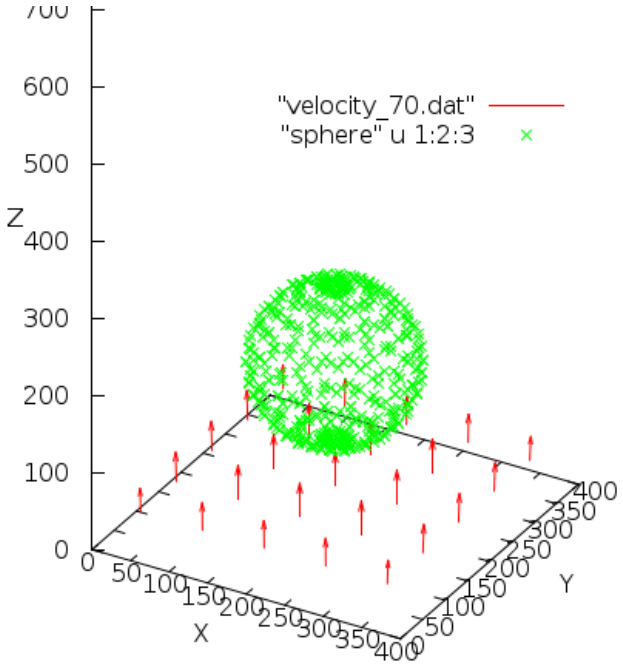

Figure 13.1: PI - flow around sphere, time 70

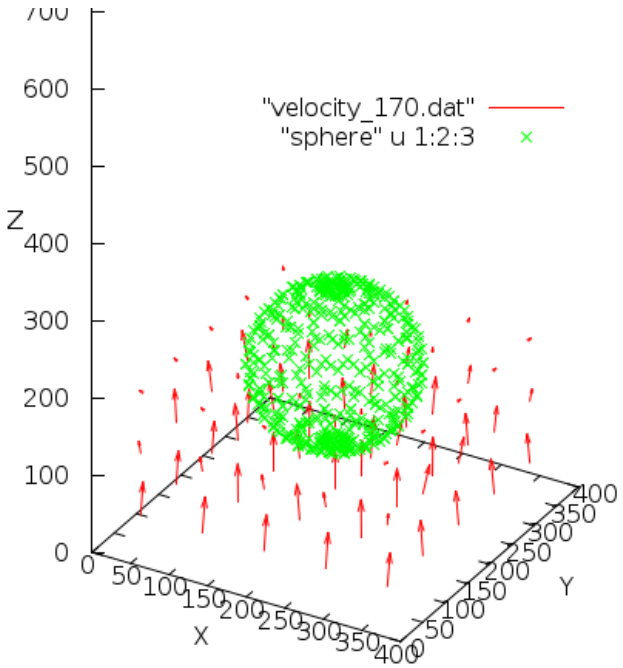

Figure 13.2: PI - flow around sphere, time 170

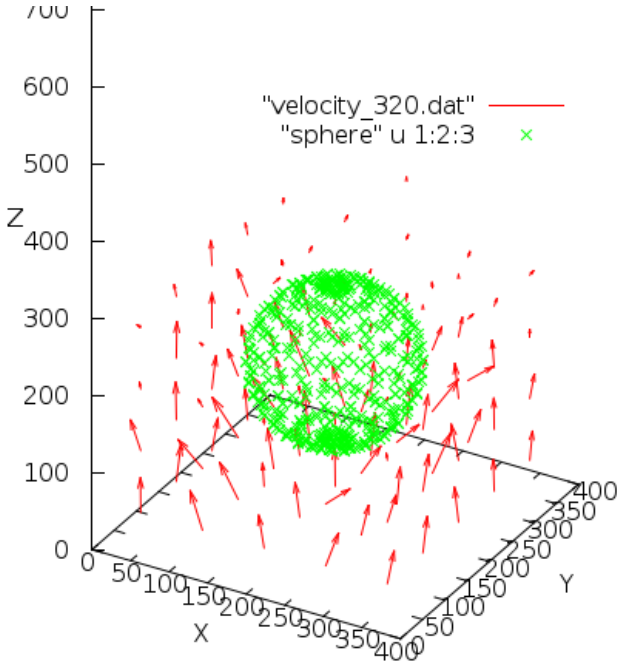

Figure 13.3: PI - flow around sphere, time 320

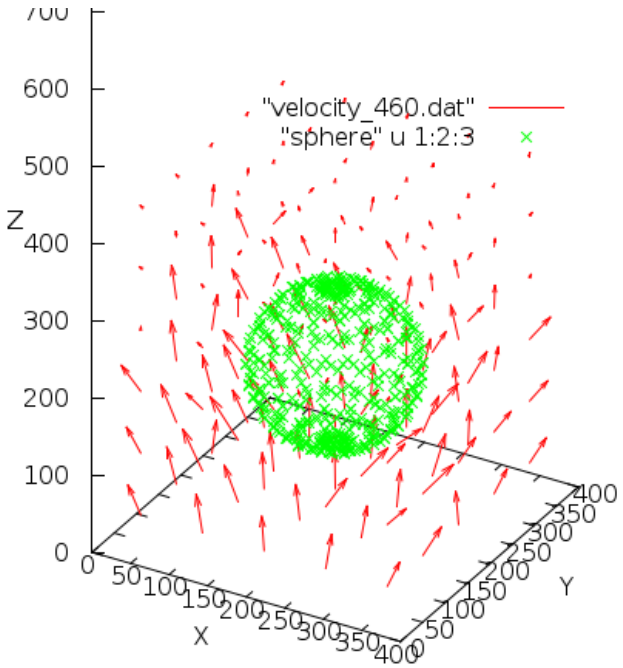

Figure 13.4: PI - flow around sphere, time 460

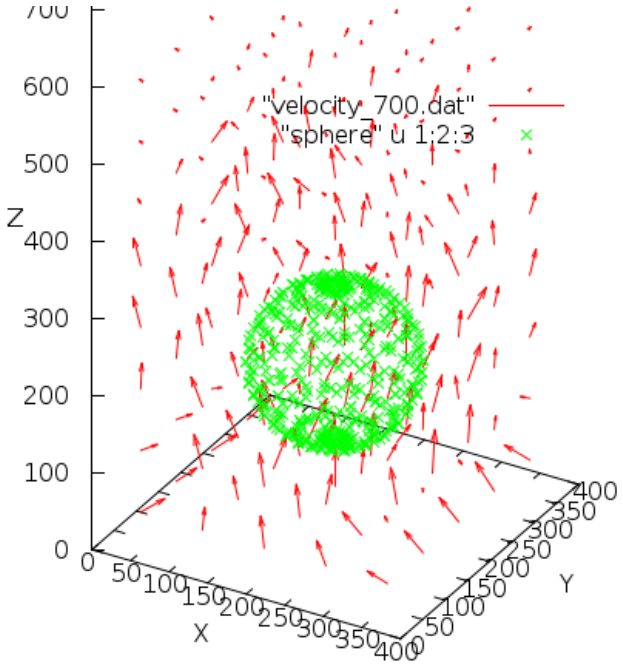

Figure 13.5: PI - flow around sphere, time 700

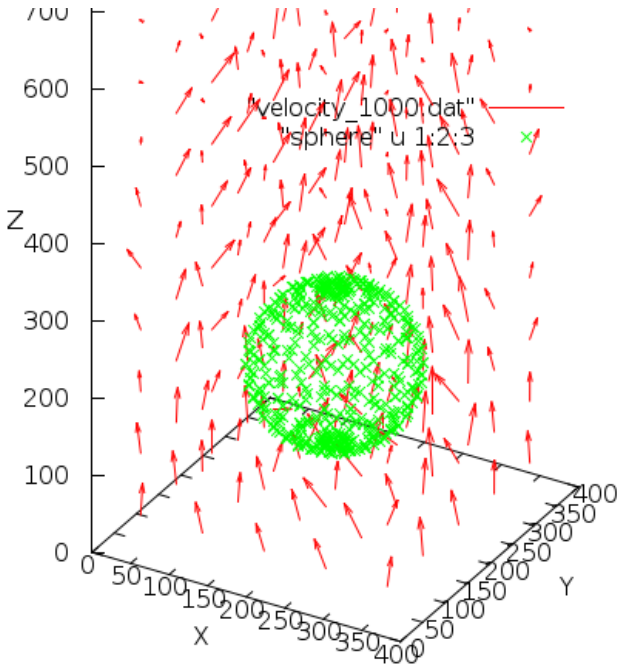

Figure 13.6: PI - flow around sphere, time 1000

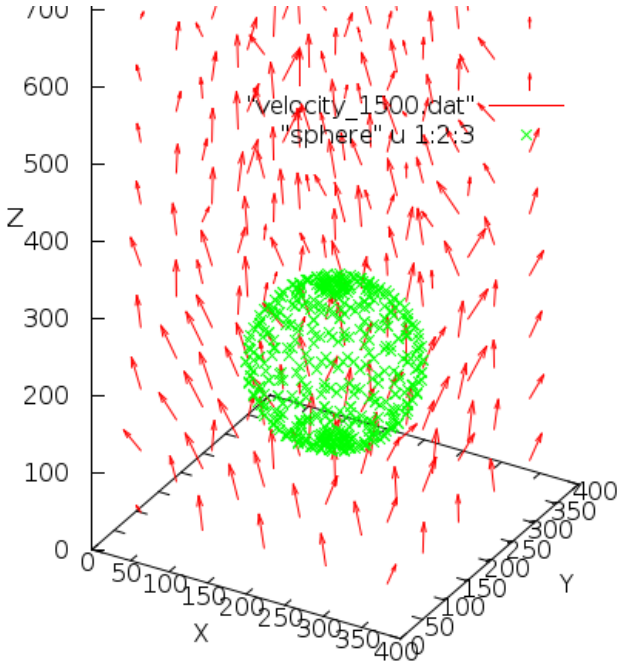

Figure 13.7: PI - flow around sphere, time 1500

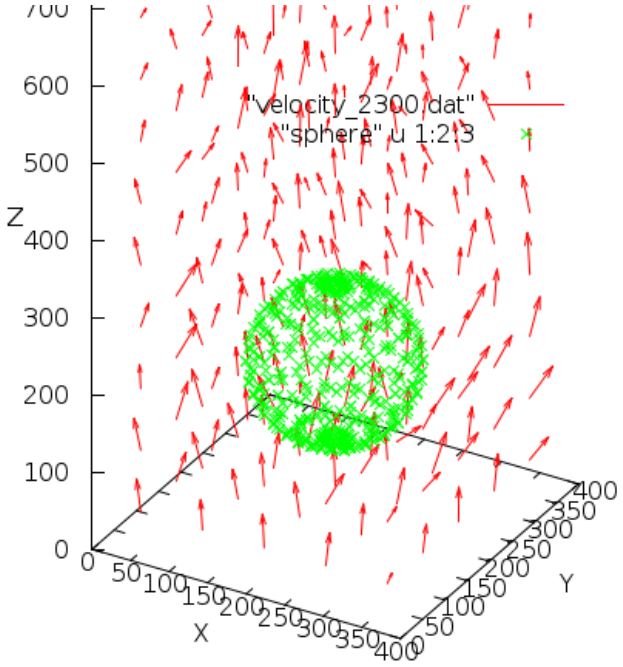

Figure 13.8: PI - flow around sphere, time 2300

13.2 Flow around the disk

Flow around the disk was performed on the Pair-interaction model only, the macroscopic velocity field was obtained by averaging over $N = 40^3/8 = 8000$ nodes.

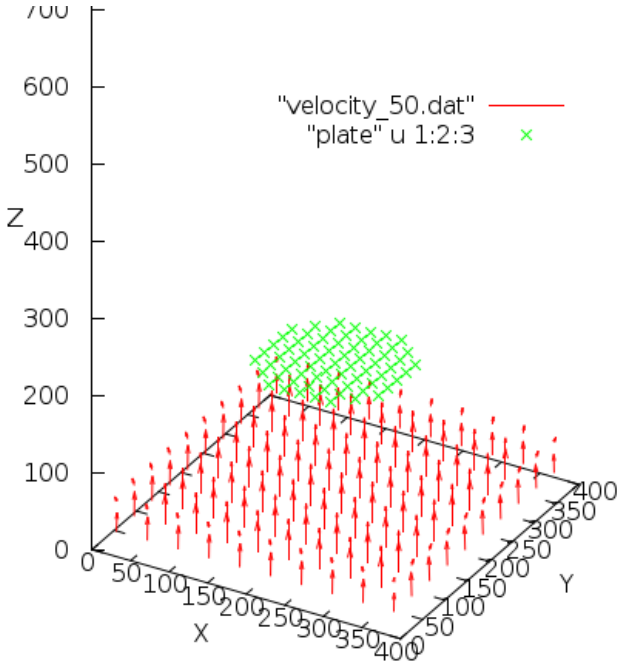

Figure 13.9: PI - flow around plate, time 50

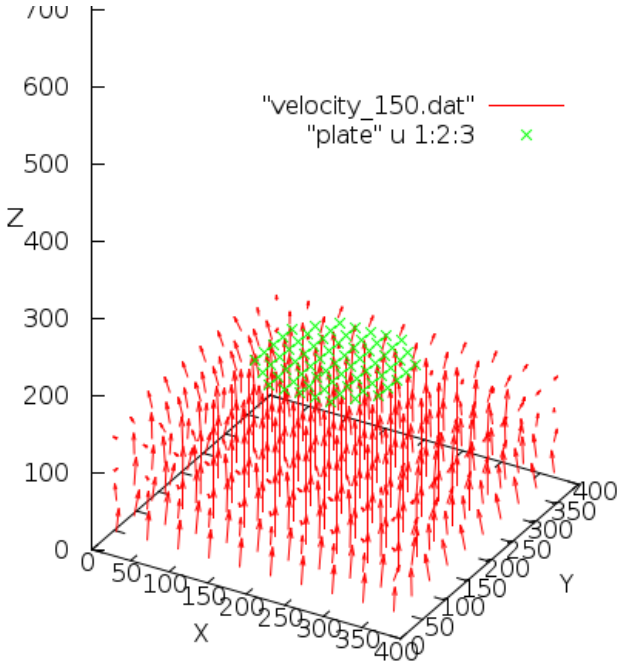

Figure 13.10: PI - flow around plate, time 150

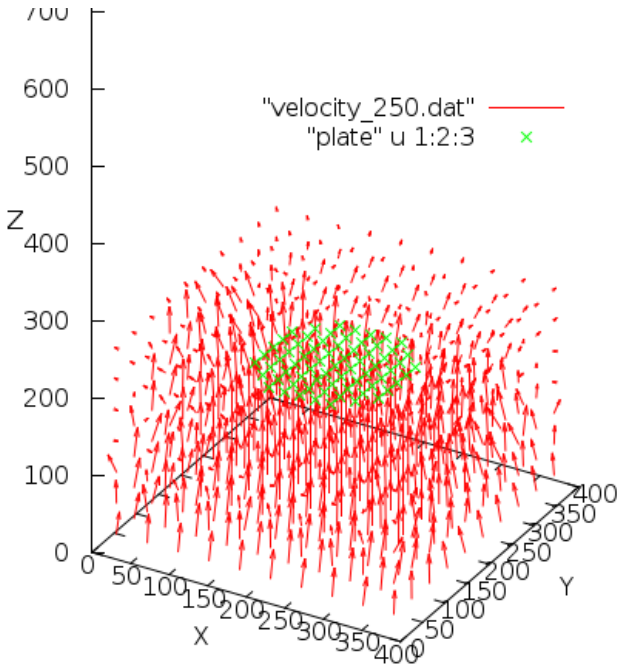

Figure 13.11: PI - flow around plate, time 250

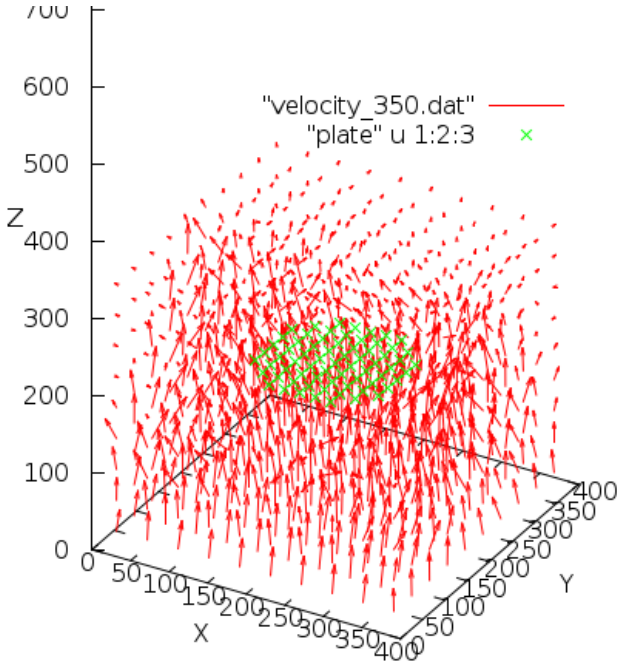

Figure 13.12: PI - flow around plate, time 350

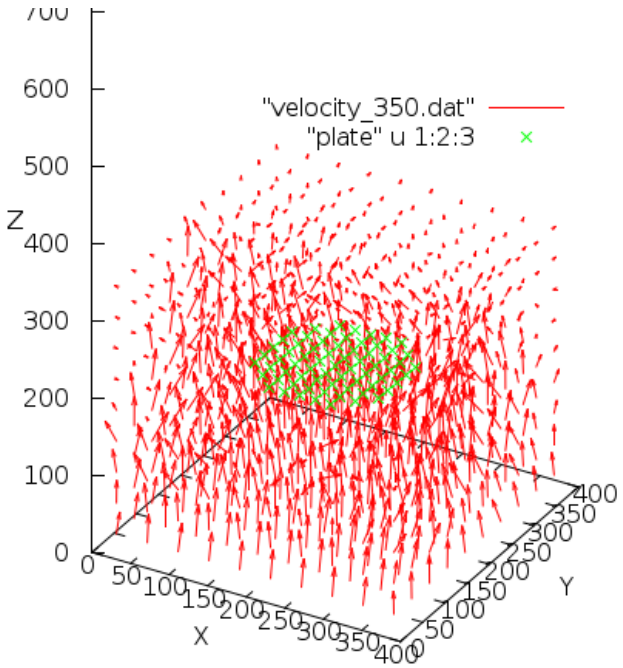

Figure 13.13: PI - flow around plate, time 350

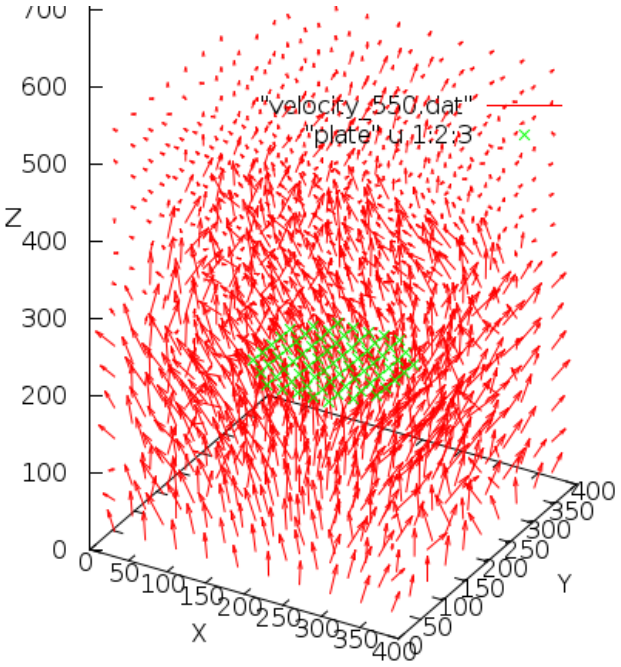

Figure 13.14: PI - flow around plate, time 550

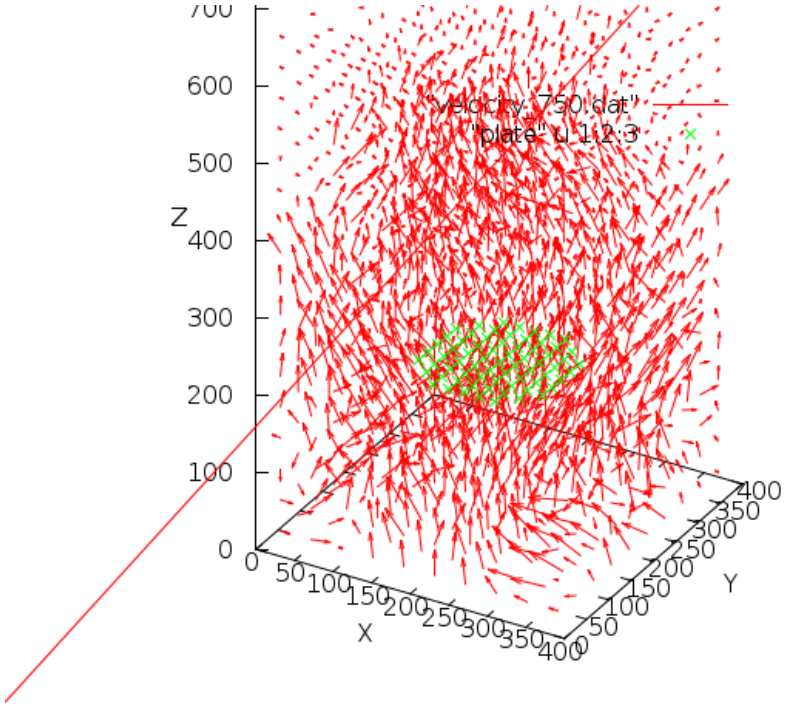

Figure 13.15: PI - flow around plate, time 750

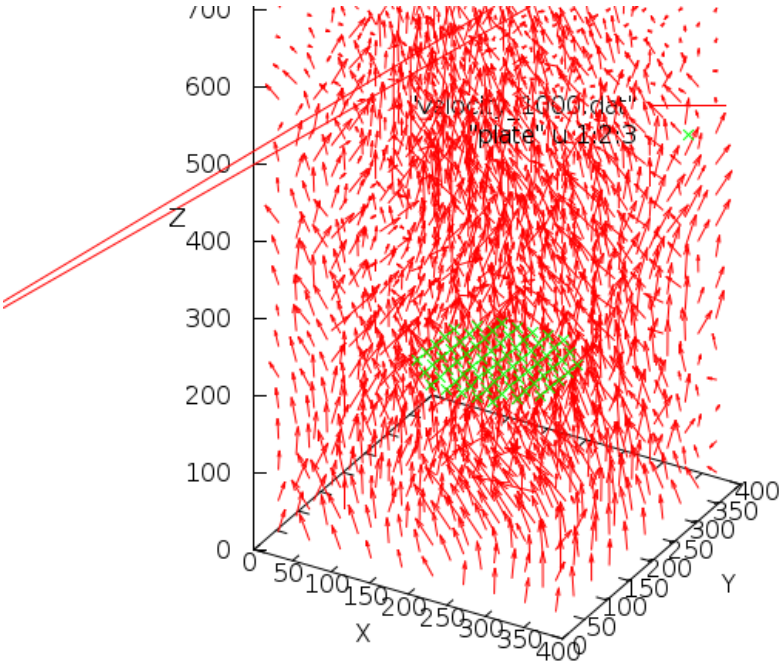

Figure 13.16: PI - flow around plate, time 1000

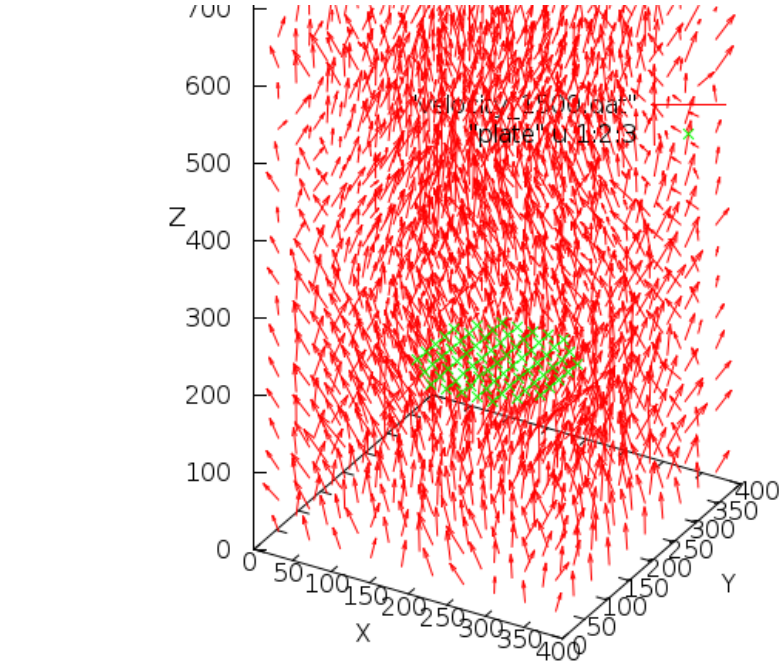

Figure 13.17: PI - flow around plate, time 1500

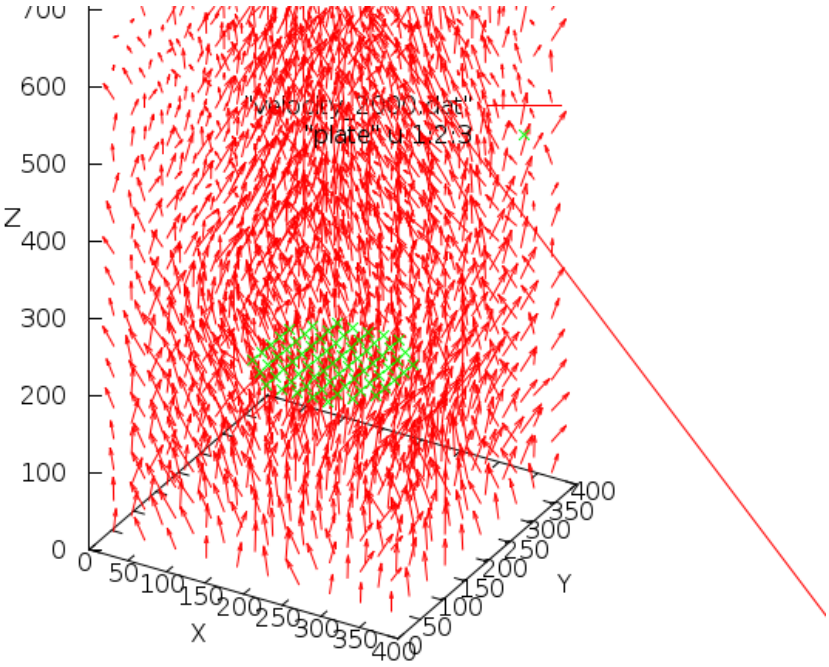

Figure 13.18: PI - flow around plate, time 2000

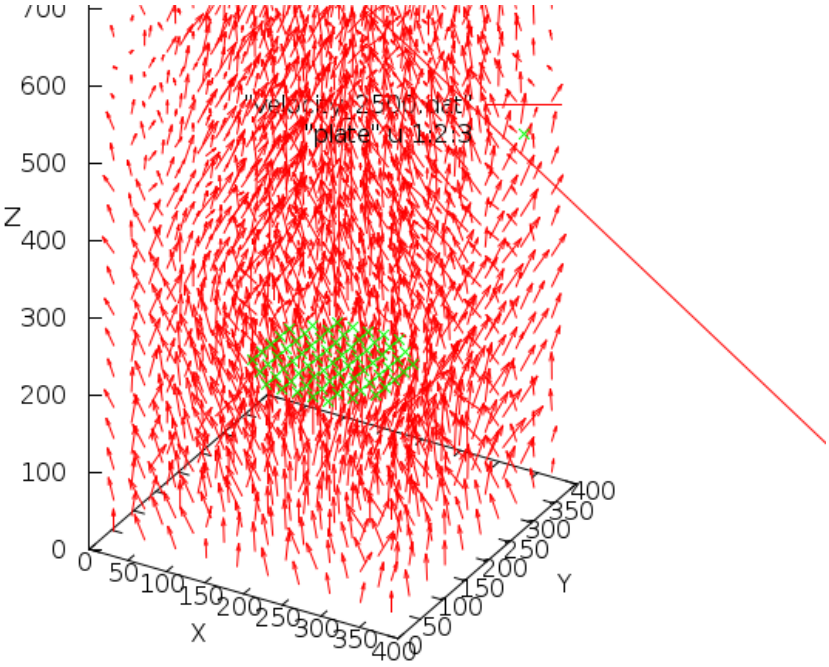

Figure 13.19: PI - flow around plate, time 2500

14. Fully developed turbulence simulated on LGCA

We are intending to simulate the fully developed turbulent flow using FCHC and PI-3D model and see how close we can get to the theoretical prediction of K41 theory and experimental results.

14.1 Inward flow on the sphere

To develop the turbulent flow that would be isotropic, we chose following setting for simulation:

1. We defined sphere with diameter 800 nodes.
2. Every time step, a new layer of the particles was created with the momenta directed into the middle of the sphere.
3. If the particle strayed out the sphere, it was forgotten.

Since the particles have discrete momenta, most of them cannot be directed from the sphere to the middle, but we can impose any direction on the mean flow (up to the precision allowed by coarse graining).

To see what directions of particle momenta are allowed, consider the cube inscribed in the sphere as on the figure 14.1.

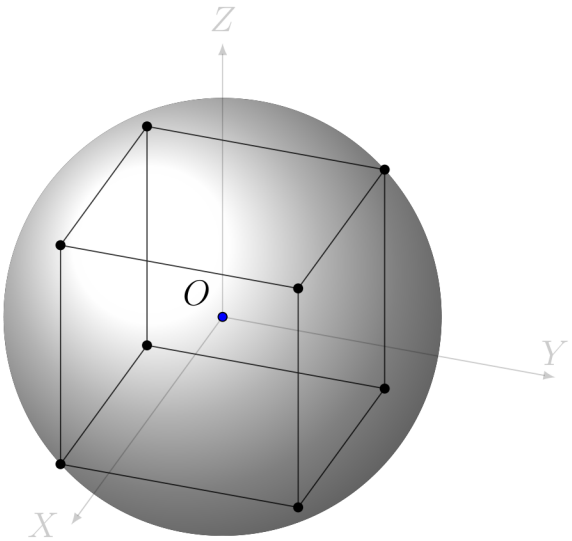

Figure 14.1: State of a node before collision

From a single node, we can direct particle in 26 basic direction, corresponding to the faces, edges and vertices of the cube.

Six directions correspond to the vectors, that are normal of the faces of the cube

$$[1,0,0],\ [-1,0,0],\ [0,1,0],\ [0,-1,0],\ [0,0,1],\ [0,0,-1]. \tag{14.1}$$

Eight directions corresponds to the "diagonal" vectors

$$[1,1,1],\ [-1,1,1],...,[-1,-1,-1] \tag{14.2}$$

and the other twelve vectors read

$$[1,1,0],\ [1,0,1],\ [-1,1,0],...,[0,-1,-1]. \tag{14.3}$$

Therefore, we divide the cube on the 26 surface areas. On each of these areas, particles have momentum in the direction corresponding to one of the vectors above, that points to the middle of the sphere.

Following figures indicate that setting described above results in the mean flow that is symmetric and directs to the middle of the sphere.

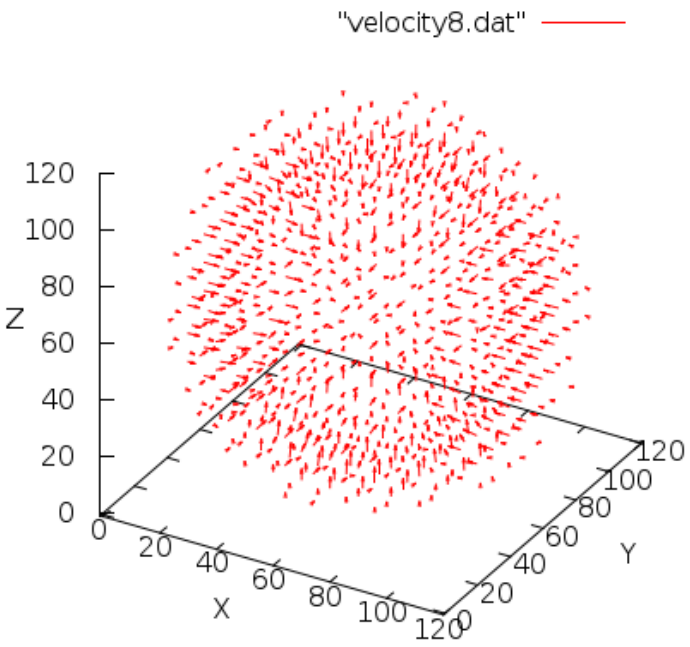

Figure 14.2: Velocity field at time 8 - FCHC inward flow

14.1.1 FCHC implementation of inward flow from the sphere

Functions that are imposing inward flow on the sphere are similar for PI and FCHC, so we explain the algorithm only on one of them.

```
// Cells in CELL_DIR[0] sum-up to momentum [6,0,0,0]
// Cells in CELL_DIR[1] sum-up to momentum [0,6,0,0]
// ...
// Cells in CELL_DIR[3] sum-up to momentum [-6,0,0,0]
// ...
```

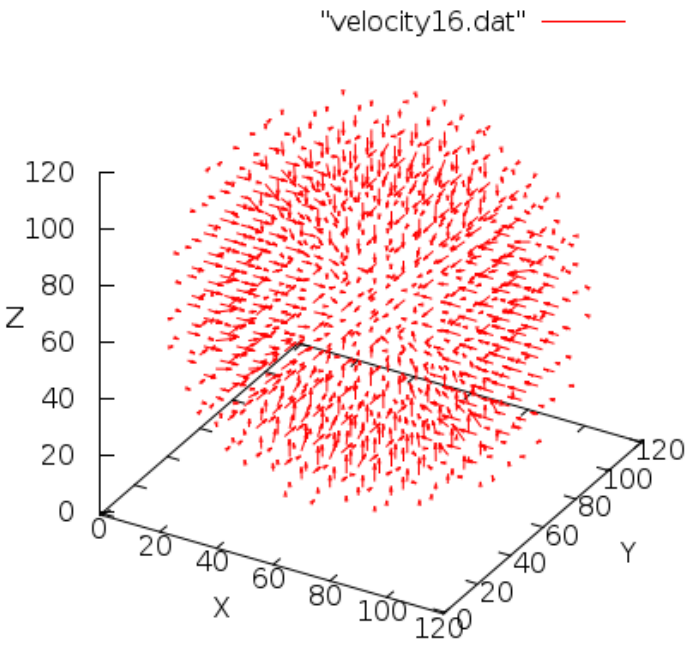

Figure 14.3: Velocity field at time 16 - FCHC inward flow

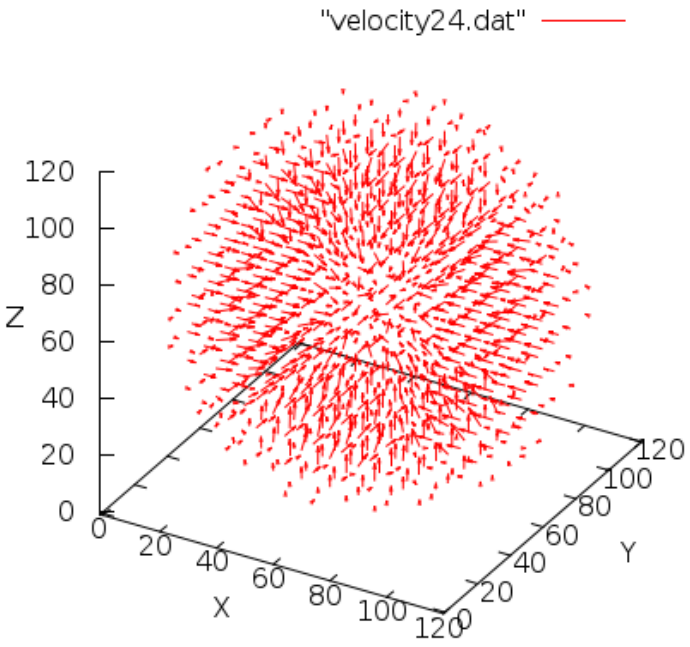

Figure 14.4: Velocity field at time 24 - FCHC inward flow

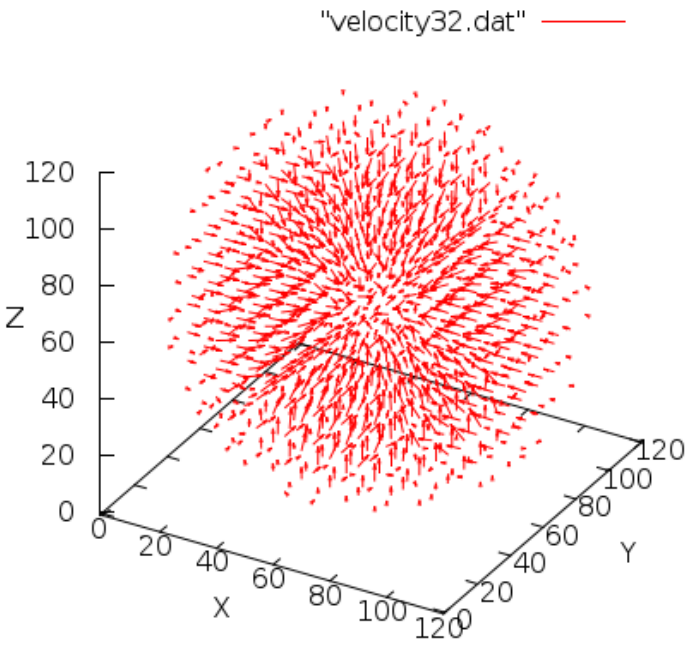

Figure 14.5: Velocity field at time 32 - FCHC inward flow

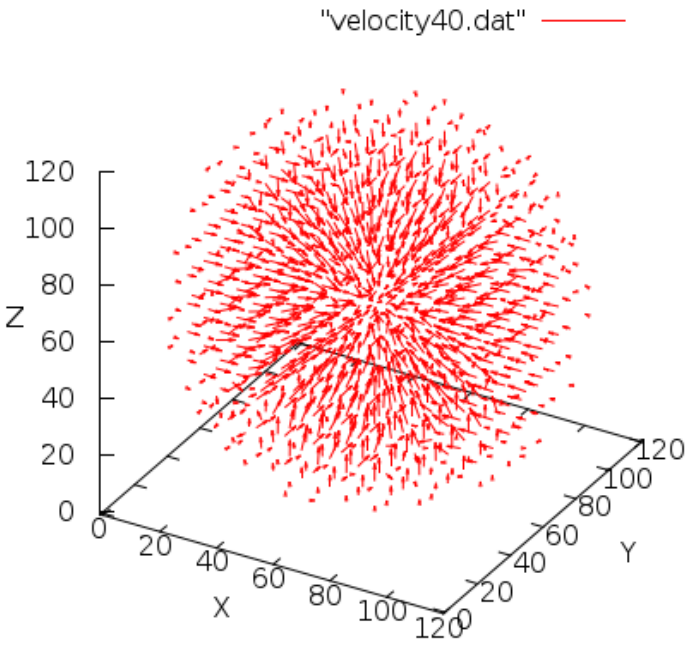

Figure 14.6: Velocity field at time 40 - FCHC inward flow

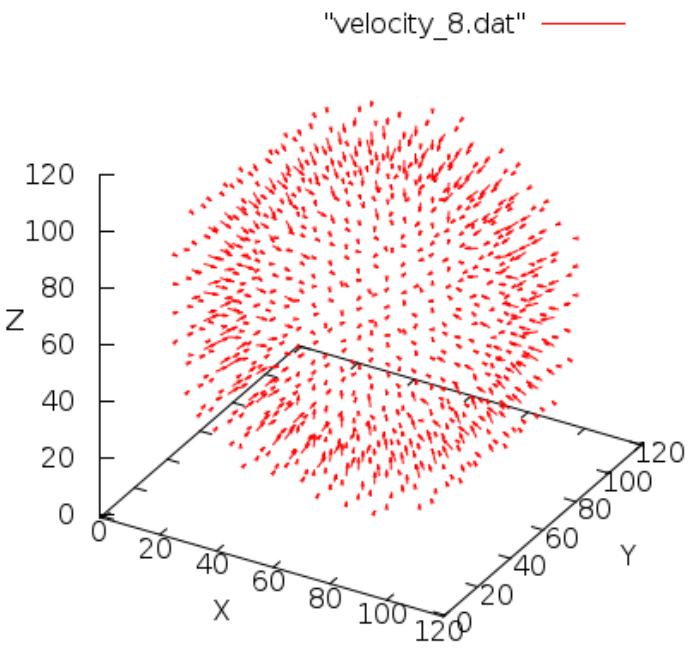

Figure 14.7: Velocity field at time 8 - PI inward flow

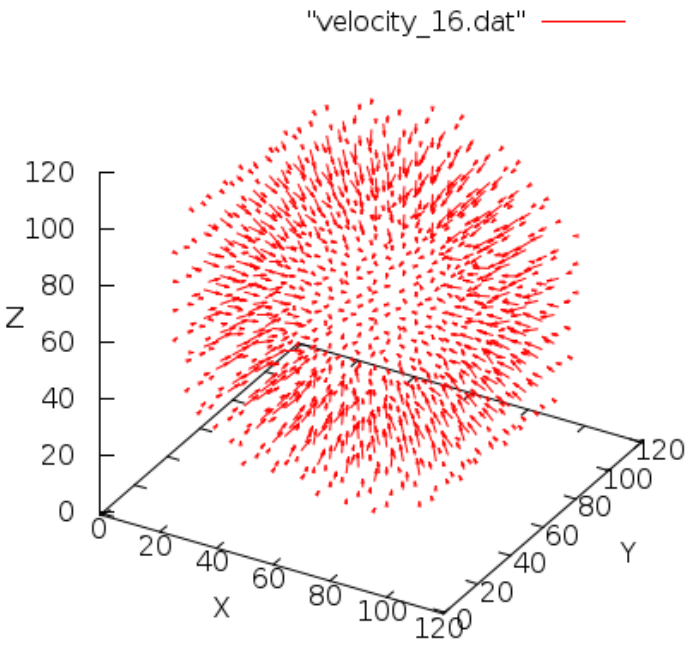

Figure 14.8: Velocity field at time 16 - PI inward flow

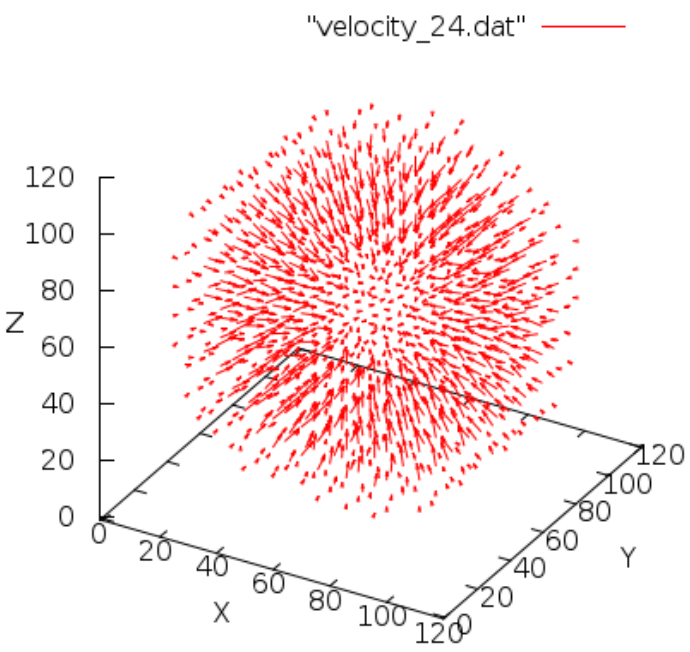

Figure 14.9: Velocity field at time 24 - PI inward flow

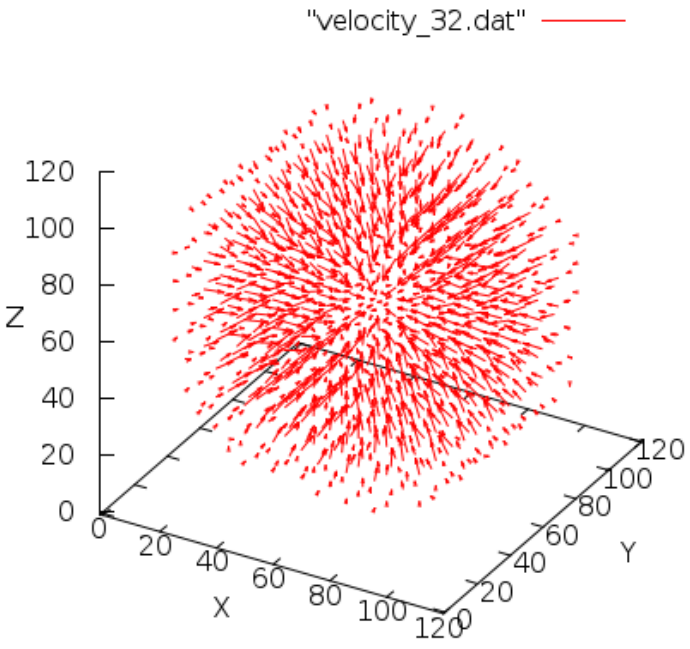

Figure 14.10: Velocity field at time 32 - PI inward flow

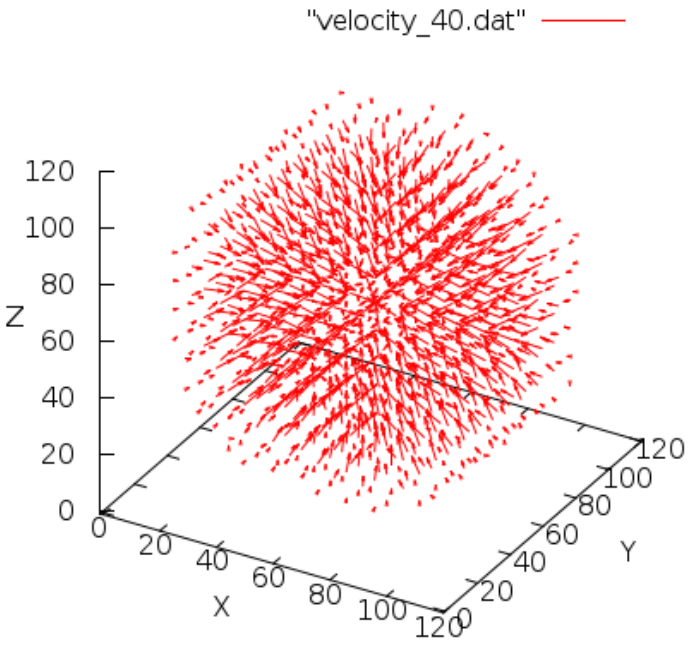

Figure 14.11: Velocity field at time 40 - PI inward flow

```
// Cells in CELL_DIR[5] sum-up to momentum [0,0,-6,0]
int CELL_DIR[6][6] = {
   { C1, C2, C5, C6, C9, C10 },
   { C1, C3, C13, C14, C17, C18 },
   { C5, C7, C13, C15, C21, C22 },
   { C3, C4, C7, C8, C11, C12 },
   { C2, C4, C15, C16, C19, C20 },
   { C6, C8, C14, C16, C23, C24 }
};

/*
 To achieve momentum in XY direction, we should not use all cells from
    CELL_DIR[0] and CELL_DIR[1].
 For example, particle in C3 has positive momentum in Y direction, but
    negative momentum in X direction, so we do not include it.
 The case is even stronger for 3 non-zero components of required
    momentum.
 Hence we implemented function flow_dir that computes which cells
    should be occupied.
 Arguments a, b and c specify components of momentum:
 0: positive X component (CELL_DIR[0])
 1: positive Y component (CELL_DIR[1])
 2: positive Z component ...

 3: negative X component ...
```

```
 4: negative Y component ...
 5: negative Z component (CELL_DIR[5])
 */
int flow_dir(int a, int b, int c = -1)
{
   int dir;
   int not_dir;
   int i, j, k;

   for (i = 0; i < 6; i++)
   {
      // Into dir, we add all cells that have positive momentum in the
         direction 'a' and 'b'
      // We want to occupy these cells by particles.
      dir |= CELL_DIR[a][i];
      dir |= CELL_DIR[b][i];

      // Into not_dir, we add all cells with negative momenta in
         direction in 'a' and 'b'.
      // These cells must not be occupied by particles.
      not_dir |= CELL_DIR[(a + 3) % 6][i];
      not_dir |= CELL_DIR[(b + 3) % 6][i];

      // Same procedure for another component of momentum, if it is
         specified.
      if (c > 0)
      {
         dir |= CELL_DIR[c][i];
         not_dir |= CELL_DIR[(c + 3) % 6][i];
      }
   }
   // To conclude:
   // dir are cells that we want to occupy,
   // not_dir are cells that must not be occupied,
   // so ~not_dir are cells that can be occupied (negation of not_dir
      flips its bits).

   //We return cells that we want to occupy and can be occupied.
   return dir & (~not_dir);
}


/* Set_initial_sphere is called just before Collision and Propagation
    at every time step. */
void set_initial_sphere(int***a, int X, int Y, int Z, int R)
{
   // The particles will be created on the layer between R and R-2.
   int R2out = R*R;
   int R2in = (R - 2)*(R - 2);

   // We will identify segments of the sphere by its distance from the
```

```
      middle.
   int up = R*cos(PI / 4);
   int down = R*sin(PI / 4);

   // These will identify position of node on lattice
   int x, y, z;

   // These are x-R, y-R and z-R, so that [0,0,0] is in the middle of
      the sphere.
   int x1, y1, z1;

   // These are squared x1, y1, z1.
   int x2, y2, z2;

   int i;
   int c;
#pragma omp parallel for private (x, y, z, x1, y1, z1, x2, y2, z2, i,
    c)
   for (x = 0; x < X; ++x)
   {
      x1 = x - R;
      x2 = x1*x1;
      for (y = 0; y < Y; ++y)
      {
         y1 = y - R;
         y2 = y1*y1;
         for (z = 0; z < Z; ++z)
         {
            z1 = z - R;
            z2 = z1*z1;

            // If the node is on the layer between R and R-2, we occupy
               it by particles.
            if (x2 + y2 + z2 > R2in && x2 + y2 + z2 < R2out)
            {
               c = 0;
               // If the node is on the upper-most segment of sphere,
                  particles have momentum in negative Z direction only
               if (z1 > up)
               {
                  for (i = 0; i < 6; ++i)
                  {
                     c |= CELL_DIR[5][i];
                  }
               }
               // If the node is on the downer-most segment, particles
                  have momentum in positive Z direction.
               else if (z1 < -up)
               {
                  for (i = 0; i < 6; i++)
                  {
```

```
      c |= CELL_DIR[2][i];
   }
}
// Similarly for segments on axis Y and Z.
else if (y1 > up)
{
   for (i = 0; i < 6; i++)
   {
      c |= CELL_DIR[4][i];
   }
}
else if (y1 < -up)
{
   for (i = 0; i < 6; i++)
   {
      c |= CELL_DIR[1][i];
   }
}
else if (x1 > up)
{
   for (i = 0; i < 6; i++)
   {
      c |= CELL_DIR[3][i];
   }
}
else if (x1 < -up)
{
   for (i = 0; i < 6; i++)
   {
      c |= CELL_DIR[0][i];
   }
}
// If x1 is close to 0, then particles should sustain
    X-component of position.
// Hence X-component of momentum of particles should be
    zero.
else if (x1 < down && x1 > -down)
{
   // If y1 is positive, we send particles in negative Y
       direction, and vice versa.
   // Same for z1.
   c = flow_dir(y1 > 0 ? 4 : 1, z1 > 0 ? 5 : 2);
}
else if (y1 < down && y1 > -down)
{
   c = flow_dir(x1 > 0 ? 3 : 0, z1 > 0 ? 5 : 2);
}
else if (z1 < down && z1 > -down)
{
   c = flow_dir(x1 > 0 ? 3 : 0, y1 > 0 ? 4 : 1);
}
```

```
                // Else the node is on the segment corresponding to one
                    of 8 corners of the inscribed cube.
                else
                {
                   c = flow_dir(x1 > 0 ? 3 : 0, y1 > 0 ? 4 : 1, z1 > 0 ?
                       5 : 2);
                }
                a[x][y][z] = c;
             }
          }
       }
    }
}
```

14.2 Statistical properties of the flow

So far, the best understanding of the phenomena arising in turbulent flow is by them means of statistical analysis.

In previous chapter, we described setting of the simulation that should lead to the fully-developed turbulent flow.

In this chapter, we will inspect statistical properties of this flow to see whether isotropy and homogenity was recovered in our model, as predicted by K41 theory and confirmed by experimental data.

The weak point of our approach might be implicit assumption of the ergodicity of the models. All the statistical quantities that we computed and visualized were obtained by averaging over 10 000 to 15 000 time-steps, or equivalently $1000-1500$ units of time.

14.2.1 First statistical moment - the mean velocity field

Assuming ergodicity, we define the first statistical moment of the velocity field $v(t, \boldsymbol{r})$ as

$$\langle v(\boldsymbol{r}) \rangle = \sum_{t=T_1}^{T_2} v(t, \boldsymbol{r}), \tag{14.4}$$

In both our models, we used similar implementation.

```
/* Every-time that velocity is updated, its value is counted */
void compute_mean(double****v, double****mean, int I, int J, int K,
    int div)
{
   // i,j,k denotes position vector, l denotes component of the vector
   int i, j, k, l;

#pragma omp parallel for private (i, j, k, l)
   for ( i = 0; i < I; i++)
      for ( j = 0; j < J; j++)
         for ( k = 0; k < K; k++)
```

```
            for ( l = 0; l < 3; l++)
               mean[i][j][k][l] += v[i][j][k][l];

}

/*  So far we have sum of velocities over specific time interval, only
    now we compute the mean */
void finalize_mean(double****mean, int I, int J, int K, int steps)
{
   int i, j, k, l;

#pragma omp parallel for private (i, j, k, l)
   for ( i = 0; i < I; i++)
      for ( j = 0; j < J; j++)
         for ( k = 0; k < K; k++)
            for ( l = 0; l < 3; l++)
               mean[i][j][k][l] /= steps;
}
```

14.2.2 Second statistical moment – the covariance tensor

As discussed in chapter on probabilistic methods, all higher statistical moments can be obtained from the second moment (for the quantities that have normal distribution). That makes it one of the most important quantities that characterize velocity field.

Intuitively speaking, this tensor measure how strong are correlated components of the velocities.

For the centered functions, the covariance tensor reads

$$\Gamma^c_{ij} = \langle v_{ij} \rangle, \tag{14.5}$$

but for the functions with non-zero mean value (that will be our case), formula has to be modified

$$\Gamma_{ij} = \langle v_{ij} \rangle - \langle v_i \rangle \langle v_j \rangle \,. \tag{14.6}$$

Implementing this formula is very straight-forward.

```
/* The covariant tensor double*****g was initialized by zero values. */
/* Each update of velocity field v is followed by function
    'covariance_tensor', */
void covariance_tensor(double****v,double*****g, int I, int J, int K)
{
   int i,j,k,d,e;
#pragma omp parallel for private (i,j,k,d,e)
   for(i=0; i<I; ++i)
      for(j=0; j<J; ++j)
         for(k=0; k<K; ++k)
            for(d=0; d<3; ++d)
               for(e=0; e<3; ++e)
```

```
                g[i][j][k][d][e] += (v[i][j][k][d]*v[i][j][k][e]);
}

/* After specified number of 'steps', finalize_covariance_tensor is
    called */
void finalize_covariance_tensor(double****mean, double*****g, int I,
    int J, int K, int steps)
{
   // Variables i,j,k stands for position vector in the velocity field,
   // d,e are indexes of the tensor 'g'
   int i,j,k,d,e;
#pragma omp parallel for private (i,j,k,d,e)
   for(i=0; i<I; ++i)
      for(j=0; j<J; ++j)
         for(k=0; k<K; ++k)
            for(d=0; d<3; ++d)
               for(e=0; e<3; ++e)
               // Avaraging by number of 'steps' and subtracting mean
                   velocity product, we obtained the covariant tensor at
                   r = (i,j,k)
                  g[i][j][k][d][e] = (g[i][j][k][d][e] / steps ) -
                      mean[i][j][k][d]*mean[i][j][k][e];
}
```

In order to interpret the data obtained in the simulation, we have to compare the correlation tensor to one predicted by Kolmogorov's K41 theory of fully-developed turbulence.

In the isotropic situation, there is no preferred direction and, thus, the only second-order tensor at our disposal is the Kronecker delta δ_{ij}. Hence, the correlation tensor must be of the form

$$\Gamma_{ij} = K\,\delta_{ij}, \tag{14.7}$$

where K is, in general, function of spatial coordinates, having dimension of velocity-squared. However, the requirement of global isotropy implies global homogeneity, so that K is in fact constant. Physically speaking, this form of correlation tensor means that different Cartesian components of the velocity field at given point are uncorrelated, i.e. independent.

In the anisotropic situation, on the other hand, there is a preferred direction which can be represented by a unit vector $\boldsymbol{n}$. In that case, the most general second-order tensor is given by

$$\Gamma_{ij} = K_1\,\delta_{ij} + K_2\,n_i\,n_j, \tag{14.8}$$

where K_1 and K_2 are functions in general. In other words, there are just two independent components of the correlation tensor.

In the most general situation, when the anisotropy is specified by three linearly independent vectors, we get six independent components, which simply corresponds to a general second-order symmetric tensor.

Any such tensor defines a quadratic form and a family of surfaces parametrized by constant C via equation

$$\Gamma_{ij}\,x_i\,x_j = C. \tag{14.9}$$

In the isotropic case these surfaces are concentric spheres. In the anisotropic case, we will get ellipsoids, because correlation tensor is positive-definite[1]. We can conclude that the deviation of the surfaces from spherical shape measures the failure of the system to be isotropic.

The Kolmogorov theory then makes assumptions known as Kolmogorov hypotheses, asserting that the correlation functions inside the inertial interval are independent of the external scale (energy injection) and of the dissipation scale.

These assumptions, together with isotropy and dimensional analysis, then restrict possible functional dependence of correlators on the parameters of the system, namely the dissipation rate and viscosity (see, e.g. [8] and references therein). In this thesis, we do not go into details of Kolmogorov's theory, instead we focus on the question to what extent the assumption of isotropy is satisfied in the cellular automaton model.

14.2.3 Structure functions

Another important quantity characterizing the velocity field are the structure functions.

For the centered velocity field, formula for the second-order structure functions reads

$$S_2^c = \langle\, [v_r(x_M) - v_r(x_R)]^2 \,\rangle, \tag{14.10}$$

where v_r is the projection of the velocity vector onto radial vector connecting the points x_M (middle of the sphere) and x_R (variable, running over the sphere with radius R).

Because velocity field that we study has non-zero mean value, we need to implement modified formula

$$S_2 = \langle\, [v_r(x_M) - v_r(x_R)]^2 \,\rangle - [\, u_r(x_M) - v_r(x_R)\,]^2. \tag{14.11}$$

where $\boldsymbol{u}$ is the mean velocity.

In this way, we examine the dependence of the structure function S_2 on the angles θ and ϕ. In the fully developed turbulent flow, S_2 should be constant function of θ and ϕ. For our imperfect models, we can expect certain dependence.

```
/* After every update of velocity field, struct_on_sphere sums
    [v_r(x_M) - v_r(x_R)] so at the end of computaton, we can compute
    the structure function by formul \ref{str2} */
/* The angular distance between various points x_R on the sphere is PI
    / N */
void struct_on_sphere(double****v, double**Cor, int I, int J, int K,
    int N=CIRC)
{
   /* x and y iterates over the sphere */
   int x, y;
```

[1]This can be easily seen by the following argument. In the frame of main axes of Γ_{ij}, this tensor is diagonal and its diagonal terms are $\Gamma_{ii} = \langle v_i^2 \rangle \geq 0$. Since quadratic forms are inertial with respect to rotations, this property is preserved in any frame.

```
   /* Cartesian coordinates of x_R */
   int i, j, k;

   /* Radius of of the sphere that i,j,k parametrize */
   int R = I/4;

   double sin_theta, sin_phi, cos_theta, cos_phi;

   /* Initialization of angles */
   double theta = 0;
   double phi = 0;

   /* The angles theta and phi will grow by PI / N */
   double step = PI / N;

   /* coordinates of v_M are fixed, it is the middle of the sphere */
   double* v_s = v[I/2][J/2][K/2];

   double* v_r = new double[3]();

   double v_x, v_y, v_z;


//#pragma omp parallel for private (i,j,k, x,y, sin_theta,sin_phi,
    cos_theta,cos_phi, theta, phi, v_r, v_x, v_y, v_z)
   for (x = 0; x < 2*N; ++x)
   {
      phi += step;
      sin_phi = sin(phi);
      cos_phi = cos(phi);

      for (y = 0; y < N; ++y)
      {
         theta += step;
         sin_theta = sin(theta);
         cos_theta = cos(theta);

         /* We transform theta and phi into Cartesian coordinates i, j,
            k
         i = R*cos_phi*cos_theta;
         j = R*sin_phi*cos_theta;
         k = R*sin_theta;

         // We transform i, j, k into coordinate frame of the lattice
         v_r = v[i + I/2][j + J/2][k + K/2];

         /* Projection onto the radial vector
         v_x = (v_s[0] - v_r[0])*cos_phi*cos_theta;
         v_y = (v_s[1] - v_r[1])*sin_phi*cos_theta;
         v_z = (v_s[2] - v_r[2])*sin_theta;
```

```
            /* Add it to the previous sum */
            /* It will be processed by another function at the end of
                computation to obtain mean value */
            struc[x][y] += pow(v_x + v_y + v_z , 2);
        }
    }
}

/* This function implements the formula \ref{str2} */
/* Implementation is similar to previous function, but it uses mean
    velocities and differs in final line */
void finalize_struct(double**str, double****mean, int I, int J, int K,
    int d, int N=CIRC)
{
    int x,y;
    int i, j, k;

    int R = I/4;
    int I2 = I/2;
    int J2 = J/2;
    int K2 = K/2;

    double sin_theta, sin_phi, cos_theta, cos_phi;

    double theta = 0;
    double phi = 0;
    double step = PI / N;

    double* v_s = mean[I2][J2][K2];
    double* v_r;

    //projections
    double v_x, v_y, v_z;


//#pragma omp parallel for private
    (i,j,k,x,y,sin_theta,sin_phi,cos_theta,cos_phi,theta,phi,v_r,v_x,v_y,v_z)
    for (x = 0; x < 2*N; ++x)
    {
        sin_phi = sin(phi);
        cos_phi = cos(phi);
        phi += step;

        for (y = 0; y < N; ++y)
        {
            sin_theta = sin(theta);
            cos_theta = cos(theta);
            theta += step;

            // coordinates of v_r
            i = R*cos_phi*cos_theta;
```

```
        j = R*sin_phi*cos_theta;
        k = R*sin_theta;


        v_r = mean[i + I2][j + J2][k + K2];

        v_x = (v_s[0] - v_r[0])*cos_phi*cos_theta;
        v_y = (v_s[1] - v_r[1])*sin_phi*cos_theta;
        v_z = (v_s[2] - v_r[2])*sin_theta;

        str[x][y] = ( str[x][y] / d ) - pow(v_x + v_y + v_z , 2);
      }
   }
}
```

14.3 Graphical representation of the obtained results

The figures 14.3 and 14.3 show that the correlation tensor is represented by highly ellipsoidal surfaces and hence, the isotropy seems to be significantly violated. This can have several reasons. First, an obvious possibility is a mistake in the code, but after careful inspection and previous applications with reasonable outcomes, we believe this is not the case.

Another and the most plausible source of anisotropy is the limited size of the grid. Based on the theoretical analysis, we expect that (much) larger grids will produce more isotropic configurations. Anisotropy can also be attributed to the initial and boundary conditions on the sphere, which are isotropic only to extent allowed by the geometry of the lattice and the coarse-graining of the velocity field. This question is left for the future investigation.

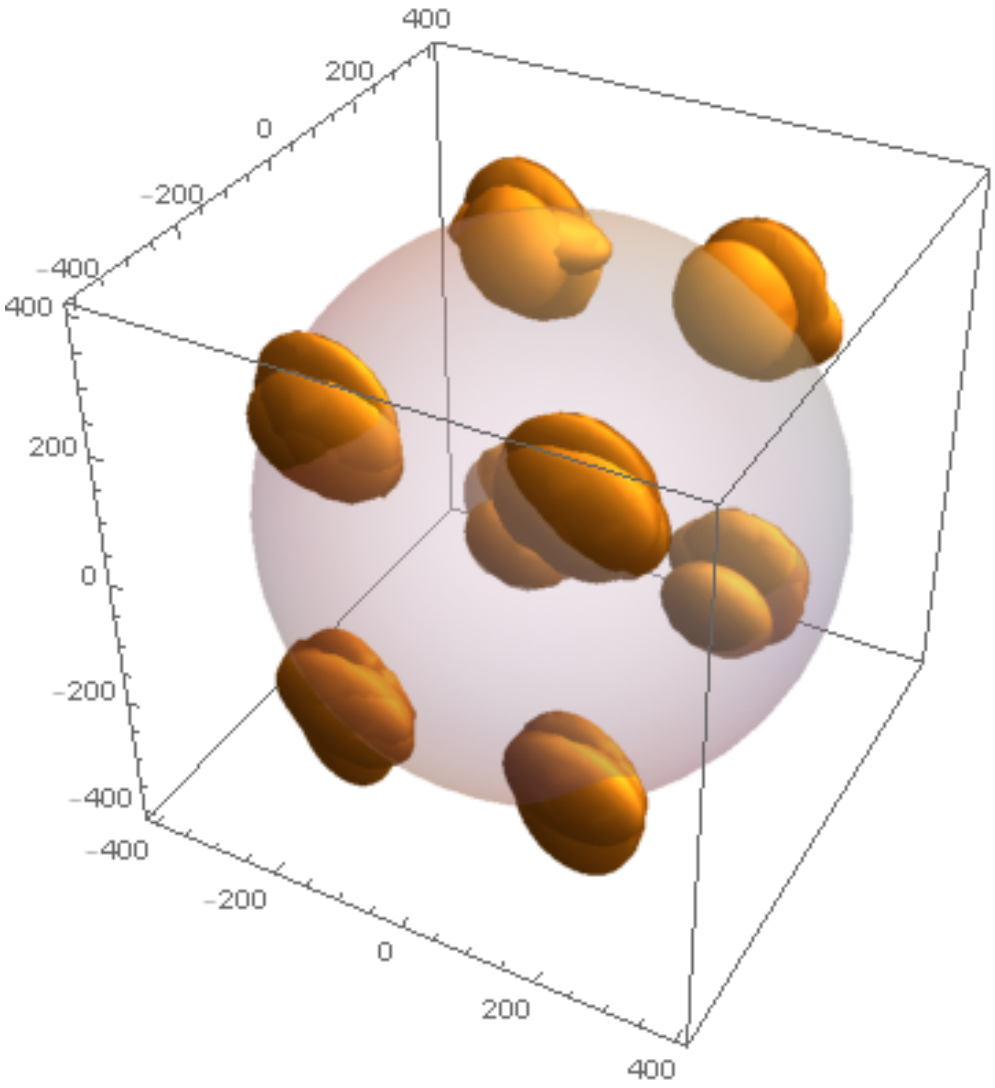

Figure 14.12: Covariance tensor field for PI with deterministic (standard) algorithm - only the tensors with highest norm are presented

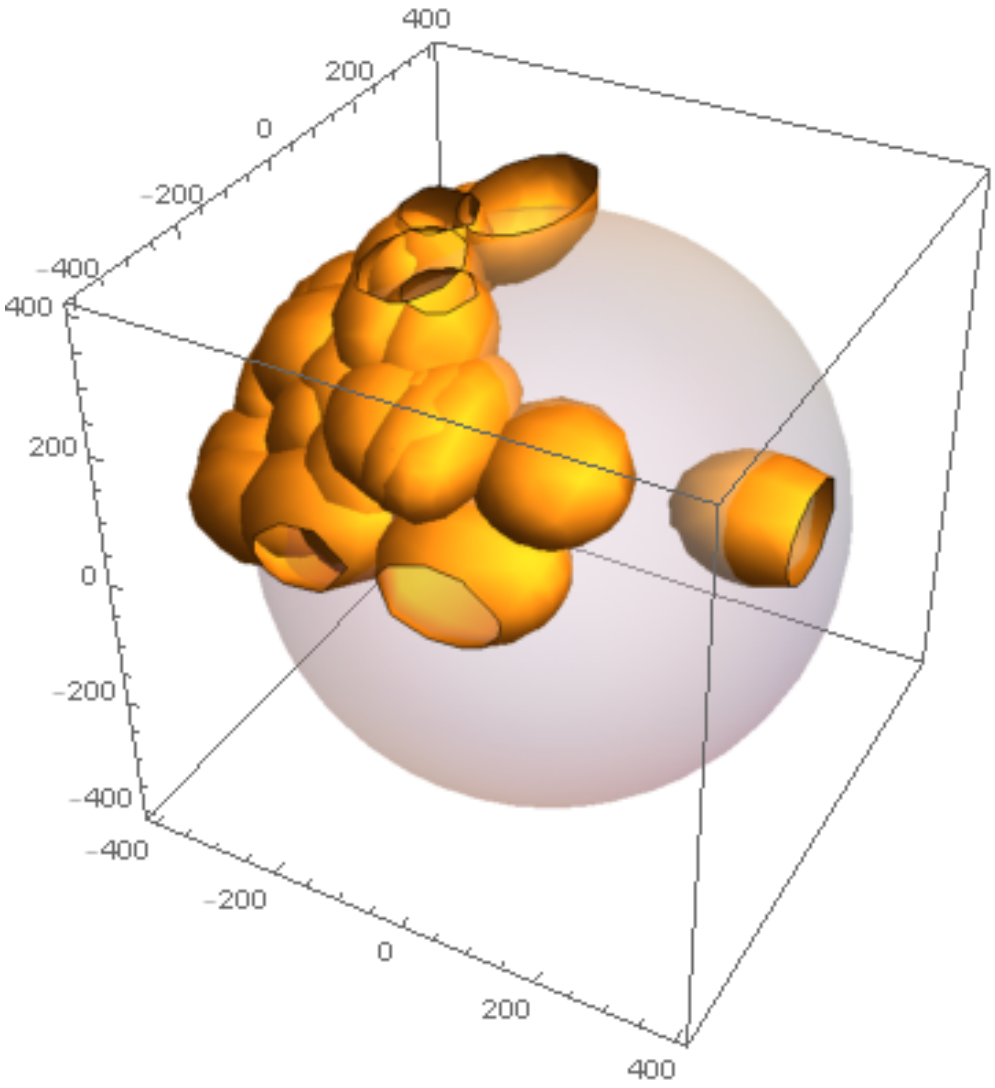

Figure 14.13: Covariance tensor field for PI with non-deterministic algorithm - future simulations are required to confirm and explain the discrepancy

Bibliography

[1] Cook, M.: *Universality in Elementary Cellular Automata*. Complex Systems 15, 1-40, 2004.

[2] Wolf-Gladrow, Dieter A.: *Lattice-Gas Cellular Automata and Lattice Boltzmann Models – An Introduction* . New York: Springer, 2005.

[3] Henon, Michel: *Isometric collision rules for the four dimensional FCHC Lattice Gas*. Complex Systems 1, 1987

[4] Wolfram, Stephen: *New kind of science* . Wolfram Media, Inc., 2002

[5] Frisch, Uriel: *Lattice Gas Hydrodynamics in Two and Three Dimensions*. Complex Systems 1, 1987

[6] Bodenheimer, Michel, Laughlin, Gregory P., Rozyczka, Michal, Yorke, Harold W.: *Numerical methods in Astrophysics - An Introduction*. Taylor & Francis Group, LLC, 2007

[7] Nasilowski, Ralf : *A Cellular-Automaton Fluid Model with Simple Rules in Arbitrarily Many Dimensions*. Journal of Statistical Physics, Vol. 65, Nos. 1/2, 1991

[8] Scholtz, Martin: *Vplyv anizotropie na stabilitu skalovacich rezimov v modeli advekcie pasivnej vektorovej primesi*. Kosice, 2007

[9] Aaronson, Scott : *BOOK REVIEW on A New Kind of Science*. Quantum Information and Computation, Vol. 1, No. 0, 2001

[10] 't Hooft, Gerald : *The Cellular Automaton Interpretation of Quantum Mechanics*. arXiv:1405.1548v3 [quant-ph] 21 Dec 2015

[11] Levy, Steven : *The man who cracked the code to everything*. https://www.wired.com/2002/06/wolfram/

List of Figures

List of Tables

List of Abbreviations

Attachments